Photoinduced Generation of Hydroxyl Radical in Natural Waters

Khan M. G. Mostofa, Cong-qiang Liu, Hiroshi Sakugawa, Davide Vione, Daisuke Minakata, M. Saquib and M. Abdul Mottaleb

1 Introduction

Hydroxyl radical ($HO^\bullet$) is a short-lived free radical, and it is the most potent oxidizing transient among the reactive oxygen species. It is an effective, nonselective and strong oxidant that is ubiquitously formed in natural sunlit surface waters (rivers, lakes and seawater and so on), rain, dew, cloud, fog, snow, aerosol, and in all living organisms. The $HO^\bullet$ is photolytically formed from a variety of sources in natural waters. The first experimental report of a reaction that is now known to produce $HO^\bullet$ dates back to Henry John Horstman Fenton, who described the oxidation

---

K. M. G. Mostofa (✉) · C. Q. Liu
State Key Laboratory of Environmental Geochemistry, Institute of Geochemistry,
Chinese Academy of Sciences, Guiyang 550002, China
e-mail: mostofa@vip.gyig.ac.cn

H. Sakugawa
Department of Environmental Dynamics and Management,
Graduate School of Biosphere Science, Hiroshima University, 1-7-1, Kagamiyama,
Higashi-Hiroshima 739-8521, Japan

D. Vione
Dipartimento di Chimica Analitica, University of Turin, I-10125 Turin, Italy

Centro Interdipartimentale NatRisk, I-10095 Grugliasco, (TO), Italy

D. Minakata
School of Civil and Environmental Engineering, Georgia Institute of Technology,
828 West Peachtree Street, Suite 320, Atlanta, GA 30332, USA

M. Saquib
Department of Chemistry, Aligarh Muslim University, Aligarh 202002, Uttar Pradesh, India

M. A. Mottaleb
Department of Chemistry/Physics Northwest Missouri State University, Center for Innovation and Entrepreneurship (CIE), 800 University Drive, Maryville, MO 64468, USA

K. M. G. Mostofa et al. (eds.), *Photobiogeochemistry of Organic Matter*,
Environmental Science and Engineering, DOI: 10.1007/978-3-642-32223-5_3,

of Fe(II) with H_2O_2 in aqueous media (Fenton 1894). The Fenton's reaction has been studied by several researchers afterwards (Haber and Weiss 1934; Barb et al. 1951; Hardwick 1957; Wells and Salam 1967, 1968; Po and Sutin 1968; Skinner et al. 1980; Rush and Bielski 1985; Moffett and Zika 1987a, b; Lloyd et al. 1997; Kremer 1999; Lindsey and Tarr 2000). Haber and Weiss in 1934 firstly postulated that the reactivity of the Fenton's reagent is due to the generation of $HO^{\cdot}$ in aqueous solution, and that Fe(II) acts as a catalyst for the decomposition of H_2O_2 into $HO^{\bullet}$. The Fenton's reaction can be used to promote the oxidation of organic compounds (Walling 1975) and has been widely studied to this purpose in the last 25 years (Sychev and Isak 1995; Chen and Pignatello 1997; Gallard et al. 1998; Barbeni et al. 1987; Lindsey and Tarr 2000; Kang et al. 2002; Pignatello et al. 2006).

Hydroxyl radical is also a photo-product of many photolysis reactions that occur in natural waters (Zafiriou 1974; Zafiriou and True 1979a, b; Mill et al. 1980; Draper and Crosby 1981; Russi et al. 1982; Zafiriou et al. 1984; Cooper et al. 1988; Mopper and Zhou 1990; Gjessing and Källqvist 1991; Dister and Zafiriou 1993; Takeda et al. 2004; Vione et al. 2006, 2009a, b; al Housari et al. 2010). In particular, $HO^{\bullet}$ can be produced photolytically from NO_2^- and NO_3^- (Zafiriou and True 1979a, b; Russi et al. 1982; Takeda et al. 2004; Zafiriou and Bonneau 1987; Zepp et al. 1987; Zellner et al. 1990; Brezonik and Fulkerson-Brekken 1998; Mack and Bolton 1999) and upon irradiation of various dissolved organic matter (DOM) components (Mill et al. 1980; Mopper and Zhou 1990; Vaughn and Blough 1998; Holder-Sandvik et al. 2000). Hydroxyl radical can be experimentally determined by use of selective probe molecules such as cumene (isopropylbenzene) and pyridine in dilute solution, benzene, terephthalic acid and and *para*-chlorobenzoic acid (*p*CBA) (Mill et al. 1980; Takeda et al. 2004; Fang et al. 1996). The rate of $HO^{\bullet}$ production mostly depends on the quantity and quality of DOM, on the concentration of other chemical species such as nitrate and nitrite, and on the pH of natural waters.

The chemical reactivity of the Fenton's reaction (Fe^{2+} and H_2O_2) is significantly increased by UV/Visible irradiation ($\lambda < 580$ nm), which has for instance been shown to enhance the mineralization of organic pollutants (Haag and Hoigné 1985; Cooper et al. 1991; Zepp et al. 1992; Ruppert et al. 1993; Faust 1994; Voelker et al. 1997; Arakaki et al. 1998; Bossmann et al. 1998; Rossetti et al. 2002; Zepp 2002; Southworth and Voelker 2003; White et al. 2003). Similarly, the H_2O_2/UV process can produce $HO^{\bullet}$ that can decompose organic substances in aqueous solution (Draper and Crosby 1981; Zellner et al. 1990; Hunt and Taube 1952; Baxendale and Wilson 1956; Volman and Chen 1959; Ho 1986; Vel Leitner and Dore 1996; Berger et al. 1999; Wang et al. 2001; Goldstein and Rabani 2008) as well as in ice (Chu and Anastasio 2005). An advanced process that exploits the photo-Fenton system is the photo-ferrioxalate/H_2O_2 reaction, where UV/visible irradiation ($\lambda < 550$ nm) is combined with the presence of excess oxalate (Huston and Pignatello 1996; Safazadeh-Amiri et al. 1996, 1997; Wu et al. 1999; Arslan et al. 2000; Nogueira and Guimaraes 2000; Emilio et al. 2002; Lee et al. 2003; Hislop and Bolton 1999; Jeong and Yoon 2005). The $HO^{\bullet}$ radical can also be generated in aqueous suspensions of

TiO_2, which plays a key role in the heterogeneous photocatalytic degradation of organic contaminants (Sun and Bolton 1996; Ullah et al. 1998; Konstantinou and Albanis 2004). However, an important difference between TiO_2 photocatalysis and the other processes of $HO^\bullet$ generation described before is that the irradiation of TiO_2 mainly causes the production of surface-bound $HO^\bullet$ groups, which are somewhat less reactive than homogeneous $HO^\bullet$ (Serpone and Pelizzetti 1989). The hydroxyl radical has been detected in rainwater, dew, cloud and fog (Arakaki et al. 1998, 1999a, b; Arakaki and Faust 1998; Nakatani et al. 2001; Kobayashi et al. 2002), snow (Chu and Anastasio 2005; Anastasio et al. 2007; Matykiewiczová et al. 2007), aerosols (Anastasio and Jordan 2004), in aqueous extracts of cigarette tar (Zang et al. 1995), and in living organisms (Buettner et al. 1978; Buettner 1987; Miller et al. 1990; Buettner and Jurkiewicz 1996; Cadet et al. 1999; Bourdat et al. 2000; Paradies et al. 2000; Blokhina et al. 2003; Li et al. 2008). The $HO^\bullet$ is rapidly consumed in natural waters by the subsequent reactions with dissolved organic compounds (Schuchmann and von Sonntag 1979; Neta et al. 1988; Westerhoff et al. 1999; Goldstone et al. 2002; Miller and Chin 2002; Miller et al. 2002; Ervens et al. 2003) and several inorganic species (Zafiriou et al. 1984, 1987; Brezonik and Fulkerson-Brekken 1998; Neta et al. 1988; Song et al. 1996).

The generation of $HO^\bullet$ and its interaction with the dynamics of DOM and nutrient as well as with aquatic organisms are very important in natural waters. There are a number of factors that can control the production and consumption of $HO^\bullet$ in that ecosystem. However, there is no general overview published on $HO^\bullet$ in natural waters. A short review by von Sonntag (2007) covers the formation of free radicals and their reactions in aqueous solution.

This review will provide a general overview on sources, production mechanisms, steady state concentration and biogeochemical functions of $HO^\bullet$ in water environment. This paper also discusses the analytical methods that can be adopted to measure the photoinduced generation of $HO^\bullet$, the factors controlling its production and decay, as well as the significance and impact of $HO^\bullet$ in the aquatic ecosystems. It is shown how the production of $HO^\bullet$ differs among DOM components, as well as between freshwaters and marine environments.

2 Hydroxyl Radical ($HO^\bullet$) and Other Free Radical Species

The hydroxyl radical ($HO^\bullet$) is the most powerful oxidizing agent among the photolytically generated ones. It is a short-lived, highly reactive and non-selective transient, able to oxidize dissolved organic substances and other chemical species in natural waters. The oxidation potentials for a series of common oxidants in surface waters is as follows: Fluorine ($E = 3.03$ V) > $HO^\bullet$ (2.80 V) > Atomic oxygen (2.42 V) > Ozone (2.07 V) > Peracetic acid (ROOH) (1.80 V) > H_2O_2 (1.78 V) > Perhydroxyl radical (1.70 V) > Potassium permanganate (1.68 V) > Chlorine dioxide (1.57 V) > Hypochlorous acid (1.49 V) > Chlorine

Table 1 Oxidation potentials of major oxidants

Free radicals	Oxidation potentials (E°) (V)
Fluorine	3.03
Hydroxyl radical	2.80
Atomic oxygen	2.42
Ozone	2.07
Hydrogen peroxide	1.78
Perhydroxyl radical	1.7
Permanganate	1.68
Chlorine dioxide	1.57
Hypochlorous acid	1.49
Chlorine	1.36

Data source Sun et al. (1997)

(1.36 V) whilst one (Table 1) (Sun et al. 1997). The oxidizing capacity of the hydroxyl radical can be described in terms of its reduction potential (E), which allows the comparison with other powerful oxidants (Buettner and Jurkiewicz 1996; Buettner 1993; Ross et al. 1994). One-electron reduction potentials at pH 7.0 for selected radical couples are 2.31 V for $HO^\bullet$, H^+/H_2O; 1.60 V for $RO^\bullet$, H^+/ROH (aliphatic alkoxyl radical); 1.00 V for $ROO^\bullet$, $H^+/ROOH$ (alkyl peroxyl radical); 0.92 V for $GS^\bullet/GS^-$ (glutathione); 0.60 V for $PUFA^\bullet$, H^+/PUFA-H) (*bis*-allylic-H); 0.59 V for $HU^{\bullet-}$, H^+/UH^{2-} (urate); 0.48 V for $TO^\bullet$, H^+/TOH (tocopherol); 0.32 V for H_2O_2, H^+/H_2O, $HO^\bullet$; 0.28 V for ascorbate$^{\bullet-}$, H^+/ascorbate monoanion; 0.12 V for Fe(III)EDTA/Fe(II)EDTA; and −3.30 V for $O_2/O_2^\bullet$ (Buettner and Jurkiewicz 1996; Buettner 1993). The $HO^\bullet$ reacts with organic compounds at close to diffusion-limited rate constants, which are the fastest after equilibrium reactions and the rate constants (k_{obs}) for the reaction of the equilibrium mixture of ascorbic acid species ($AscH_2/AscH^-/Asc^{2-}$ at pH 7.4) are 1.1×10^{10} M^{-1} s^{-1} for $HO^\bullet$; 1.6×10^9 M^{-1} s^{-1} for tert-Butyl alkoxyl radical ($RO^\bullet$); 1–2 $\times 10^6$ M^{-1} s^{-1} for Alkyl peroxyl radical, e.g. $CH_3OO^\bullet$ ($ROO^\bullet$); 1.8×10^8 M^{-1} $s^{-1}$for $ClCOO^\bullet$; 6×10^8 M^{-1} s^{-1} for glutathiol radical ($GS^\bullet$); 1×10^6 M^{-1} s^{-1} for urate radical ($HU^{\bullet-}$); 2×10^5 M^{-1} s^{-1} for tocopheroxyl radical ($TO^\bullet$); 2×10^5 M^{-1} s^{-1} for dismutation ($Asc^{\bullet-}$); 1.4×10^9 M^{-1} s^{-1} for chlorpromazine radical action ($CPZ^{+\bullet}$); $\approx 10^2$ M^{-1} s^{-1} for Fe^{III}-EDTA/Fe^{II}-EDTA; and 1×10^5 M^{-1} s^{-1} for $O_2^{\bullet-}/HO_2^\bullet$ (Buettner and Jurkiewicz 1996; Buettner 1988; Ross et al. 1994). The $HO^\bullet$ radical is formed by a variety of sources such as NO_2^- and NO_3^- under UV irradiation, the Fenton and the photo-Fenton reaction, the photo-ferrioxalate/H_2O_2 system and so on (Legrini et al. 1993). It is directly responsible for a number of important biogeochemical functions in natural waters.

Among other radical species present in natural waters, organic peroxy radicals ($ROO^\bullet$) are intermediates formed photolytically and thermally from organic peroxides, or directly from the degradation of dissolved organic matter. These radicals are short-lived and highly reactive transients. An important process that involves $ROO^\bullet$ is the formation of new organic compounds upon rapid combination of peroxide radicals with organic substances in aqueous solution (Mill et al. 1980; Mageli and Kolczynski 1966; Faust and Hoigne 1987; Blough 1988; Kieber and Blough 1990; Sakugawa et al. 1990; Faust and Allen 1992; Mostofa and Sakugawa 2009). Furthermore, the thermal decomposition of organic peroxides can initiate the polymerization of vinyl monomers or induce cross-linking of a polymeric substrate upon formation of free radical sites on the polymer (Mageli and Kolczynski 1966). The overall (unspeciated) photostationary-state concentration of peroxyl radicals in sunlit cloud and fog waters is around 1–30 nM (Faust and Allen 1992).

The superoxide radical anion ($O_2^{\bullet -}$) is the one-electron reduction product of molecular oxygen. It is an early photoinduced and short-lived intermediate that is formed in chemical reactions occurring in natural waters, where oxygen acts as the ultimate electron acceptor (Jeong and Yoon 2005; Bielski et al. 1985; Petasne and Zika 1987; Zafiriou 1990; Micinski et al. 1993; Zafiriou et al. 1998; Millington and Maurdev 2004). It has been shown that the photoinduced superoxide production rates are 0.1–6.0 nM min^{-1} under full-sun irradiation in spring, and 0.2–8.0 nM min^{-1} in fall in a variety of Eastern Caribbean waters (Micinski et al. 1993). A key reaction of $O_2^{\bullet -}$ is the production of H_2O_2 by dismutation; hydrogen peroxide is then able to generate $HO^{\bullet}$ by direct photolysis or upon photo-Fenton type reactions in sunlit aqueous solutions (Cooper et al. 1988; Micinski et al. 1993; Fischer et al. 1985). Interestingly, the organic complexes of Cu as well as the copper-catalyzed dismutation (involving Cu^{+} and Cu^{2+}) can be significant sinks of photoproduced $O_2^{\bullet -}$ in seawater (Zafiriou et al. 1998; Voelker et al. 2000).

The carbon dioxide radical anion ($CO_2^{\bullet -}$) is a short-lived and highly reactive intermediate that is photolytically formed in the ferrioxalate reaction system. It is a strong oxidizing agent that is able to oxidize metals and other chemical species in aqueous solution. The $CO_2^{\bullet -}$ is formed photolytically ($C_2O_4^{\bullet -} \rightarrow CO_2^{\bullet -} + CO_2$; $k = 2 \times 10^6\ \text{s}^{-1}$) upon decomposition of the oxalyl radical anion ($C_2O_4^{\bullet -}$). The latter is produced by the photoinduced decomposition of the highly photosensitive ferrioxalate complex $[Fe(C_2O_4)_3]^{3-}$ in aqueous solution (Hislop and Bolton 1999; Jeong and Yoon 2004, 2005; Mulazzani et al. 1986). A key role played by $CO_2^{\bullet -}$ is its ability to oxidize the metal ions, therefore affecting the biogeochemical cycling of metal-containing species. These processes can have an impact on the generation of $HO^{\bullet}$ and of the superoxide radical anion in natural waters (Hislop and Bolton 1999; Jeong and Yoon 2004, 2005; Wang et al. 2010). Another potentially important process is the transformation of organic substances induced by $CO_2^{\bullet -}$, which is formed photolytically from ferrioxalate complexes in the aqueous solution (Huston and Pignatello 1996).

In addition, it has been reported that quinones photolytically produce species capable of hydroxylation (Alegria et al. 1997; Pochon et al. 2002; Gan et al. 2008; Maurino et al. 2008; Maddigapu et al. 2010; Page et al. 2011). Some of these quinone-derived hydroxylating species exhibit reactivity that is around one order of magnitude lower than free $HO^{\bullet}$ (Pochon et al. 2002; Gan et al. 2008). It is hypothesized that quinone-derived hydroxylating species may contribute at least in part to the photoinduced $HO^{\bullet}$ production by DOM (Vaughn and Blough 1998; Page et al. 2011).

2.1 Sources of $HO^{\bullet}$ in Natural Waters

The $HO^{\bullet}$ radical is formed photolytically from various sources in natural waters. In rivers, contributions to $HO^{\bullet}$ photoproduction are 1–89 % from NO_2^-, 2–70 % from NO_3^-, 1–50 % from H_2O_2, and 2–70 % from the photo-Fenton reaction and/or irradiated CDOM (Takeda et al. 2004; Vione et al. 2006; White et al. 2003; Page et al. 2011; Nakatani et al. 2007; Mostofa KMG and Sakugawa H, unpublished data). Experimental studies show that DOM isolates from rivers may contribute up to 50 % of the hydroxylation through production of H_2O_2 (Page et al. 2011). The results demonstrate that NO_2^- is a key contributor (48–80 %) for $HO^{\bullet}$ production in sewerage-polluted river waters, but NO_3^- can be a major contributor (16–49 %) in clean river waters. In seawater the major sources of $HO^{\bullet}$ are 7–75 % from NO_2^-, 1–8 % from NO_3^-, 0–1 % from H_2O_2, and 24–93 % from unknown sources. These data were obtained from a study carried out in Seto Inland and the Yellow Sea (Takeda et al. 2004). The formation of $HO^{\bullet}$ from different sources in natural waters can be distinguished as: (i) the photolysis of nitrite and nitrate in the aqueous solution (Mopper and Zhou 1990; Takeda et al. 2004; Zepp et al. 1987); (ii) the irradiation of CDOM components via formation of H_2O_2 in the aqueous solution. In this case the production of $HO^{\bullet}$ depends on the nature of the CDOM components (Fig. 1) (White et al. 2003; Mostofa and Sakugawa 2009; Mostofa KMG and Sakugawa H, unpublished data), but a useful correlation has been found between the formation rate of $HO^{\bullet}$ and the content of dissolved organic carbon in different lake water samples (Vione et al. 2006); (iii) the Fenton reaction (Fenton 1894; Walling 1975; Kang et al. 2002), the photo-Fenton reaction (Zepp et al. 1992; Arakaki et al. 1998; Southworth and Voelker 2003) as well as the photo-ferrioxalate/H_2O_2 system in natural waters (Southworth and Voelker 2003; Safazadeh-Amiri et al. 1997; Hislop and Bolton 1999); (iv) the direct photolysis of hydrogen peroxide, i.e. UV/H_2O_2 processes in aqueous solution (Draper and Crosby 1981; Wang et al. 2001). The UV irradiation of natural waters can produce H_2O_2 that further yields $HO^{\bullet}$ (Gjessing and Källqvist 1991; Cooper et al. 1996); (v) the reaction of hydroperoxide radical ($HO_2^{\bullet}$) with NO ($HO_2^{\bullet} + NO \rightarrow HO^{\bullet} + NO_2$) (Sakugawa et al. 1990); (vi) the photolysis of dimeric $\left[Fe_2\,(OH)_2\,(H_2O)_8\right]^{4+}$ species in aqueous solution (Langford and Carey 1975); (vii) the photolysis of $Fe^{III}(OH)^{2+}$ in aqueous solution. The generation of $HO^{\bullet}$ upon photolysis of $Fe^{III}(OH)^{2+}$ is very efficient (quantum yield ~0.2), but the Fe(III) hydroxocomplex is present in significant concentration only at strongly acidic pH values that have little environmental significance(Jeong and Yoon 2005; Pozdnyakov et al. 2000); (viii) the generation of singlet states of oxygen atoms ($^1O_1$) by ozonolysis, followed by reaction with H_2O to form $HO^{\bullet}$ (Hoigné and Bader 1978, 1979; Staehelin and Hoigné 1985; Takahashi et al. 1995); (ix) the reaction of O_3 with H_2O_2 (peroxone process), which generates $HO^{\bullet}$ ($H_2O_2 + 2O_3 \rightarrow 2HO^{\bullet} + 3O_2$) (Hoigné 1998); (x) the production of $HO^{\bullet}$ by auto-oxidation of cytotoxic agents (Cohen and Heikkila 1974); (xi) chemical effects of ultrasound, which can generate $HO^{\bullet}$ in aqueous solution (Makino et al. 1983); (xii) ultrasound-induced cavitation in aqueous solution, yielding $HO^{\bullet}$ upon water splitting (H_2O + ultrasound $\rightarrow HO^{\bullet}$,

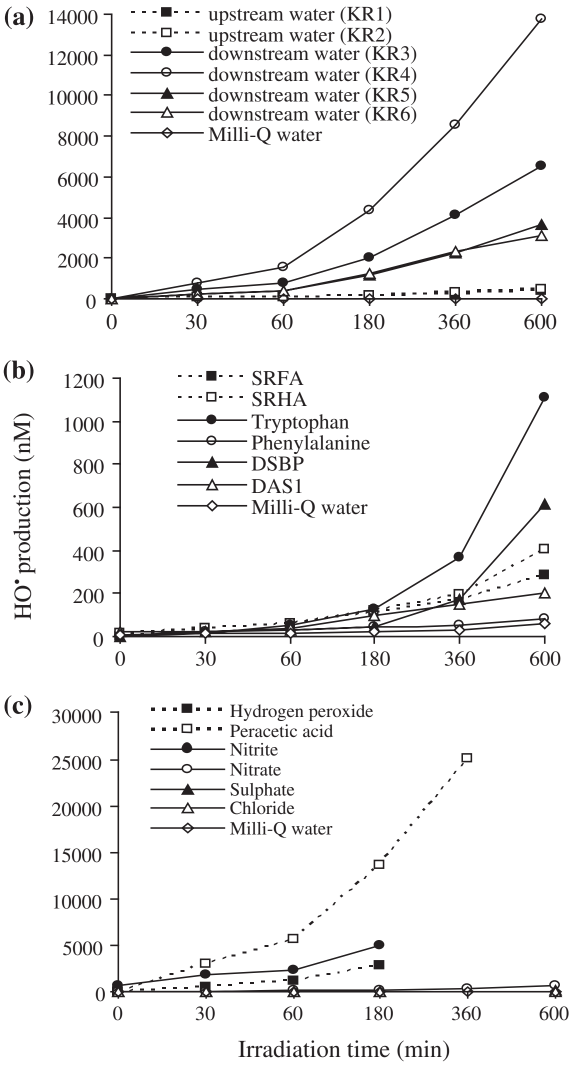

Fig. 1 Photoinduced generation of $HO^{\bullet}$ from river waters (**a**), various standard organic substances (**b**) and various (inorganic and organic) chemical species (**c**) in photoexperiments conducted using a solar simulator. Aqueous solutions ($1\ \text{mg}\ L^{-1}$) of standard all organic substances are used for production of HO radicals in (**b**) and all chemical species in (**c**) are adjusted to 100 μM. All data depicted in these figures are calibrated for natural sunlight on 6 July 2004 at Hiroshima University Campus at noon under clear sky conditions. *Data source* Mostofa KMG and Sakugawa H (unpublished data)

H_2O_2, H_2) (Henglein 1987); (xiii) autooxidation of aqueous extracts of cigarette tar (ACT), giving $HO^{\bullet}$ in air-saturated, buffered aqueous solutions. It is thought that the process is caused by the autooxidation of hydroquinone- and catechol-related species in ACT (Zang et al. 1995); (xiv) photoinduced $HO^{\bullet}$ production from aqueous suspensions of algae(Li et al. 2008); and (xv) photoinduced $HO^{\bullet}$ production can occur from DOM, the reactive triplet states of which could be involved in oxidation of water and/or OH^{-} and in the production of lower energy hydroxylating species that simulate DOM reactivity (Alegria et al. 1997; Pochon et al. 2002; Gan et al. 2008; Maurino et al. 2008; Maddigapu et al. 2010; Page et al. 2011; Maddigapu et al. 2011; Brigante et al. 2010; Sur et al. 2011).

2.2 Biogeochemical Functions of $HO^\bullet$ in Natural Waters

The $HO^\bullet$ is responsible for the occurrence of many important biogeochemical functions in natural waters: (i) photoinduced decomposition of DOM, which causes the production of a number of low molecular weight (LMW) photoproducts. The latter are microbiologically labile and constitute a significant source of carbon and energy to the microbial food chains, as well as an important pathway for DOM turnover in natural waters (Zhou and Mopper 1990; Blough and Zepp 1995; Tranvik 1992; Moran and Zepp 1997; Bertilsson and Tranvik 1998; Mopper and Kieber 2000; Mostofa et al. 2009a, b). However, despite the major role played by $HO^\bullet$ in the mineralization processes of organic pollutants in the framework of the AOPs, the $HO^\bullet$ is expected to contribute to a minor extent to the photomineralization of natural DOM in surface waters (Vione et al. 2009); (ii) photoinduced production of low-molecular weight chemical species such as H_2O_2 and CO_2 (both dissolved and gaseous forms). These processes play some role in the occurrence of photosynthesis, which produces algal biomass that is involved into the generation of autochthonous DOM in natural waters (Mostofa et al. 2009a, b; Komissarov 2003; Fu et al. 2010). However, the importance of such reactions is limited by the relatively low generation rate of $HO^\bullet$ in surface waters (Brezonik and Fulkerson-Brekken 1998); (iii) photo-bleaching of DOM induced by solar radiation in waters (Moran et al. 2000; del Vecchio and Blough 2002; Mostofa et al. 2005, 2007); (iv) photodegradation of persistent organic pollutants, which are usually recalcitrant to biological, chemical, and direct photodegradation in water (Brezonik and Fulkerson-Brekken 1998; Haag and Yao 1992; Grannas et al. 2006; Vione et al. 2009); (v) cycling of transition metal ions that can be oxidized by $HO^\bullet$ (Jeong and Yoon 2004; Faust and Zepp 1993; Kwan and Voelker 2002); (vi) use of $HO^\bullet$ in water treatment processes such as the Advanced Oxidation Technology (AOT), to purify sewerage or industrial wastewater effluents, with the purpose of controlling the organic pollution for sustainable development (Safazadeh-Amiri et al. 1996, 1997; Kang et al. 2000); (vii) damage to macromolecules such as DNA, proteins and lipids, membrane leakage, breakdown of the cellular metabolism, and finally of tissues in biological systems. These processes can be induced by the $HO^\bullet$, alkoxyl ($RO^\bullet$) and peroxyl ($ROO^\bullet$) radicals, which may be produced by the autooxidation of biomolecules such as ascorbate, catecholamines or thiols in organisms (Paradies et al. 2000; Blokhina et al. 2003; Berlett and Stadtman 1997; von Sonntag 2006).

2.3 Steady-State Concentration and Life-Time of $HO^\bullet$ in Natural Waters

The steady state concentration of $HO^\bullet$ can be determined on the basis of its major sources, which control the total photoinduced formation rate constants, and on sinks or scavengers of $HO^\bullet$ that control the total consumption rate constants in natural waters (al Housari et al. 2010; Brezonik and Fulkerson-Brekken 1998; Arakaki et al. 1999b; Hoigné et al. 1989; Schwarzenbach et al. 1993; Nakatani et al. 2004). DOM and carbonate are the major scavengers or sinks of $HO^{\bullet}$ in freshwaters (White et al. 2003; Nakatani et al. 2004), but in seawater the bromide (Br^-) ions are actually the main scavengers (Song et al. 1996; Nakatani et al. 2004; Zafiriou et al. 1987). The steady-state concentration of $HO^{\bullet}$ shows a large variability in natural waters. Examples of concentration values reported in the literature are $(3.0–8.5) \times 10^{-16}$ M in rivers (Brezonik and Fulkerson-Brekken 1998; Arakaki et al. 1999b; Nakatani et al. 2004), $(9.41 \pm 0.12) \times 10^{-17}$ M to $(1.72 \pm 0.01) \times 10^{-16}$ M in estuarine waters (al Housari et al. 2010), 12×10^{-18} M in coastal surface seawater and 1.1×10^{-18} M in the open ocean (Mopper and Zhou 1990). In Antarctic waters the steady-state concentrations have been determined as 4.3×10^{-19} M in coastal waters and 2.6×10^{-19} M in the open ocean (Qian et al. 2001). Elevated $HO^{\bullet}$ concentration values (from 6.7×10^{-15} to 4.0×10^{-12} M) have been described in surface stream waters contaminated with acidic mine drainage (AMD). These waters have pH ~2.1–3.4, are highly rich of iron (6–1203 mg L^{-1}) and have a high concentration of NO_3^- (5.9×10^{-6}–5.8×10^{-3} M) (Allen et al. 1996). The reported data suggest that the steady-state concentration of $HO^{\bullet}$ can be very variable in different water systems. A major caveat that should be considered while comparing different studies is that the irradiation conditions are usually unequal, which accounts for at least part of the variability. However, variations in the steady-state $HO^{\bullet}$ concentration have also been observed with waters of different origin under the same irradiation conditions. The major factors that account for the variation of the steady-state concentration of $HO^{\bullet}$ in the aquatic environments are: (i) presence of elevated concentrations of NO_2^- and NO_3^- ions; (ii) presence of the elevated amounts of Fe^{3+}-containing complexes; (iii) occurrence of photo Fenton-type reactions that take place between H_2O_2 and reduced transition metal ions; (iv) amount and nature of the dissolved organic matter (DOM).

The reciprocal of the consumption rate constant allows the assessment of the life-time of $HO^{\bullet}$, which is $(2.6–6.0) \times 10^{-6}$ s in river, dew and cloud water (Arakaki and Faust 1998; Arakaki et al. 1999b; Nakatani et al. 2004) and several times higher ($3.0–66.0 \times 10^{-6}$ s) in remote polluted clouds, as estimated from a modeling study (Jakob 1986).

2.4 An HPLC Method for Measuring $HO^{\bullet}$ in Irradiated Natural Waters, Based on Benzene as Probe Molecule

This section reports a detailed description of a possible method that can be adopted for the determination of $HO^{\bullet}$, based on benzene as a probe. The description is very detailed to enable the reader easily reproducing a similar experimental set-up. Note that other probe molecules can also be used for $HO^{\bullet}$ determination, e.g. cumene (isopropylbenzene), pyridine and terephthalic acid (Mill et al. 1980;

Fang et al. 1996). Other substrates, such as benzoic acid and nitrobenzene are less suitable as $HO^{\bullet}$ probe molecules (Vione et al. 2010). The photoinduced generation of $HO^{\bullet}$ can be quantitatively determined by measuring the phenol (Eq. 2.1) that is produced photolytically from benzene + $HO^{\bullet}$, when natural waters under illumination are added with benzene. For irradiation it is possible to adopt a quartz cell under a Xe lamp or sunlight (Takeda et al. 2004; Mostofa KMG and Sakugawa H, unpublished data). Note that the light of a xenon lamp should be equipped with special glass filters to filter out the radiation below 300 nm, if one wants to simulate sunlight irradiation.

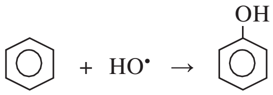

(2.1)

The phenol concentration can be determined by a HPLC method.

Experimental Details

The benzene solutions (e.g. a ~1 mM stock solution) should be prepared by benzene addition to water, followed by gentle shaking. The solution should be kept for 24-h under dark conditions to mix up benzene well with the water sample. The light intensity of the artificial Xe lamp or sunlight can be determined by measuring the photo-degradation rate of 8-μM standard aqueous solution of 2-nitrobenzaldehyde (2-NB) after illumination in a quartz cell (e.g. 60 mL). The illumination time of 2-NB should usually be kept short, e.g. up to 5 min for an irradiation intensity comparable to that of sunlight. In the case of the transformation reaction of benzene into phenol the irradiation time should be longer (up to 10–20 h), except for samples with unusually elevated $HO^{\bullet}$ production rate. 2-NB can be measured by HPLC–UV. Elution can be carried out with a C18 reverse-phase column. Upon adoption of $H_2O:CH_3CN = 40:60$ as isocratic eluent at a flow rate of 1 ml min^{-1}, if one employs a (5 μm, 4.6 × 250 mm) column the retention time of 2-NB could be something around 5 min. The recommended detection wavelength is 260 nm. It is also recommended to remove the air from the eluent before use, by 20–30 min sonication or by magnetic stirring under vacuum.

Phenol can be determined under the same elution conditions, setting the UV detection wavelength at 210 nm or adopting a fluorescence detector. In the latter case, recommended wavelengths are 270 nm for excitation and 297 nm for emission.

Calculations: The concentration of phenol that are produced can be estimated by comparison with a standard. The photo-formation rate of $HO^{\bullet}$ (r_{HO}) can be calculated from Eq. 2.2 (Takeda et al. 2004; Nakataniet al. 2004):

$$r_{\mathrm{HO}} = \frac{r_p}{F_{B,HO} \times Y_P} \qquad (2.2)$$

where r_P is the photo-formation rate of phenol obtained experimentally (M s^{-1}), $F_{B,HO}$ is the fraction of HO radicals that react with benzene [i.e., $k_{HO/Ph} \times C_{HO} \times C_{Ph}/(k_{HO/Ph} \times C_{HO} \times C_{Ph} + \sum k_i\ C_{HO}\ C_i)$, where i is scavenger], and Y_P is the yield of phenol formed per benzene oxidized by $HO^{\bullet}$. It is $Y_P = 0.75 \pm 0.07$ in natural waters (Arakaki and Faust 1998). The $F_{B,OH}$ values are much variable for a variety of natural waters, also depending on the concentration of added benzene and on the amount of the natural $HO^{\bullet}$ scavengers. For addition of 1.2 mM benzene it has been found $F_{B,HO} = 0.94$ for cloud waters (Arakaki and Faust 1998), 0.92 and 0.99 for rivers, and 0.68 for seawaters (Takeda et al. 2004). The high values of $F_{B,HO}$ in rivers and cloud suggest that most of the HO radicals formed photolytically reacts with benzene. In contrast, the low value in seawater samples suggests the 32–34 % of photolytically formed HO radicals reacts with various scavengers of HO radical other than benzene. There are many scavengers, DOM components, HCO_3^-, CO_3^{2-}, NO_2^-, halides (X^-, but chloride only in acidic medium) etc. that can interact with $HO^{\bullet}$ in aqueous solution (Zafiriou 1974; Mopper and Zhou 1990; Vione et al. 2006; Zepp et al. 1987; Voelker and Sulzberger 1996; Minakata et al. 2009). In seawater, the bromide ion (Br^-) alone scavenges approximately 93 % of photo-generated $HO^{\bullet}$ (Mopper and Zhou 1990).

To mathematically derive the terms in Eq. 2.2 for any added benzene concentration, one requires a kinetic model where the scavengers and benzene simultaneously react with photogenerated $HO^{\bullet}$ at the rates R_{SC} and R_B, respectively (Takeda et al. 2004). Under the steady-state condition, the formation rate of $HO^{\bullet}$ is equal to the consumption rate as follows (Takeda et al. 2004):

$$r_{HO} = r_{SC} + r_B \tag{2.3}$$

$$r_{SC} = k_{SC}[SC][HO]_{SS} = k'_{SC}[HO]_{SS} \tag{2.4}$$

$$r_S = k_B[B][HO]_{SS} \tag{2.5}$$

where k_{SC} is the reaction rate constant of HO radicals with various scavengers in the water sample, $k'_{SC} = k_{SC}\ [SC]$ is the apparent scavenging rate constant of the HO radical, k_B is the reaction rate constant of $HO^{\bullet}$ with benzene (i.e., 7.8×10^9 M^{-1} s^{-1}), [B] is the concentration of benzene added to the water sample (e.g. ~1 mM), and $[HO]_{SS}$ is the steady-state concentration of $HO^{\bullet}$. Under conditions where benzene is in excess (i.e., $r_B >> r_{SC}$), most of the photo-generated $HO^{\bullet}$ react with benzene, thus $F_{B,HO} \approx 1$. In contrast, in the most general case it is:

$$F_{B,HO} = \frac{r_B}{r_B + R_{SC}} = \frac{[B]}{[B] + k'_{SC}/k_B} \tag{2.6}$$

From Eqs. 2.3–2.6, the phenol formation rate (r_P) can be expressed as:

$$\frac{1}{r_P} = \frac{1}{r_{HO} + Y_P} + \frac{[k'_{sc}]}{r_{HO} + Y_P \times k_B[B]} \tag{2.7}$$

According to Eq. 2.7, the plot of $1/r_P$ versus $1/[B]$ should be straight line (Takeda et al. 2004) and k'_{SC}/k_B can be calculated from the slope and intercept of the plot. Thus, $F_{B,HO}$ can be calculated with Eq. 2.6 using the values of k'_{SC}/k_B and $[B]$.

2.5 *Levels of Photoinduced Generation of HO$^\bullet$ in Natural Waters*

The production rates of HO$^\bullet$ that have been estimated in a variety of waters, in the presence of standard chemical species (NO_2^-, NO_3^- and H_2O_2) or of standard organic substances under sunlight are summarized in Table 2 (Mopper and Zhou 1990; Takeda et al. 2004; Zepp et al. 1987; Haag and Hoigné 1985; White et al. 2003; Arakaki and Faust 1998; Nakatani et al. 2007; Mostofa KMG and Sakugawa H, unpublished data; Nakatani et al. 2004; Qian et al. 2001; Allen et al. 1996; Mabury 1993; Grannas et al. 2006; Anastasio and Newberg 2007). The rates are typically varied in a range from 10^{-7} to 10^{-10} M s^{-1} in aqueous solution (Table 2). Production rates in rivers are (0.6–7.5) × 10^{-11} M s^{-1} in upstream waters, (0.4–7.4) × 10^{-8} M s^{-1} in upstream waters contaminated with AMD, (1.0–2.9) × 10^{-11} M s^{-1} in non-polluted river waters, 2.4 × 10^{-11} M s^{-1} in Ogeechee River, (2.0–6.0) × 10^{-10} M s^{-1} in Wetland on Lake Erie and Artificial Agricultural wetland, 6.4 × 10^{-11} M s^{-1} in Rice field water, (2.0–17.0) × 10^{-10} M s^{-1} in Satilla River and Pine Barrens that have iron-rich waters (Table 2). It is noticeable that the production rates of HO$^\bullet$ are higher by two to five orders of magnitude in stream waters contaminated with AMD (Allen et al. 1996) than in typical river waters. Such an effect might be caused by the photo-Fenton reaction that is considerably favored in the presence of elevated iron contents (Allen et al. 1996; McKnight et al. 1988). Similarly, high production rates of HO$^\bullet$ have been observed in Satilla River water (White et al. 2003), where more than 70 % of the total HO$^\bullet$ production is accounted for by the photo-Fenton reaction. Therefore, the latter process is expected to be the main contributor to HO$^\bullet$ photo-production in iron-rich waters. In contrast, upstream waters mainly contain DOM components (mostly fulvic and humic acids) that are the major contributors to HO$^\bullet$ photo-production in these systems. A possible pathway that yields HO$^\bullet$ from DOM is the photoinduced formation of H_2O_2 (Eqs. 3.13–3.18, see chapter "Photoinduced and Microbial Generation of Hydrogen Peroxide and Organic Peroxides in Natural Waters"), which could induce the photo-Fenton reaction in the presence of Fe or produce HO$^\bullet$ by direct photolysis (Nakatani et al. 2007; Mostofa KMG and Sakugawa H, unpublished data). An alternative explanation for the production of HO$^\bullet$ from DOM is the oxidation of water by the excited triplet states (^{3}DOM*) (Brigante et al. 2010).

In lake water the production rates of HO$^\bullet$ are very variable, ranging from 1.8 × 10^{-13} to 4.6 × 10^{-11} M s^{-1} (Table 2). The HO$^\bullet$ photo-production depends on the irradiation wavelength. For instance, the formation rate of HO$^\bullet$ observed on extracted lake DOM under sunlight is higher [(1.6–1.8) × 10^{-10} Ms^{-1} at 308 nm]

Table 2 Production rates of hydroxyl radical ($HO^{\bullet}$) reported from natural waters, standard nitrite (NO_2^-) nitrate (NO_3^-) and various standard organic substances

Type of samples/substances	Sample	Source of light/ wavelength (nm)	Production rate of $HO^{\bullet} \times 10^{-11}$ (Ms^{-1})	References
Rivers				
Stream, contaminated with acid mine drainage	Freshwater-polluted	Sunlight	400–7,400	Allen et al. (1996)
Kurose River (upstream): 1 site	Freshwater	Xe lamp[b]	1.8	Takeda et al. (2004)
Kurose River (downstream regions): 7 sites	Freshwater-sewage polluted	Xe lamp[b]	17–89	Takeda et al. (2004)
Ohta River (upstream regions): 4 sites	Freshwater	Xe lamp[b]	0.6–1.1	Takeda et al. (2004)
Ohta River (downstream regions): 4 sites	Freshwater	Xe lamp[b]	1.0–2.6	Takeda et al. (2004)
Kurose River (upstream regions): 2 sites	Freshwater	Xe lamp[b]	7.0–0.5	Nakatani et al. (2004)
Kurose River (downstream): 2 sites	Freshwater-sewage polluted	Xe lamp[b]	17–33	Nakatani et al. (2007)
River waters: upstream & downstream: 33 sites	Freshwater-sewage polluted	Xe lamp[b]	0.78–530	Nakatani et al. (2007)
Kurose River (upstream regions): 2 sites	Freshwater	Xe lamp[b]	0.9–2.5	Mostofa KMG and Sakugawa H (unpublished data)[a]
Kurose River (downstream regions): 4 sites	Freshwater-sewage polluted	Xe lamp[b]	8.0–570	Mostofa KMG and Sakugawa H (unpublished data)[a]
Ohta River (upstream regions): 3 sites	Freshwater	Xe lamp[b]	1.3–1.8	Mostofa KMG and Sakugawa H (unpublished data)[a]
Ohta River (downstream regions): 3 sites	Freshwater	Xe lamp[b]	1.7–2.9	Mostofa KMG and Sakugawa H (unpublished data)[a]
Ogeechee River	Freshwater	Xe lamp[b]	24.0	White et al. (2003)
Satilla River	Freshwater	Xe lamp[b]	45.0	White et al. (2003)
Satilla River (bleached)	Freshwater	Xe lamp[b]	20.0	White et al. (2003)
Pine Barrens	Freshwater	Xe lamp[b]	170.0	White et al. (2003)
Wetland on Lake Erie	Freshwater	Xe lamp[b]	20–26	White et al. (2003)
Artificial agricultural wetland	Freshwater	Xe lamp[b]	23.0	White et al. (2003)
Rice Field water	Freshwater	Xe lamp[b]	64.0	Mabury (1993)

(continued)

Table 2 (continued)

Type of samples/substances	Sample	Source of light/ wavelength (nm)	Production rate of $HO^\bullet \times 10^{-11}$ (Ms^{-1})	References
Lakes				
Lake Greifensee, Switzerland	Freshwater	Xe lamp^b	1.0	Haag and Hoigné (1985)
Lake Greifensee, Switzerland	Freshwater	Xe lamp^b	2.5	Zepp et al. (1987)
Clear Lake	Freshwater	Xe lamp^b	4.6	Mabury (1993)
Lake Tahoe	Freshwater	Xe lamp^b	2.2	Mabury (1993)
Nitrate-rich shallow water body	Freshwater	Xe lamp^b	0.018	Zepp et al. (1987)
DOM extracted-XAD, Toolik Lake	Freshwater	308 nm	18	Grannas et al. (2006)
DOM extracted-XAD, Toolik Lake	Freshwater	330 nm	8.1	Grannas et al. (2006)
DOM extracted-XAD, Toolik Lake	Freshwater	355 nm	5.6	Grannas et al. (2006)
DOM extracted-C-18, Toolik Lake	Freshwater	308 nm	18	Grannas et al. (2006)
DOM extracted-C-18, Toolik Lake	Freshwater	330 nm	6.4	Grannas et al. (2006)
DOM extracted-C-18, Toolik Lake	Freshwater	355 nm	6.1	Grannas et al. (2006)
DOM extracted-UF, Toolik Lake	Freshwater	308 nm	16	Grannas et al. (2006)
DOM extracted-UF, Toolik Lake	Freshwater	330 nm	8.1	Grannas et al. (2006)
DOM extracted-UF, Toolik Lake	Freshwater	355 nm	4.7	Grannas et al. (2006)
Seawaters				
Everglades	Seawater	Sunlight	42.0	Mopper and Zhou (1990)
Biscayne Bay	Seawater	Sunlight	2.9	Mopper and Zhou (1990)
Vineyard Sound	Seawater	Sunlight	2.7	Mopper and Zhou (1990)
Mississippi River Plume	Seawater	Xe lamp^b	6.2	White et al. (2003)
Florida Keys	Seawater	Xe lamp^b	0.43	White et al. (2003)
Seto Inland Sea: 0 m depth	Seawater	Xe lamp^b	1.5	Takeda et al. (2004)
Seto Inland Sea: 5 m depth	Seawater	Xe lamp^b	0.57	Takeda et al. (2004)

(continued)

Table 2 (continued)

Type of samples/substances	Sample	Source of light/ wavelength (nm)	Production rate of $HO^{\bullet} \times 10^{-11}$ (Ms^{-1})	References
Seto Inland Sea: 10 m depth	Seawater	Xe lamp[b]	0.91	Takeda et al. (2004)
Seto Inland Sea: 15 m depth	Seawater	Xe lamp[b]	1.0	Takeda et al. (2004)
Seto Inland Sea: 20 m depth	Seawater	Xe lamp[b]	2.4	Takeda et al. (2004)
Seto Inland Sea: 30 m depth	Seawater	Xe lamp[b]	4.9	Takeda et al. (2004)
Yellow Sea: 0 m depth	Seawater	Xe lamp[b]	0.39	Takeda et al. (2004)
Yellow Sea: 20 m depth	Seawater	Xe lamp[b]	0.36	Takeda et al. (2004)
Yellow Sea: 30 m depth	Seawater	Xe lamp[b]	0.49	Takeda et al. (2004)
Yellow Sea: 40 m depth	Seawater	Xe lamp[b]	0.82	Takeda et al. (2004)
Yellow Sea: 50 m depth	Seawater	Xe lamp[b]	0.73	Takeda et al. (2004)
Yellow Sea: 60 m depth	Seawater	Xe lamp[b]	0.72	Takeda et al. (2004)
Gulf Stream	Seawater	Sunlight	0.31	Mopper and Zhou (1990)
Sargasso Sea	Seawater	Sunlight	0.28	Mopper and Zhou (1990)
Weddel Sea, Antarctic	Seawater	Sunlight	0.10	Qian et al. (2001)
Crystal Sound, Antarctic	Seawater	Sunlight	0.10	Qian et al. (2001)
Paradise Harbor, Antarctic	Seawater	Sunlight	0.01	Qian et al. (2001)
Standard substances				
NO_2^-	Seawater	Sunlight	2.30	Mopper and Zhou (1990)
NO_2^-	Milli-Q water	Sunlight	2.80	Arakaki and Faust (1998)
NO_2^-	Milli-Q water	Sunlight	2.30	Takeda et al. (2004)
NO_2^-	Milli-Q water	Xe lamp[b]	2.20	Mostofa KMG and Sakugawa H (unpublished data)[a]
NO_3^-	Fresh water	Sunlight	0.03	Zepp et al. (1987)
NO_3^-	Seawater	Sunlight	0.03	Mopper and Zhou (1990)
NO_3^-	Milli-Q water	Sunlight	0.02	Arakaki and Faust (1998)
NO_3^-	Milli-Q water	Sunlight	0.02	Takeda et al. (2004)

(continued)

Table 2 (continued)

Type of samples/substances	Sample	Source of light/ wavelength (nm)	Production rate of HO$^{\bullet}$ × 10^{-11} (Ms^{-1})	References
NO_3^-	Milli-Q water	Xe lamp[b]	0.01	Mostofa KMG and Sakugawa H (unpublished data)[a]
Suwannee River Fulvic Acid (SRFA)	Milli-Q water	Xe lamp[b]	1.20	Mostofa KMG and Sakugawa H (unpublished data)[a]
SRFA	Milli-Q water	Xe lamp[b]	6.00	White et al. (2003)
Tryptophan	Milli-Q water	Xe lamp[b]	1.70	Mostofa KMG and Sakugawa H (unpublished data)[a]
Suwannee River Humic Acid (SRHA)	Milli-Q water	Xe lamp[b]	1.10	Mostofa KMG and Sakugawa H (unpublished data)[a]
Phenylalanine	Milli-Q water	Xe lamp[b]	0.40	Mostofa KMG and Sakugawa H (unpublished data)[a]
DAS1	Milli-Q water	Xe lamp[b]	0.31	Mostofa KMG and Sakugawa H (unpublished data)[a]
DSBP	Milli-Q water	Xe lamp[b]	0.30	Mostofa KMG and Sakugawa H (unpublished data)[a]
H_2O_2	Milli-Q water	Xe lamp[b]	0.26	Mostofa KMG and Sakugawa H (unpublished data)[a]
Peracetic acid	Milli-Q water	Xe lamp[b]	0.25	Mostofa KMG and Sakugawa H (unpublished data)[a]
Sea-salt particulate matter, extracted from coastal waters	Seawater	summer, midday, sunlight	~2778–27778	Anastasio and Newberg (2007)

[a] Production rates (Mostofa and Sakugawa) calculated for initial 60 min irradiation and normalized to sunlight intensity (noon time) using 2 nitro benzaldehyde solution (8 mM) at the Campus of Hiroshima University, Japan as well as the rates for standard substances mentioned here is calculated after deduction of rate of MQ water

Rates for standard organic substances adjusted for 1 mg L^{-1} of each substances

[b] Xe light intensity is normalized to sunlight intensity

for shorter wavelength than for longer one [(4.7–6.1) × 10^{-11} Ms^{-1} at 355 nm] in a variety of lake waters (Table 2) (Grannas et al. 2006). Thus, the production of $HO^{\bullet}$ greatly depends on the light wavelength.

In seawater, the $HO^{\bullet}$ production rate is higher [(4.3–42.0) × 10^{-12} M s^{-1}] in coastal waters than in the open ocean [(2.8–3.1) × 10^{-12} M s^{-1}], and it is very low [(1.04–10.3) × 10^{-13} M s^{-1}] in Antarctic waters (Table 2). The production rates of $HO^{\bullet}$ are lower in surface seawater and gradually increase with increasing depth (Takeda et al. 2004; Zafiriou and Dister 1991). For example, the production rate of $HO^{\bullet}$ is (5.7–15.0) × 10^{-12} M s^{-1} at 0–20 m depth, 4.9 × 10^{-11} M s^{-1} at 30 m, and 7.2 × 10^{-11} M s^{-1} at 60 m in Seto Inland Sea and the Yellow Sea (Takeda et al. 2004), obviously under the same irradiation conditions that is not the case of the real environment. The lower production rates at the surface compared to the deeper layers may be caused by the fact that the natural solar radiation is active in surface waters where it produces $HO^{\bullet}$ and other reactive transients. These species can lead to the photo-degradation of DOM (e.g. photo-bleaching that reduces the ability of DOM to absorb sunlight), a process to which the direct photolysis could also contribute. Therefore, the sources of $HO^{\bullet}$ in surface waters can be reduced, e.g. by decreasing the concentration of NO_2^- and the capability of DOM to photo-generate $HO^{\bullet}$. The intensity of solar radiation that reaches the deeper layers is quite limited. Therefore, the deep water has the double feature of generating the highest potentiality to produce $HO^{\bullet}$, but also of being involved to a very limited extent into $HO^{\bullet}$ photo-production in the real natural environment. An important exception could be represented by the sites where the deep oceanic water emerges to the surface.

Studies observe that the sea-salt particulate matter (SS PM) extracted from coastal seawaters can demonstrate substantially high $HO^{\bullet}$ production (rate: ~2778–27778 M s^{-1}), approximately 3–4 orders of magnitude greater than $HO^{\bullet}$ photoformation rates in surface seawater (Anastasio and Newberg 2007). The results show that photolysis of nitrate is a dominant source of $HO^{\bullet}$ (on average 59±25 %) in the SS PM whilst other source is presumably considered the organic compounds. The fact behind the other phenomenon is that irradiated organic compounds or DOM can induce photoinduced production of H_2O_2 that is a $HO^{\bullet}$ source via photolysis or the Fenton reaction, and the photoinduced generation of H_2O_2 is enhanced by salinity. Salinity or NaCl solutions are capable of generating high production of aqueous electrons (e_{aq}^-) photolytically in aqueous media (Gopinathan et al. 1972; Assel et al. 1998) that may enhance the H_2O_2 production from DOM components in waters (Mostofa and Sakugawa 2009; Moore et al. 1993) (see also chapter "Photoinduced and Microbial Generation of Hydrogen Peroxide and Organic Peroxides in Natural Waters"). In fact, photogeneration of H_2O_2 from river DOM was substantially increased with salinity, from 15 to 368 nM h^{-1} at circumneutral pH that may enhance the H_2O_2 production from DOM components in waters (Osburn et al. 2009). Salinity effect on irradiated CDOM might be another most important source of high photoproduction of $HO^{\bullet}$ in sea-salt particulate matter in seawaters.

3 Mechanisms for Photoinduced Generation of HO• in Natural Waters

The photoinduced generation of HO• significantly depends on several important factors such as the presence of NO_2^- and NO_3^- and their concentration, the chemical nature of DOM and its quantity, and finally the total content of Fe. The most important mechanisms for HO• formation in natural waters are discussed below.

3.1 In situ Generation of HO• from DOM

One of the main HO• sources in natural waters (Table 2) (Vione et al. 2006; Mostofa KMG and Sakugawa H, unpublished data) is the photoinduced generation of HO• from DOM components (either Fluorescent Dissolved Organic Matter-FDOM or Colored Dissolved Organic Matter-CDOM). This process can be accounted for either by the oxidation of water by the triplet states $^3DOM^*$, or by the generation of H_2O_2 upon DOM irradiation (reaction 3.1) and its detailed mechanisms are discussed in earlier chapter (see chapter "Photoinduced and Microbial Generation of Hydrogen Peroxide and Organic Peroxides in Natural Waters"). In the latter case, HO• could be produced upon photolysis of H_2O_2 (Eq. 3.2) (Legrini et al. 1993; von Sonntag et al. 1993).

$$DOM + O_2 + H_2O + H^+ \xrightarrow{h\upsilon} H_2O_2 + DOM^{\bullet +} + O_2 + HO^- \tag{3.1}$$

$$H_2O_2 \xrightarrow{h\upsilon} 2HO^{\bullet} \tag{3.2}$$

The quantum yield of reaction 3.2 has been determined as 0.5 under UVC irradiation (Legrini et al. 1993; von Sonntag et al. 1993). The quantum yield varies with wavelength, but it also depends on the band that absorbs radiation. In the case of H_2O_2, the same band is responsible for radiation absorption and photolysis in both the UVC and UVB regions. The hypothesis that the formation of HO• by irradiated DOM is accounted for by H_2O_2 photoproduction. It is consistent with the observed, gradual and parallel increase of H_2O_2 concentration and of phenol formation from benzene, upon irradiation of natural river waters and of relevant standard organic substances (Fig. 2). A similar, parallel trend of both phenol (its formation being used as HO• probe) and H_2O_2 has been observed upon irradiation of upstream DOM mostly containing fulvic acid (Fig. 2a), of standard Suwannee River Fulvic Acid (SRFA) (Fig. 2c) and of diaminostilbene type (DAS1) (Fig. 2d). The same trend has not been observed in sewage polluted river waters (Fig. 2b), which might be the effect of additional production from other HO• sources such as the NO_2^- and NO_3^- ions, present in high amount (Takeda

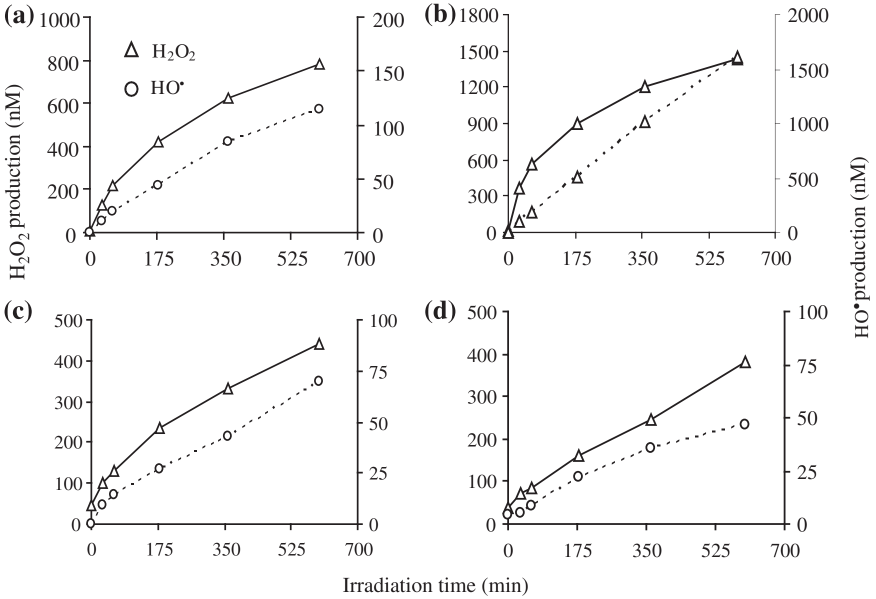

Fig. 2 In-situ generation of H_2O_2 and $HO^\bullet$ for river waters and standard organic substances during the 10 h of irradiation period in photoexperiments conducted using a solar simulator. Upstream DOM having mostly fulvic acid (**a**); polluted river waters, mostly affected by mixture of sewage effluents and upstream DOM (**b**); standard Suwannee River Fulvic Acid (**c**); and standard diaminostilbene (DAS1) (**d**). *Data source* Mostofa KMG and Sakugawa H (unpublished data)

et al. 2004; Mostofa KMG and Sakugawa H, unpublished data; Nakatani et al. 2004). Therefore, the generation of H_2O_2 by DOM could account for most of the production of $HO^\bullet$ by unpolluted water samples, with a relatively elevated content of fulvic acid in DOM (Fig. 3) and a relatively low concentration of other $HO^\bullet$ sources, such as nitrate, nitrite and Fe.

3.2 Direct Photolysis of Nitrate and Nitrite

The direct photolysis of nitrite and nitrate induces $HO^\bullet$ photoproduction (Zafiriou and True 1979a, b; Takeda et al. 2004; Zepp et al. 1987; Mack and Bolton 1999). There is evidence that irradiation in the 200–400 nm wavelength region can convert NO_2^- into $NO^\bullet$ and $O^{\bullet-}$ (Eqs. 3.3, 3.4) (Zepp et al. 1987; Mack and Bolton 1999):

$$NO_2^- + h\upsilon \rightarrow [NO_2^-]^* \qquad (3.3)$$

$$[NO_2^-]^* \rightarrow NO^\bullet + O^{\bullet-} \qquad (3.4)$$

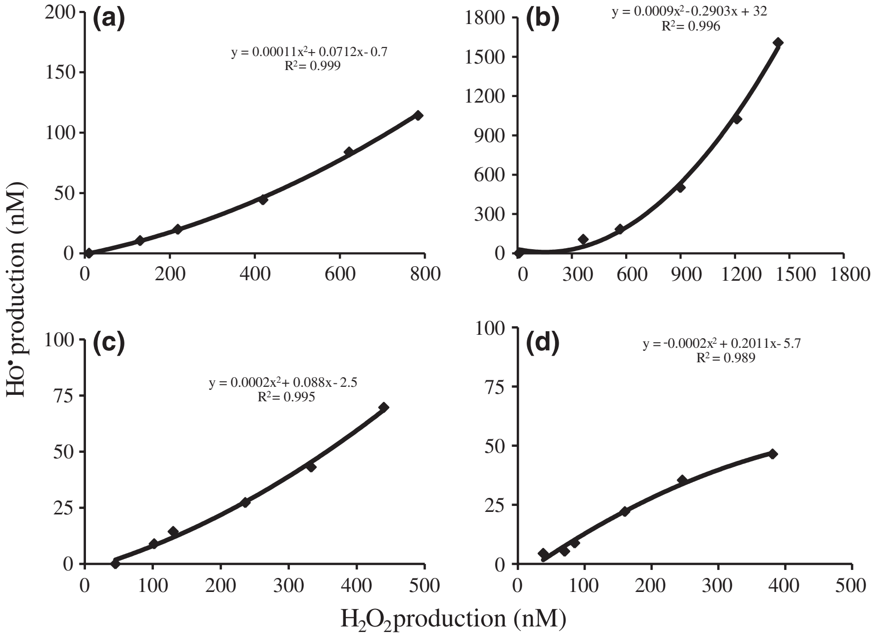

Fig. 3 Relationship between H_2O_2 and $HO^\bullet$ in situ produced from river waters and standard organic substance during the 10 h of irradiation period in photoexperiments conducted using a solar simulator. The relationships of the (**a**, **b**, **c** and **d**) are the same samples of Fig. 1. *Data source* Mostofa KMG and Sakugawa H (unpublished data)

At pH < 12 in aqueous solution, $O^{\bullet -}$ is protonated to form $HO^\bullet$:

$$O^{\bullet -} + H_2O \underset{k_{-3.5}}{\overset{k_{3.5}}{\rightleftharpoons}} HO^\bullet + HO^- \tag{3.5}$$

where $k_{3.5} = 1.7 \times 10^6\ M^{-1}\ s^{-1}$ for the $HO^\bullet$ formation reaction and $k_{-3.5} = 1.2 \times 10^{10}\ M^{-1}\ s^{-1}$ for the reverse reaction. The radical $HO^\bullet$ can significantly recombine with $NO^\bullet$ and $NO_2{}^{—}$; such reactions are very fast (diffusion-controlled) in aqueous media (Mack and Bolton 1999):

$$HO^\bullet + NO^\bullet \rightarrow HNO_2 \tag{3.6}$$

where $k_{3.6} = 1.0 \times 10^6\ M^{-1}\ s^{-1}$.

$$HO^\cdot + NO_2^- \rightarrow NO_2{}^\cdot + OH^- \tag{3.7}$$

where $k_{3.7} = 1.0 \times 10^{10}\ M^{-1}\ s^{-1}$. These reactions can limit the steady-state concentration of $HO^\bullet$ and, therefore, the ability of the hydroxyl radical to take part in photooxidation reactions of organic compounds in natural waters. Note, however, that the main $HO^\bullet$ scavengers are DOM in freshwater and bromide in seawater (Takeda et al. 2004).

As far as NO_3^- photolysis is concerned (Eq. 3.8), the process can be expressed as follows (Zepp et al. 1987; Mack and Bolton 1999):

$$NO_3^- + h\upsilon \rightarrow NO_2^- + 1/2O_2 \tag{3.8}$$

This stoichiometry can be followed in the absence of $HO^\bullet$ scavengers, over the entire pH range and at irradiation wavelength around 200 nm (Shuali et al. 1969; Wagner et al. 1980). However, irradiation above 280 nm results into two primary photoinduced pathways (Zepp et al. 1987; Mack and Bolton 1999):

$$NO_3^- + h\upsilon \rightarrow [NO_3^-]^* \tag{3.9}$$

$$[NO_3^-]^* \rightarrow NO_2^- + O(^3P) \tag{3.10}$$

$$[NO_3^-]^* \rightarrow NO_2^\bullet + O^{\bullet -} \xrightarrow{H_2O} HO^\bullet + HO^- + NO_2^\bullet \tag{3.11}$$

In this mechanism, NO_3^- absorbs a UVB photon yielding an excited state, $[NO_3^-]^*$ (Eq. 3.9), which undergoes disintegration following two pathways: the first one produces the nitrite ion (NO_2^-) and atomic oxygen, $O(^3P)$ (Eq. 3.10). The second pathway produces nitrogen dioxide ($NO_2^\bullet$) and $O^{\bullet -}$. The latter is rapidly protonated to form $HO^\bullet$ (Eq. 3.11). The formation of NO_2^- in Eq. 3.10 can be followed by nitrite photolysis to give $HO^\bullet$, as shown in (Eqs. 3.3–3.5). It can be noted that $HO^\bullet$ is a strong oxidant that can react with DOM more quickly than does atomic oxygen, $O(^3P)$. Indeed, the main fate of $O(^3P)$ (Eq. 3.4) would be the reaction with oxygen to form ozone, which is rapidly consumed in natural waters by reaction with NO_2^- or decomposition to $HO^\bullet$ (Zepp et al. 1987).

3 $HO^\bullet$ Production from the Fenton Reaction

The ferrous ions (Fe^{2+}) catalyzes the formation of $HO^\bullet$ in the presence of H_2O_2 (Fenton 1894). An aqueous solution of H_2O_2 and ferrous or ferric salts is termed as Fenton's reagent. The oxidation efficiency of the Fenton reaction is the highest at pH values ranging from 2 to 5 and at a 1:1 molar ratio of H_2O_2 and Fe^{2+} (Walling 1975). The reactivity of the Fenton's reagent is the effect of the generation of $HO^\bullet$ in the reaction media (Haber and Weiss 1934). The mechanism for the chain Fenton reaction was initially depicted as follows (Eqs. 3.12–3.16) (Barb et al. 1951):

$$Fe^{2+} + H_2O_2 \rightarrow Fe^{3+} + HO^\bullet + HO^- \tag{3.12}$$

$$Fe^{2+} + HO^{\bullet} \rightarrow Fe^{3+} + HO^{-} \tag{3.13}$$

$$HO^{\bullet} + H_2O_2 \rightarrow HO_2^{\bullet} + H_2O \tag{3.14}$$

$$Fe^{2+} + HO_2^{\bullet} \rightarrow Fe^{3+} + HO_2^{\bullet -} \tag{3.15}$$

$$Fe^{3+} + O^{2-} \rightarrow Fe^{2+} + O_2 \tag{3.16}$$

Recently, the reaction rate constants of the Fenton system have been measured at various pH values, an issue that will be discussed later (Kwan and Voelker 2002; Duesterberg et al. 2008). At low $[H_2O_2]/[Fe^{2+}]$ ratios in both reactions (3.12) and (3.13), only the reactions are important, and the overall process is second-order with respect to the reactants. At high $[H_2O_2]/[Fe^{2+}]$ ratios, there is also an important contribution from the competitive reactions (3.15, 3.16) (Rush and Bielski 1985). The earlier studies have examined the Fenton reaction at low pH (<1.0) with the reactants at mM levels. The production of $HO^{\bullet}$ from $Fe^{2+} + H_2O_2$ is also important in AOTs, as it allows the use of transition metals to catalyze the oxidation of organic compounds.

Recent studies demonstrate that the formation of $HO^{\bullet}$ increases linearly with the H_2O_2 concentration (Lindsey and Tarr 2000). Experiments carried out using ESR spin trapping together with water labeled with ^{17}O suggest that $HO^{\bullet}$ is derived exclusively from hydrogen peroxide, and that there is no exchange of oxygen atoms between H_2O_2 and the water solvent (Lloyd et al. 1997). It has been demonstrated that fulvic and humic acid reduce the $HO^{\bullet}$ formation in the Fenton reaction under most conditions, but fulvic acid increases $HO^{\bullet}$ formation at certain pH values (Lindsey and Tarr 2000; Voelker and Sulzberger 1996). Fulvic acid can inhibit the degradation of dissolved aromatic compounds (e.g. phenol, fluorene and phenanthrene) by the Fenton reagent in aqueous solution (Lindsey and Tarr 2000). Accordingly, natural organic matter could inhibit the remediation of pollutants by the Fenton process in water and soil environments. However, it has also been shown that humic acids are able to enhance the degradation of phenol in the second step of the Fenton process. Indeed, after the reaction between Fe^{2+} and H_2O_2 is completed, further degradation of the organic substrate can be directed by the reduction of Fe(III) to Fe^{2+}. The latter process is enhanced by humic substances (Vione et al. 2004).

Indeed, the ferric ion (Fe^{3+}) catalyzes the decomposition of H_2O_2 into $HO^{\bullet}$ and Fe^{2+} ($Fe^{3+} + H_2O_2 \rightarrow Fe^{2+} + HO_2^{\bullet} + H^{+}$) (Barb et al. 1951; Walling and Weil 1974; Lee et al. 2003; Lee and Sedlak 2009). The rate of the Fenton process is greatly enhanced when the temperature is raised from 10 to 50 °C, because of the high activation energy (≈126 kJ mol^{-1}) of the reaction (Lee et al. 2003). A high production of Fe^{2+} causes a correspondingly high production of $HO^{\bullet}$ in the reaction system (Eq. 3.12).

The effective catalytic oxidation of organic compounds by the system Fe^{3+}/H_2O_2 is usually limited to the acidic pH region, because of the low solubility of Fe^{3+} and of the low efficiency of the oxidant generation at neutral pH values (Lee and Sedlak 2009). The addition of polyoxometalate ions (POM) greatly increases the yield of oxidant species in the reaction. Under acidic conditions, POM can mediate the electron transfer from nanoparticle zerovalent iron or Fe(II) to oxygen, thereby increasing the production of H_2O_2. The latter is subsequently converted to $HO^{\bullet}$ through the Fenton reaction (Lee et al. 2008).

3.4 *$HO^{\bullet}$ Production from the Photo-Fenton Reaction*

The reactivity of the Fenton's reagent, and in particular of $Fe^{3+} + H_2O_2$ is greatly enhanced by UV/Visible irradiation ($\lambda < 580$ nm), which can for instance increase the extent of mineralization of organic pollutants (Zepp et al. 1992; Voelker et al. 1997; Southworth and Voelker 2003; Nakatani et al. 2007; Vermilyea and Voelker 2009). The photo-Fenton reaction is defined as the reaction of photoproduced Fe^{2+} with H_2O_2 to form the highly reactive $HO^{\bullet}$ (Eqs. 3.17, 3.18). The main chemical reactions occurring in the photo-Fenton system are the following:

$$Fe^{3+} + h\upsilon \rightarrow Fe^{2+} + O_2 + H^+ \tag{3.17}$$

$$Fe^{2+} + H_2O_2 \xrightarrow{h\upsilon} Fe^{3+} + HO^{\bullet} + HO^- \tag{3.18}$$

Irradiation of Fe(III) species causes the production of Fe^{2+} and possibly of $HO^{\bullet}$ (e.g. in the photolysis of the complex $FeOH^{2+}$). In the presence of H_2O_2, further $HO^{\bullet}$ is produced by the Fenton process between H_2O_2 itself and the photogenerated Fe^{2+}. The latter reaction yields again Fe(III), but continuing irradiation may recycle Fe(III) to Fe(II) in the reaction media. Therefore, it is possible to continuously generate $HO^{\bullet}$ under irradiation without any net consumption of Fe(II), which significantly accelerates the overall reaction rate in the photo-Fenton system. The $HO^{\bullet}$ formation in the photo-Fenton system is limited only by the availability of radiation and by the content of H_2O_2 in the reaction medium. The photo-Fenton reaction is observed in open ocean whereas vertical profiles of Fe(II) show maxima consistent with the plume of the iron infusion whilst H_2O_2 profiles demonstrate a corresponding minima showing the effect of oxidation of Fe(II) by H_2O_2 (Croot et al. 2005). Observations also show that the detectable Fe(II) concentrations can exist for up to 8 days after an iron infusion (Croot et al. 2005).

3.5 *$HO^{\bullet}$ Production from Photo-Ferrioxalate/H_2O_2 Reaction*

The photo-ferrioxalate/H_2O_2 reaction is an advanced modification of the photo-Fenton reaction and an effective technique of generating Fe(II) in the reaction media. The addition of oxalate to the photo-Fenton system significantly accelerates the $HO^{\bullet}$ production under UV/visible irradiation ($\lambda < 550$ nm) (Eqs. 3.19–3.25; Table 3) (Hislop and Bolton 1999; Jeong and Yoon 2005;

Table 3 The reaction rate constants for the production of $HO^{\bullet}$ in photo-ferrioxalate/H_2O_2 reaction

Reaction type	Rate constant (k) ($M^{-1}\ s^{-1}$)	Equations	References
$Fe^{III}(C_2O_4)^{3-2n} + h\upsilon \rightarrow Fe^{2+} + (n\text{-}1)C_2O_4^{2-} + C_2O_4^{\bullet -}$	–	3.19	Jeong and Yoon (2005)
$C_2O_4^{\bullet -} \rightarrow CO_2 + CO_2^{\bullet -}$	2×10^{12}	3.20	Mulazzani et al. (1986)
$Fe^{III}(C_2O_4)_n^{3-2n} + CO_2^{\bullet -} \rightarrow CO_2 + Fe^{II}(C_2O_4)_n^{2-2n}$	$\approx 8 \times 10^9$	3.21	Jeong and Yoon (2004)
$CO_2^{\bullet -} + O_2 \rightarrow CO_2 + O_2^{\leftarrow\leftarrow\bullet}$	2.4×10^9	3.22	Hislop and Bolton (1999)
$Fe^{III}(C_2O_4)_n^{3-2n} + O_2^{\bullet -} \rightarrow O_2 + Fe^{II}(C_2O_4)_n^{2-2n}$	$<1 \times 10^6$	3.23	Sedlak and Hoigné (1993)
$Fe^{III}(C_2O_4)_n^{3-2n} + HO_2^{\bullet} \rightarrow O_2 + Fe^{II}(C_2O_4)_n^{2-2n}$	$<1.2 \times 10^5$	3.24	Sedlak and Hoigné (1993)
$Fe^{II}(C_2O_4) + H_2O_2 \rightarrow Fe^{III}(C_2O_4)^+ + HO^{\bullet} + OH^-$	3.1×10^4	3.25	Sedlak and Hoigné (1993)
$Fe^{2+} + HO\bullet \rightarrow Fe^{III}(OH)^{2+}$	4.3×10^8	3.26	Zuo and Hoigné (1992)
$Fe^{III}(OH)^{2+} + h\upsilon \rightarrow Fe^{2+} + HO\bullet$	Negligible	3.27	Jeong and Yoon (2005)
$Fe^{3+} + O_2^{\bullet -} \rightarrow Fe^{2+} + O_2$	1.5×10^8	3.28	Balmer and Sulzberger (1999)
$C_2O_4^{2-} + HO\bullet \rightarrow CO_2 + CO_2^{\bullet -} + OH^-$	7.7×10^6	3.29	Buxton et al. (1988)
$HC_2O_4^- + HO\bullet \rightarrow CO_2 + CO_2^{\bullet -} + H_2O$	4.7×10^7	3.30	Buxton et al. (1988)
$CPAA^a + HO\bullet \rightarrow$ products	3.0×10^9	3.31	Pignatello (1992)
Equilibrium reactions	*Equilibrium constants* (M^{-1})		
$Fe^{3+} + C_2O_4^{2-} \leftrightarrow Fe^{III}(C_2O_4)^+$	2.5×10^9	3.32	Faust and Zepp (1993)
$Fe^{III}(C_2O_4)^+ + C_2O_4^{2-} \leftrightarrow Fe^{III}(C_2O_4)_2^-$	6.3×10^6	3.33	Faust and Zepp (1993)
$Fe^{III}(C_2O_4)^- + C_2O_4^{2-} \leftrightarrow Fe^{III}(C_2O_4)_3^{3-}$	3.8×10^4	3.34	Faust and Zepp (1993)
$Fe^{2+} + C_2O_4^{2-} \leftrightarrow Fe^{II}(C_2O_4)$	2.0×10^5	3.35	Faust and Zepp (1993)
$Fe^{II}(C_2O_4) + C_2O_4^{2-} \leftrightarrow Fe^{II}(C_2O_4)_2^{2-}$	1.2×10^2	3.36	Faust and Zepp (1993)
$HC_2O_4^+ \leftrightarrow C_2O_4^{2-} + H^+$	6.2×10^1	3.37	Zuo and Hoigné (1992)
$HO_2^{\bullet} \leftrightarrow O_2^{\bullet -} + H^+$	6.2×10^1	3.38	Bielski et al. (1985)

[a] CPAA means the 2,4-dichlorophenoxyacetic acid

Bielski et al. 1985; Mulazzani et al. 1986; Jeong and Yoon 2004; Buxton et al. 1988; Pignatello 1992; Zuo and Hoigné 1992; Sedlak and Hoigné 1993; Balmer and Sulzberger 1999). In the photo-Fenton reaction, the $HO^{\bullet}$ radical is formed photolytically from $Fe(OH)^{2+}$ (Eq. 3.27). The relevant reaction mainly takes place at pH 2.5–5 (Eq. 3.26), but its quantum yield is relatively low: $\varphi_{Fe(II)} = 0.14 \pm 0.04$ at 313 nm and $\varphi_{HO} = 0.195 \pm 0.03$ at 310 nm (Hislop and Bolton 1999). When Fe(III) is complexed with a carboxylic anion (e.g. oxalate), the quantum yield of Fe(II) production ($\varphi_{Fe(II)}$) is significantly increased to $\varphi_{Fe(II)} = 1.24$, at 300 nm, pH = ~2 and 6 mM ferrioxalate (Murov et al. 1993). This result is accounted for by the considerable photosensitive nature of the ferrioxalate complex $[Fe(C_2O_4)_3]^{3-}$, which combines elevated absorption of visible radiation with a very high quantum yield of Fe^{2+} photoproduction. Interestingly, the photolysis of the ferrioxalate complex generates an additional reactive radical species, the carbon dioxide radical anion ($CO_2^{\bullet-}$) (Eqs. 3.19–3.21; Table 3).

The radical $CO_2^{\bullet-}$ can produce Fe(II) via reaction (Eq. 3.21) and by other reaction pathways (Eqs. 3.23, 3.24). The kinetic and equilibrium constants for the photo-ferrioxalate/H_2O_2 reaction are shown in Table 3. $CO_2^{\bullet-}$ can react with oxygen to form the superoxide anion ($O_2^{\bullet-}$) (Eq. 3.22), which can further enhance the quantum yield for the generation of Fe^{2+} (Eqs. 3.23, 3.24, 3.28) and contributes to the production of H_2O_2 (Eq. 3.17). When ferrioxalate is irradiated in the presence of H_2O_2 under ideal conditions, a radical $HO^{\bullet}$ is produced by the Fenton reaction per every Fe(II) generated (Eq 3.25, Table 3). In the reaction media (Eq. 3.25), both uncoordinated Fe^{2+} and $Fe^{II}(C_2O_4)$ can react with H_2O_2. Therefore one gets an overall, apparent second-order rate constant for the reaction between Fe(II) and H_2O_2. In the presence of excess oxalate, Fe(III) will be coordinated with either two or three oxalate ligands. Fe(III) is recycled to Fe(II) in both the photo-Fenton and the photo-ferrioxalate/H_2O_2 reaction. In the latter case the formation of $HO^{\bullet}$ depends on the availability of radiation, H_2O_2 and oxalate, the latter two components being consumed by the reaction. The enhancement of $HO^{\bullet}$ photoproduction that is observed upon addition of oxalate depends on the very high photolysis quantum yield of the Fe(III)-oxalate complex(es), which largely compensates for the facts that the photolysis of Fe(III)-oxalate, unlike that of $FeOH^{2+}$, does not yield $HO^{\bullet}$, and that oxalate is a $HO^{\bullet}$ scavenger.

3.6 $HO^{\bullet}$ Production from Photocatalytic Metal Oxide (TiO_2) Suspensions

Titanium dioxide is the most frequently used metal oxide photocatalyst, which undergoes excitation at near-UV wavelengths. The irradiation by sunlight of aqueous suspensions of TiO_2 can induce very significant generation of $HO^{\bullet}$ in aqueous solution. Below it is reported a general scheme of $HO^{\bullet}$ photo-production, proposed in early studies to describe the behavior of aqueous suspensions of TiO_2 in the presence of DOM (Konstantinou and Albanis 2004; Murov et al. 1993; Tseng and Haung 1991; Fox 1993; Chen et al. 2001; Han et al. 2009) (Eqs. 3.13–3.18, see chapter “Photoinduced and Microbial Generation of Hydrogen Peroxide and Organic Peroxides in Natural Waters”):

$$\mathrm{DOM} + h\upsilon \rightarrow {}^{1}\mathrm{DOM}^{*} \xrightarrow{\mathrm{ISC}} {}^{3}\mathrm{DOM}^{*} \tag{3.39}$$

$$\mathrm{T_iO_2} + h\upsilon \rightarrow \mathrm{T_iO_2^{*}} \rightarrow \mathrm{T_iO_2}\,(e^{-} + h^{+}) \tag{3.40}$$

$${}^{3}\mathrm{DOM}^{*} + \mathrm{O_2} \rightarrow \mathrm{DOM}^{*+} + \mathrm{O_2}^{\bullet -} \tag{3.41}$$

$$\mathrm{TiO_2}(e^{-} + h^{+}) + \mathrm{O_2} \rightarrow \mathrm{TiO_2}(h^{+}) + \mathrm{O_2}^{\bullet -} \tag{3.42}$$

$$\mathrm{O_2^{\bullet -}} + \mathrm{H^{+}} \rightarrow \mathrm{HO_2}^{\bullet} \quad \mathrm{pK_a} = 4.8 \tag{3.43}$$

$$2\mathrm{O_2}^{\bullet -} \rightarrow \mathrm{O_2^{2-}} + \mathrm{O_2} \quad \mathrm{pK_a} = < 0.35\,\mathrm{M^{-1}s^{-1}} \tag{3.44}$$

$$\mathrm{HO_2}^{\bullet} + \mathrm{HO_2}^{\bullet} \rightarrow \mathrm{H_2O_2} + \mathrm{O_2} \quad k = 8.6 \times 10^{5}\,\mathrm{M^{-1}s^{-1}} \tag{3.45}$$

$$\mathrm{HO_2}^{\bullet} + \mathrm{O_2}^{\bullet -} + \mathrm{H_2O} \rightarrow \mathrm{H_2O_2} + \mathrm{O_2} + \mathrm{OH^{-}} \quad k = 1.0 \times 10^{8}\,\mathrm{M^{-1}s^{-1}} \tag{3.46}$$

$$\mathrm{H_2O_2} + h\upsilon \rightarrow 2\mathrm{HO}^{\bullet} \tag{3.47}$$

$$\mathrm{H_2O_2} + \mathrm{HO}^{\bullet} \rightarrow \mathrm{HO_2}^{\bullet} + \mathrm{HO_2} \quad k = 3.0 \times 10^{7}\,\mathrm{M^{-1}s^{-1}} \tag{3.48}$$

$$\mathrm{DOM}^{\bullet +} + \mathrm{HO}^{\bullet} \rightarrow \text{the photo degraded products} \tag{3.49}$$

Major oxidants arising upon UV irradiation of $\mathrm{TiO_2}$ are the valence-band holes (h^{+}), which can be trapped by surface Ti–$\mathrm{OH^{-}}$ groups to yield Ti-$\mathrm{HO}^{\bullet}$ radical species (surface-bound $\mathrm{HO}^{\bullet}$ or $\mathrm{HO}^{\bullet}_{\mathrm{ads}}$). In contrast, the conduction-band electrons (e^{-}) can be trapped to form surface and sub-surface $\mathrm{Ti^{III}}$ species: The latter can react with dissolved oxygen to give hydrogen peroxide radical ($\mathrm{HO_2}^{\bullet}$), which disproportionates to $\mathrm{H_2O_2}$ that is photolyzed to give $\mathrm{HO}^{\bullet}$ in solution (Murov et al. 1993; Tseng and Haung 1991; Fox 1993).

As already reported, a semiconductor photocatalyst generates electron/hole pairs upon irradiation, with free electrons produced in a nearly empty conduction band and positive holes remaining in the valence band (Bard 1979; Schiavello 1987). The lifetime of an electron/hole pair can vary from a few nano-seconds to a few hours depending on the ambient conditions (Pleskov and Gurevich 1986). Once formed the $\mathrm{HO}^{\bullet}$ radical (surface-bound or in solution) reacts with organic compounds, which results into the heterogeneous photocatalytic degradation of organic contaminants in solution (Sun and Bolton 1996; Ullah et al. 1998; Konstantinou and Albanis 2004; Tseng and Haung 1991; Fox 1993; Han et al. 2009; Prousek 1996; Vione et al. 2001; Muñoz et al. 2006; Saquib et al. 2008).

3.7 Photoinduced Generation of $HO^\bullet$ from Algae

Recent studies demonstrate that chlorophyll *a* and algae can photolytically produce $HO^\bullet$ in natural waters (Li et al. 2008; Dykens et al. 1992; Oda et al. 1992). It is hypothesized that $HO^\bullet$ is produced by H_2O_2 (Eq. 3.2), which is initially formed in irradiated aqueous suspensions of algae. The photo formation of H_2O_2 from algae is a well-known phenomenon in natural waters (Lehninger 1970; Zepp et al. 1987; Collen et al. 1995), which has been explained in detail in the second chapter (see chapter "Photoinduced and Microbial Generation of Hydrogen Peroxide and Organic Peroxides in Natural Waters"). As found by in vitro studies carried out in aerated water–acetone mixtures, the generation of H_2O_2 proceeds through the photo-formation of superoxide ion by chlorophyll *a* (You and Fong 1986). It has been shown that the $HO^\bullet$ photoproduction increases with increasing algal concentration and irradiation time (Li et al. 2008). It has also been shown that for the marine microalga *Dunaliella salina*, the $HO^\bullet$ production is significantly enhanced by the addition of Pb(II), or by Pb(II) and methylmercury. However, the $HO^\bullet$ production is decreased by addition of methylmercury only, suggesting a complex effect of metal pollution on the $HO^\bullet$ production from algae suspensions (Li et al. 2008).

4 Factors Controlling the Production and Decay of $HO^\bullet$ in Natural Waters

Major sources of $HO^\bullet$ in irradiated natural waters are NO_2^-, NO_3^-, H_2O_2, photo-Fenton reaction (which depends on the concentrations of Fe and H_2O_2), humic substances (fulvic and humic acids), tryptophan amino acid, autochthonous and even unknown DOM components as well as anthropogenic DOM such as components of household detergents or fluorescent whitening agents (FWAs) such as (DAS1) and distyryl biphenyl (DSBP) (Table 2). The concentration values and, in the case of DOM, also the nature of these species are very variable among rivers, lakes and oceans, which significantly affects the $HO^\bullet$ sources in natural waters (Takeda et al. 2004; White et al. 2003; Nakatani et al. 2007; Mostofa KMG and Sakugawa H, unpublished data; Mostofa et al. 2005; Zika et al. 1993). Interestingly, the concentration values of NO_2^- and NO_3^- in surface seawaters are lowered by solar irradiation that induces transformation reactions. This is a key factor that limits the role of nitrite and nitrate as $HO^\bullet$ sources in the surface seawater layer. Unknown or little known photoinduced $HO^\bullet$ sources in natural waters are still poorly characterized DOM components such as humic substances (fulvic and humic acid), amino acids, proteins, components of detergents or FWAs, as well as their daughter photoproducts, unidentified organic compounds and photo-Fenton reactions. Therefore, the production of $HO^\bullet$ in natural waters depends on several factors, which can be listed as: (1) Wavelength spectrum of solar radiation; (2) Nature and contents of DOM; (3) Consumption of $HO^\bullet$ by DOM and other chemical species; (4) Nitrite and nitrate: Effect of wavelength spectrum, temperature, and pH; (5) H_2O_2: Effect of wavelength spectrum and temperature; (6) Fenton reaction: Effect of pH, temperature and salinity; (7) Photo-Fenton reaction; and (8) Photo-ferrioxalate/H_2O_2 reaction: Dependence of pH and reactants. These issues will be discussed below.

4.1 Wavelength Spectrum of Solar Radiation

The production of $HO^\bullet$ significantly depends on the spectrum of the incident radiation in the ultraviolet (UVC = 200–280 nm; UVB = 280–320 nm; UVA = 320–400 nm) and visible (400–700 nm) regions. Note that UVC radiation is not present in the sunlight spectrum in the troposphere. The maximum $HO^\bullet$ photo-production has been observed upon UVB irradiation of three DOM fractions isolated from lake water, and it decreased at higher wavelengths (Grannas et al. 2006). A rough estimation shows that the $HO^\bullet$ production is approximately 191–247 % and 103–178 % higher at 308 nm than at 355 and 330 nm, respectively. The photoproduction of $HO^\bullet$ by nitrate is only induced by UVB radiation, while the production of $HO^\bullet$ by nitrite and DOM can take place under both UVB and UVA. Note that UVA radiation is able to penetrate more deeply than UVB into the water bodies (Mopper and Zhou 1990; Zafiriou and Bonneau 1987; Zellner et al. 1990; Qian et al. 2001). H_2O_2 generates $HO^\bullet$ (Eq. 3.2) mostly by non-environmental UVC with quantum yield around 0.5, but the radiation absorption by H_2O_2 is extended to the UVB region and the photolysis quantum yield is expected to be similar (Legrini et al. 1993; von Sonntag et al. 1993). During non-ozone hole conditions, $HO^\bullet$ formation from nitrate contributed ~33 % to the total $HO^\bullet$ photoinduced generation in open oceanic surface waters, while the role of DOM plus nitrite was ~67 % (Qian et al. 2001). During an ozone hole event (e.g., 151 Dobson units) the corresponding results were ~40 and 60 % for nitrate and DOM plus nitrite, respectively, because of an increase in UVB irradiance that enhanced the photolysis of nitrate. A model estimation of $HO^\bullet$ photoinduced generation in Antarctic seawater during an ozone hole (151 Dobson units) shows that the production is enhanced by at least 20 %, mostly from nitrate photolysis and to a minor extent from DOM photoinduced reactions (Qian et al. 2001). Similar results have been obtained for Arctic water (Rex et al. 1997; Randall et al. 2005).

4.2 Nature and Amount of DOM Components

The radical $HO^\bullet$ is generated photolytically from various organic substances in natural waters (Table 2) (Mill et al. 1980; Mopper and Zhou 1990; Vaughn and Blough 1998; Holder-Sandvik et al. 2000; Page et al. 2011; Grannas et al. 2006). The most common dissolved organic compounds are humic substances (fulvic and humic acid), amino acids, fluorescence whitening agents (FWAs) or components of detergents such as diaminostilbene (DAS1) and distyryl biphenyl (DSBP), phenolic compounds, various kinds of autochthonous DOM components and unknown ones (Page et al. 2011; Mostofa et al. 2011). The $HO^{\bullet}$ production greatly depends on the DOM components, an increase of which can enhance the $HO^{\bullet}$ formation rate in the aqueous solution (Fig. 1) (Page et al. 2011; Mostofa KMG and Sakugawa H, unpublished data). Study shows that DOM isolates from the Suwannee River photolytically produce free $HO^{\bullet}$, while Elliot Soil Humic Acid (ESHA), and Pony Lake Fulvic Acid (PLFA) hydroxylate arenes, at least in part, through a lower-energy hydroxylating species (Page et al. 2011). The photoinduced generation of $HO^{\bullet}$ from various standard organic substances (1 mg L^{-1} aqueous solutions) has been studied using a solar simulator (Table 2; Fig. 1) (Mostofa KMG and Sakugawa H unpublished data). The differences in production rates among different substances are attributed to the variation of the fluorophores or functional groups on the highly unsaturated aliphatic carbon chains present in various DOM components (FDOM or CDOM) (Mostofa et al. 2011; Senesi 1990). The electronic transitions involving illuminated DOM can lead to the release of free electrons, which can induce the production of H_2O_2 in natural waters. It would then follow $HO^{\bullet}$ production upon H_2O_2 photolysis, and the photogenerated hydroxyl radicals can contribute to the transformation of DOM or of the pollutants present in natural waters. That would lead to photoinduced self-transformation of DOM via photogenerated $HO^{\bullet}$. Table 2 reports the main $HO^{\bullet}$ sources that are operational in the natural environment.

In polluted sewage waters, the $HO^{\bullet}$ formation is greatly enhanced after 60 min of irradiation (Fig. 3a). This finding could be compatible with $HO^{\bullet}$ production by photogenerated H_2O_2, which would not be present in the system before irradiation and would undergo accumulation at earlier irradiation times. The $HO^{\bullet}$ generation being proportional to $[H_2O_2]$, the accumulation of hydrogen peroxide would lead to an increase of the formation rate of the $HO^{\bullet}$.

The photogenerated $HO^{\bullet}$ is rapidly consumed in natural waters upon reaction with dissolved organic compounds (Brezonik and Fulkerson-Brekken 1998; Southworth and Voelker 2003; Westerhoff et al. 1999; Goldstone et al. 2002; Miller and Chin 2002; Miller et al. 2002; Moran and Zepp 1997). A rough estimation showed that the consumption of $HO^{\bullet}$ by DOM is 12–56 % in rivers (Nakatani et al. 2004). Considering the DOM as a major sink, the maximum steady-state concentration of $HO^{\bullet}$ is equal to the production rate divided by the decay rate constant, and can be depicted by (Eq. 4.1) (Schwarzenbach et al. 1993):

$$[\mathrm{HO}]_{\mathrm{SS,Fenton}} = \sum_{\lambda} \frac{I(\lambda)\varphi(\lambda)[1 - 10^{-\varepsilon(\lambda)Cz}]}{zK_{\mathrm{DOM}}C} \tag{4.1}$$

where the $1-10^{-\epsilon(\lambda)Cz}$ is the light attenuation at the depth z (cm), φ is the apparent quantum yield for the generation of $HO^{\bullet}$ from DOM (mole Einstein^{-1}), ϵ is the absorption coefficient of DOM [(mg C $L^{-1})^{-1}cm^{-1}$], C its concentration of DOM (mg C L^{-1}), and k_{DOM} (M^{-1} s^{-1}) is the second-order reaction rate constant between $HO^{\bullet}$ and DOM. The rate constant for the reaction of $HO^{\bullet}$ with

Suwannee River Fulvic Acid is (3.8–4.4) × 10^4 (mg C)$^{-1}$ L s^{-1} (Southworth and Voelker 2003; Westerhoff et al. 2007). Rate constants in the same ranges, (1–7) × 10^4 (mg C)$^{-1}$ L s^{-1}, have been determined for the reaction between $HO^\bullet$ and DOM present in natural water samples or extracted from them (Vione et al. 2006; Westerhoff et al. 1999; Goldstone et al. 2002; Gao and Zepp 1998). The half-life of a model pollutant can be estimated as $t_{1/2} = \ln 2\ (k_{HO}[HO^\bullet]_{SS})^{-1}$, where k_{HO} is the second-order reaction rate constant with $HO^\bullet$, and $[HO^\bullet]_{ss}$ is given by Eq. (4.1). Depending on the mixed layer depths that influence $[HO^\bullet]_{ss}$, and for k_{HO} values of the order of 10^9–10^{10} M^{-1} s^{-1}, $t_{1/2}$ can vary from some days to some months.

4.2.1 Fulvic Acid as a Producer and Scavenger of HO• in Natural Waters

Fulvic acid (FA) can produce $HO^\bullet$ photolytically in aqueous solution (Table 2) (Vaughn and Blough 1998; Goldstone et al. 2002). FA can account for approximately 23–70 % of H_2O_2 production in rivers (Mostofa and Sakugawa 2009). A general reaction of FA that leads to the formation of H_2O_2 (Eq. 4.2) can be depicted on the basis of Eqs. (3.13–3.18) (see chapter "Photoinduced and Microbial Generation of Hydrogen Peroxide and Organic Peroxides in Natural Waters"):

$$FA + O_2 + H_2O \xrightarrow{h\upsilon} FA^{\bullet+} + H_2O_2 + O_2 + OH^- \quad (4.2)$$

The generation of H_2O_2 from FA can lead to $HO^\bullet$ ($H_2O_2 + h\upsilon \rightarrow 2HO^\bullet$) that could further react with FA, at the same time being consumed and causing transformation of FA (Voelker and Sulzberger 1996). Recent experimental studies indicate that at least 50 % of the hydroxylation reactions photosensitized by DOM isolates would be a result of a pathway that is independent of hydrogen peroxide (Page et al. 2011). Recently, the photo-degradation of various functional groups in DOM by $HO^\bullet$ has been observed, and the rates determined in aqueous solution (Minakata et al. 2009). The results suggest that DOM or FA is important scavengers of photolytically generated $HO^\bullet$ in aqueous solution.

4.3 Other Chemical Species or Processes as HO• Sinks

There are several processes that can inhibit $HO^\bullet$ formation or consume these radicals in the aquatic environments, which can be distinguished as:

(1) Decrease in light intensity in deeper waters, which reduces the formation rate of H_2O_2 and of Fe(II). Photo-generated H_2O_2 and Fe(II) at the surface could be moved downward through vertical mixing processes, thereby reducing their concentration in the surface layer (Southworth and Voelker 2003; Pullin et al. 2004). Such an effect can greatly decrease the $HO^\bullet$ production in water.

(2) Upon oxidation of carbonate and bicarbonate by $HO^{\bullet}$, the carbonate radical ($CO_3^{\bullet-}$) is produced (Eqs. 4.3, 4.4) in surface waters (Minella et al. 2011) and DOM is the key component to sink $CO_3^{\bullet-}$ by the reaction between them (Eq. 4.5) in surface waters (Buxton et al. 1988; Canonica et al. 2005).

$$HO^{\bullet} + CO_3{}^{2-} \rightarrow OH^- + CO_3{}^{\bullet-} \left[k_{4.3} = 3.9 \times 10^8\, M^{-1}\, s^{-1}\right] \tag{4.3}$$

$$HO^{\bullet} + HCO_3^- \rightarrow H_2O + CO_3{}^{\bullet-} \left[k_{4.4} = 8.5 \times 10^6\, M^{-1}\, s^{-1}\right] \tag{4.4}$$

$$DOM + CO_3{}^{\bullet-} \rightarrow DOM^{+\bullet} + CO_3{}^{2-} \quad \left[k_{4.5} = 10^2\, (mg\ C)^{-1}\, s^{-1}\right] \tag{4.5}$$

These reactions are all dependent on pH since pK_a of carbonate and bicarbonate has 10.3 and 6.3 (Tossell 2005). At around neutral pH, bicarbonate is dominant over carbonate so HO radical scavenging is not so significant as to higher pH (i.e., carbonate is more dominant).

(3) In seawater, $HO^{\bullet}$ is mainly consumed by Br^- ions (Zafiriou et al. 1984; Neta et al. 1988; Goldstone et al. 2002; Song et al. 1996; Zafiriou et al. 1987; Das et al. 2009). The reaction of $HO^{\bullet}$ with Br^- generates the oxidized bromine radical species ($BrOH^{\bullet-}$) (Eq. 4.6), which can be transformed into Br and $Br_2{}^{\bullet-}$ (Eq. 4.7) (Goldstone et al. 2002; Song et al. 1996; Zafiriou et al. 1987; von Gunten and Oliveras 1997; Grebel et al. 2009).

$$HO^{\bullet} + Br^- \rightarrow BrOH^{\bullet-} \tag{4.6}$$

$$BrOH^- + H^+ \rightarrow Br^{\bullet} + H_2O \xrightarrow{Br^-} Br_2{}^{\bullet-} + H_2O \tag{4.7}$$

Moreover, the bromine radical species could also react with DOM and induce transformation reactions. The half-life of $BrOH^{\bullet-}$ is less than a few seconds, for a H_2O_2 concentration of 0.1 mg L^{-1} in cloud water at pH 8. However, at pH 5 the half-life of $BrOH^{\bullet-}$ is several hours for the same H_2O_2 concentration (von Gunten and Oliveras 1997). A recent study shows that bromide scavenges the $HO^{\bullet}$ radicals formed upon photolysis of nitrate, before they leave the solvent cage, thereby inhibiting the geminate recombination between the photogenerated $HO^{\bullet}$ and $^{\bullet}NO_2$. The result is that the formation rate of $HO^{\bullet} + Br_2{}^{\bullet-}$ with nitrate + bromide is higher than that of $HO^{\bullet}$ with nitrate alone. Such an effect compensates for the lower reactivity of $Br_2{}^{\bullet-}$ compared to $HO^{\bullet}$ toward certain organic substrates, e.g. phenol and tryptophan (Das et al. 2009). It has also been shown that the radical $Br_2{}^{\bullet-}$ is an effective brominating agent for phenol (Vione et al. 2008).

(4) In stimulated polymorphonuclear leukocyte systems, a water extract from green tea and green tea polyphenols had the strongest scavenging effect on $HO^{\bullet}$, much stronger than vitamin C or vitamin E. Moreover, rosemary antioxidants and curcumin have weaker scavenging effects than vitamin C, but a stronger one than vitamin E (Zhao et al. 1989).

4.4 Dependence on NO_2^- and NO_3^- Photolysis: Effect of Wavelength Spectrum, Temperature, and pH

The photoinduced generation of $HO^\bullet$ largely depends on the presence of NO_2^- and NO_3^- in natural waters (Zafiriou and True 1979a, b; Takeda et al. 2004; Zafiriou and Bonneau 1987; Zepp et al. 1987; Zellner et al. 1990; Brezonik and Fulkerson-Brekken 1998; Mack and Bolton 1999). The quantum yield of $HO^\bullet$ (Φ_{HO}) for NO_2^- and NO_3^- photolysis significantly depends on the temperature, wavelength and pH in the aqueous solution (Tables 4 and 5) (Zepp et al. 1987; Zellner et al. 1990; Goldstein and Rabani 2008; Matykiewiczová et al. 2007; Treinin and Hayon 1970; Strehlow and Wagner 1982; Warneck and Wurzinger 1988; Mark et al. 1996; Vione et al. 2001; Chu and Anastasio 2003). The Φ_{HO} of NO_2^- photolysis has been determined for a NO_2^- concentration of 3×10^{-3} M, for $4 \le \text{pH} \le 11$ and temperatures between 278–353 K at 308 nm (Table 4) (Zellner et al. 1990). The absorption coefficient of NO_2^- at 308 nm is $\varepsilon_{308} = 4.1$ L mol^{-1} cm^{-1} (Strickler and Kasha 1963). For the same solution, Φ_{HO} has also been determined in the temperature range of 278–358 K, for pH 8 and under 351 nm irradiation (Table 4). Note that the absorption coefficient of NO_2^- is $\varepsilon_{351} = 9.4$ L mol^{-1} cm^{-1} (Strickler and Kasha 1963). The results have demonstrated that Φ_{HO} generally increases with temperature and decreases with pH (Fig. 4).

The temperature dependence of Φ_{HO} is mathematically derived, based on the results of NO_2^- photolysis at 308 (Eq. 4.8) and 351 nm (Eq. 4.9) at room temperature (Table 4) (Zellner et al. 1990). It can be expressed as:

$$\Phi_{HO}(298\ \text{K}) = 0.07 \pm 0.01 \qquad \text{for } 7 \le \text{pH} \le 9 \tag{4.8}$$

$$\Phi_{HO}(298\ \text{K}) = 0.046 \pm 0.009 \qquad \text{for pH} = 8 \tag{4.9}$$

Using the averaged data over the range $7 \le \text{pH} \le 9$, the temperature dependence of Φ_{HO} at 308 nm (Eq. 4.10) becomes:

$$\Phi_{HO}(\text{T}) = \Phi_{HO}(298\ \text{K}) \exp\left[(1560 \pm 360)\left(\frac{1}{298} - \frac{1}{T}\right)\right] \tag{4.10}$$

where the apparent activation energy is $E_A = 13 \pm 3$ kJ mol^{-1}. This equation is in good agreement with previous data (Zafiriou and Bonneau 1987), where it has been obtained $E_A = 12 \pm 6$ kJ mol^{-1} at 298.5 nm and in the temperature range of 296–322 K.

The temperature dependence of Φ_{HO} for NO_2^- photolysis at 351 nm can be expressed as (Eq. 4.11):

$$\Phi_{HO}(\text{T}) = \Phi_{HO}(298\ \text{K}) \exp\left[(1800 \pm 400)\left(\frac{1}{298} - \frac{1}{T}\right)\right] \tag{4.11}$$

Table 4 The quantum yield of $HO^{\bullet}$ (Φ_{HO}) of nitrite photolysis as a function of pH and temperature (T)

T (K)	pH							
	4	5	6	7	8	9	10	11
For wavelength 308 nm								
278	0.047 ± 0.004	0.037 ± 0.002	0.039 ± 0.005	0.040 ± 0.005	0.040 ± 0.002	0.039 ± 0.001	0.034 ± 0.002	0.030 ± 0.003
298	0.091 ± 0.011	0.080 ± 0.007	0.068 ± 0.004	0.068 ± 0.009	0.071 ± 0.009	0.068 ± 0.008	0.060 ± 0.007	0.046 ± 0.006
318	0.100 ± 0.011	0.085 ± 0.005	0.081 ± 0.006	0.082 ± 0.011	0.079 ± 0.003	0.080 ± 0.003	0.076 ± 0.003	0.069 ± 0.005
353	0.160 ± 0.011	0.159 ± 0.008	0.148 ± 0.006	0.141 ± 0.007	0.143 ± 0.003	0.132 ± 0.005	0.125 ± 0.003	0.115 ± 0.004
For wavelength 351 nm								
278	nd	nd	nd	nd	0.027 ± 0.003	nd	nd	nd
288	nd	nd	nd	nd	0.038 ± 0.004	nd	nd	nd
298	nd	nd	nd	nd	0.046 ± 0.003	nd	nd	nd
308	nd	nd	nd	nd	0.058 ± 0.002	nd	nd	nd
318	nd	nd	nd	nd	0.078 ± 0.003	nd	nd	nd
328	nd	nd	nd	nd	0.091 ± 0.010	nd	nd	nd
338	nd	nd	nd	nd	0.096 ± 0.003	nd	nd	nd
348	nd	nd	nd	nd	0.118 ± 0.008	nd	nd	nd
358	nd	nd	nd	nd	0.153 ± 0.009	nd	nd	nd

nd means ‘not detected’
Data source Zellner et al. (1990)

Table 5 The quantum yield of $HO^{\bullet}$ (Φ_{HO}) of nitrate photolysis as a function of pH and temperature (T)

T (K)	pH							
	4	5	6	7	8	9	10	11
For wavelength 308 nm								
278	0.008 ± 0.001	0.007 ± 0.001	0.008 ± 0.001	0.007 ± 0.001	0.008 ± 0.001	0.007 ± 0.001	0.007 ± 0.001	0.004 ± 0.001
298	0.016 ± 0.001	0.017 ± 0.001	0.017 ± 0.001	0.016 ± 0.001	0.017 ± 0.001	0.016 ± 0.001	0.014 ± 0.001	0.009 ± 0.001
318	0.028 ± 0.002	0.026 ± 0.003	0.027 ± 0.002	0.028 ± 0.001	0.027 ± 0.002	0.024 ± 0.002	0.015 ± 0.002	0.011 ± 0.001
353	0.038 ± 0.004	0.034 ± 0.003	0.036 ± 0.004	0.035 ± 0.002	0.036 ± 0.003	0.030 ± 0.005	0.017 ± 0.003	0.012 ± 0.001

Data source (Zellner et al. 1990)

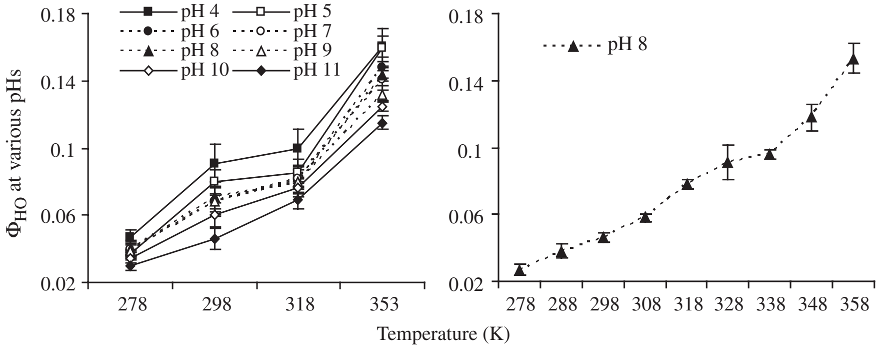

Fig. 4 Quantum yields of $HO^{\bullet}$ of NO_2^- photolysis with variation in temperature at a specific wavelength at 308 nm for various pH (**a**) and at 351 nm (**b**) at pH 8. *Data source* Zellner et al. (1990)

These results allow the hypothesis that the temperature dependence of Φ_{HO} for NO_2^- photolysis is independent of wavelength, despite a decline of the absolute Φ_{HO} value with increasing wavelength (Fig. 4) (Zellner et al. 1990).

On the other hand, the Φ_{HO} of NO_3^- photolysis has been determined for a NO_3^- concentration of 3×10^{-3} M in the range $4 \leq \text{pH} \leq 11$, at temperature between 278–353 K and 308 nm irradiation (Table 5) (Zellner et al. 1990). The absorption coefficient of NO_3^- at 308 nm is $\varepsilon_{308} = 6.5$ L mol^{-1} cm^{-1} (Meyerstein and Treinin 1961). It has been shown that the quantum yields at each temperature are generally independent of pH in the range $4 \leq \text{pH} \leq 9$. At higher pH's, the quantum yield is typically decreased (Fig. 5).

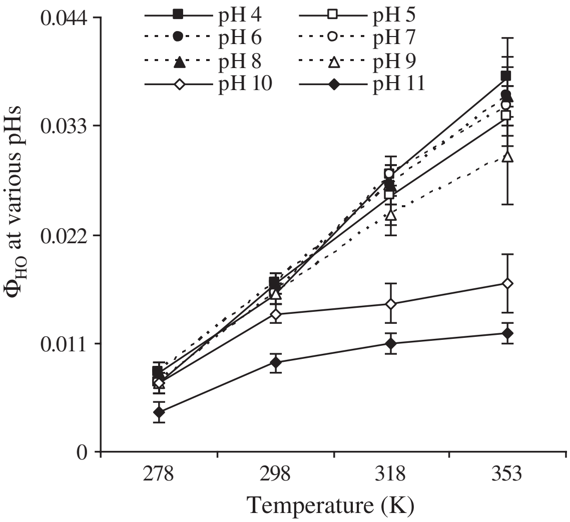

Fig. 5 Quantum yields of $HO^{\bullet}$ of NO_3^- photolysis with variation in temperature at a specific wavelength (308 nm) for various pH. *Data source* Zellner et al. (1990)

The Φ_{HO} of NO_3^- photolysis at room temperature (298 K) is (Eq. 4.12)

$$\Phi_{HO}(298\ \text{K}) = 0.017 \pm 0.03 \text{ for } 4 \leq \text{pH} \leq 9 \tag{4.12}$$

The temperature dependence of Φ_{HO} is mathematically derived from the results of NO_3^- photolysis at 308 nm, in the range of $4 \leq \text{pH} \leq 9$ (Table 5). It can be written as (Eq. 4.13) (Zellner et al. 1990):

$$\Phi_{HO}(\text{T}) = \Phi_{HO}(298\ \text{K}) \exp\left[(1800 \pm 480)\left(\frac{1}{298} - \frac{1}{T}\right)\right] \tag{4.13}$$

where the apparent activation energy $E_A = 15 \pm 4$ kJ mol^{-1}. The effect of temperature on the $HO^\bullet$ quantum yield is relatively stronger than the effect of pH: Φ_{HO} increases by almost a factor of 5 over the temperature range 278–353 K, for $4 \leq \text{pH} \leq 9$ (Zellner et al. 1990). Because of the low molar absorption coefficient of NO_3^- at 351 nm ($\varepsilon 351 \approx 0.05$ L mol^{-1} cm^{-1}) (Meyerstein and Treinin 1961), nitrate is a less effective $HO^\bullet$ source at 351 than at 308 nm. However, the results indicate that the $HO^\bullet$ quantum yield and the temperature dependence are constant at these wavelength (Zellner et al. 1990). There is an overall consistency between the results of different studies into the temperature and wavelength dependence of the $HO^\bullet$ quantum yield for NO_3^- photolysis (e.g., obtained $\Phi_{HO} = 0.015 \pm 0.003$ at 313 nm) (Zepp et al. 1987).

4.5 Dependence on H_2O_2 Photolysis: Effect of Wavelength Spectrum and Temperature

The photoinduced generation of $HO^\bullet$ from H_2O_2 ($H_2O_2 + h\upsilon \rightarrow 2\ HO^\bullet$) depends on the wavelength spectrum of UV-B radiation and on water temperature (Zellner et al. 1990; Hunt and Taube 1952; Baxendale and Wilson 1956; Volman and Chen 1959; Goldstein and Rabani 2008; Chu and Anastasio 2005; Goldstein et al. 2007). The quantum yield of $HO^\bullet$ (Φ_{HO}) has been determined for 3×10^{-3} M H_2O_2 at pH 7, at the wavelengths of 308 and 351 nm (Zellner et al. 1990). The H_2O_2 absorption coefficients for these wavelengths are $\varepsilon_{308} = 1.10$ and $\varepsilon_{351} = 0.11$ L mol^{-1} cm^{-1}, respectively (Taylor and Cross 1949). It has also been shown that the $HO^\bullet$ production gradually increases with an increase in temperature at pH 7 (Fig. 6; Table 6) (Zellner et al. 1990). Zellner and his co-workers derived the equations for the temperature dependence of Φ_{HO} upon H_2O_2 photolysis.

For the photolysis at 308 nm, Φ_{HO} can be expressed as (Eq. 4.14):

$$\Phi_{HO}(298\ \text{K}) = 0.98 \pm 0.03 \tag{4.14}$$

The temperature dependence of Φ_{HO} can be expressed as (Eq. 4.15):

$$\Phi_{HO}(T) = \Phi_{HO}(298\ \text{K}) \exp\left[(660 \pm 190)\left(\frac{1}{298} - \frac{1}{T}\right)\right] \tag{4.15}$$

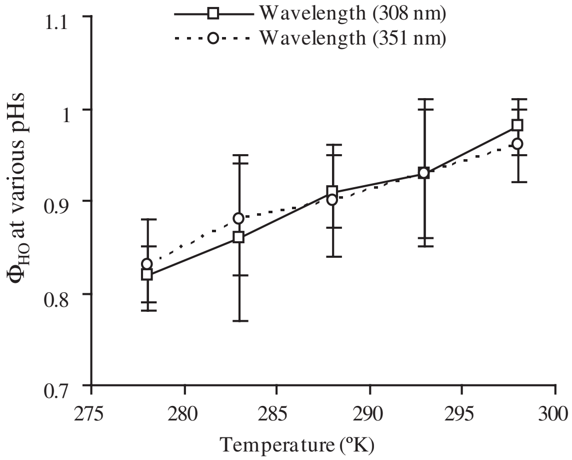

Fig. 6 Quantum yields of $HO^{\bullet}$ of H_2O_2 photolysis with variation in temperature at specific wavelengths (308 and 351 nm, respectively) at pH 7. *Data source* Zellner et al. (1990)

Table 6 Quantum yield of $HO^{\bullet}$ production (Φ_{HO}) from H_2O_2 photolysis at pH 7 as a function of temperature (T)

T (°K)	Φ_{HO} at pH 7	
	308 nm	351 nm
278	0.82 ± 0.03	0.83 ± 0.05
283	0.86 ± 0.09	0.88 ± 0.06
288	0.91 ± 0.04	0.90 ± 0.06
293	0.93 ± 0.07	0.93 ± 0.08
298	0.98 ± 0.03	0.96 ± 0.04

Data source Zellner et al. (1990)

where the activation energy is 5.5 ± 1.6 kJ mol^{-1}.

These values are essentially constant for H_2O_2 photolysis at 351 nm (Eqs. 4.16, 4.17):

$$\Phi_{HO}(298\ \mathrm{K}) = 0.96 \pm 0.04 \tag{4.16}$$

$$\Phi_{HO}(T) = \Phi_{HO}(298\ \mathrm{K}) \exp\left[(580 \pm 160)\left(\frac{1}{298} - \frac{1}{T}\right)\right] \tag{4.17}$$

A recent study has shown that the quantum yield Φ_{HO} = 1.11 ± 0.07 in the excitation range of 205–280 nm for the photolysis of H_2O_2. This is in agreement with earlier studies (Goldstein et al. 2007). Therefore, the available data suggest that the photolysis of aqueous H_2O_2 at wavelengths $\geq$ 300 nm generates $HO^{\bullet}$ with a quantum yield Φ_{HO} ~1 at room temperature (25 °C). Φ_{OH} decreases to approximately 0.82 at 5 °C (278 K). It can be noted that the effective quantum yield of H_2O_2 dissociation is approximately 0.5, but the photolysis of H_2O_2 yields two

Table 7 The reaction rate constants for generation of HO• in Fenton reaction at various pH ranges in the absence of light

Reaction type	pH 3	pH 4	pH 5	Equations
	Reaction rate constant (k) ($M^{-1}s^{-1}$)			
$Fe^{(II)} + H_2O_2 \rightarrow Fe^{(III)} + HO^{\bullet} + OH^-$	63	1.2×10^2	5.7×10^2	4.18
$Fe^{(III)} + H_2O_2 \rightarrow Fe^{(II)} + HO_2^{\bullet}/O_2^- + H^+$	2×10^{-3}	2.5×10^{-3}	2.6×10^{-3}	4.19
$H_2O_2 + HO^{\bullet} \rightarrow HO_2^{\bullet}/O_2^- + H_2O$	3.7×10^7	3.3×10^7	3.3×10^7	4.20
$Fe^{(III)} + HO_2^{\bullet}/O_2^- \rightarrow Fe^{(II)} + O_2 + H^+$	7.8×10^5	6.8×10^6	3.1×10^7	4.21
$Fe^{(II)} + HO^{\bullet} \rightarrow Fe^{(III)} + OH^-$	3.2×10^8	3.2×10^8	3.2×10^8	4.22
$Fe^{(II)} + HO_2^{\bullet}/O_2^- \rightarrow Fe^{(III)} + HO_2^{\bullet}$	1.3×10^6	2.4×10^6	6.6×10^6	4.23
$HO\bullet + HO^{\bullet} \rightarrow H_2O_2$	5.2×10^9	5.2×10^9	5.2×10^9	4.24
$HO_2^{\bullet}/O_2^- + HO_2^{\bullet}/O_2^- \rightarrow H_2O_2$	2.3×10^6	1.2×10^7	2.3×10^7	4.25
$HO^{\bullet} + HO_2^{\bullet}/O_2^- \rightarrow H_2O + O_2$	7.1×10^9	7.5×10^9	8.9×10^9	4.26

Data source (Kwan and Voelker 2002)

$HO^{\bullet}$. Therefore, the quantum yield of $HO^{\bullet}$ photoinduced generation from H_2O_2 is double compared to that of H_2O_2 photolysis (Hunt and Taube 1952; Baxendale and Wilson 1956; Volman and Chen 1959).

4.6 Fenton Reaction: Effect of pH, Temperature and Salinity

The Fenton reaction depends on the presence of Fe^{2+} (or Fe^{3+}) and H_2O_2 in natural waters. The oxidation of Fe(II) with H_2O_2 in seawater depends on pH (2–8.5), temperature (5–45 °C) and salinity (0–35 g L^{-1}) (Wells and Salam 1968; Moffett and Zika 1987a, b; Gallard et al. 1998; Bossmann et al. 1998; Duesterberg et al. 2008; Millero and Sotolongo 1989; de Laat and Gallard 1999; Duesterberg and Waite 2006; Duesterberg et al. 2005; Farias et al. 2007; Jung et al. 2009). The rate constants of the chain Fenton reactions and the relevant dependence on pH are presented in Table 7 (Kwan and Voelker 2002). The reaction rate constant between Fe^{2+} and H_2O_2 significantly increases with pH in the range from 3 to 5 (Eq. 4.18; Table 7), and a similar effect is observed with some of the chain reactions (Eqs. 4.19–4.26; Table 7).

A recent study that has been carried out in the pH range 2.5–4.0, both in the presence and absence of a target organic substance (formic acid), also highlights the importance of the Fenton system in the catalytic redox cycling of iron (Duesterberg et al. 2008). Supply of oxygen can enhance the efficiency of the Fenton oxidation, which is understandably attenuated by competition with the organic intermediates in the reaction media (Sychev and Isak 1995; Duesterberg et al. 2005).

It is shown that the addition of phosphotungstate ($PW_{12}O_{40}{}^{3-}$), a polyoxometalate, extends the working pH range of the Fenton system (Fe^{3+}/H_2O_2) up to pH 8.5. This is because $PW_{12}O_{40}{}^{3-}$ forms a soluble complex with iron that converts H_2O_2 into $HO^\bullet$ (Lee and Sedlak 2009). The Fenton reaction for the catalytic oxidation of organic compounds is usually limited to the acidic pH region, due to the low solubility of Fe(III) and the low efficiency of oxidant production at neutral pH values. The coordination of Fe^{2+} by $PW_{12}O_{40}{}^{3-}$ can alter the mechanism of the reaction of Fe(II) with H_2O_2 at neutral pH, yielding a reactive species capable of oxidizing aromatic compounds (Lee and Sedlak 2009).

An increase in temperature significantly enhances the efficiency of the Fenton reaction towards the degradation of organic pollutants in aqueous solution (Fig. 7) (Farias et al. 2007). From the results of Farias et al. (2007) it is possible to estimate a HCOOH degradation enhancement of 164–191 % at 313 K and 370–561 % at 328 K compared to 298 K, after 20 min of reaction time, with H_2O_2: formic acid molar ratios between 3 and 8 (Fig. 7). The results also show that the conversion of the organic pollutant is the highest at 328 K, with a low H_2O_2: formic acid molar ratio. Conversion gradually decreases when the H_2O_2: formic acid molar ratio is increased from 3 to 8 at the same temperature (328 K) (Fig. 7). However, at 313 K the conversion of the organic pollutant gradually increases when the H_2O_2: formic acid molar ratio is increased from 3 to 8 (Fig. 7).

The overall Fenton reaction ($Fe^{2+} + H_2O_2$) is first-order with respect to the concentration of total Fe(II) and H_2O_2. It can be expressed as follows (Eq. 4.27) (Moffett and Zika 1987a, b; Millero and Sotolongo 1989):

$$\mathrm{d}\,[\mathrm{Fe\,(II)}]\,/\mathrm{dt} \;=\; -k\,\{[\mathrm{Fe\,(II)}]\,[\mathrm{H_2O_2}]\} \tag{4.27}$$

where the brackets denote the total molar concentrations. With an excess of $[H_2O_2]$, the overall reaction becomes pseudo-first order and can be depicted as follows (Eq. 4.28):

$$\mathrm{d}\,[\mathrm{Fe\,(II)}]\,/\mathrm{dt} \;=\; -k_1'\,[\mathrm{Fe\,(II)}] \tag{4.28}$$

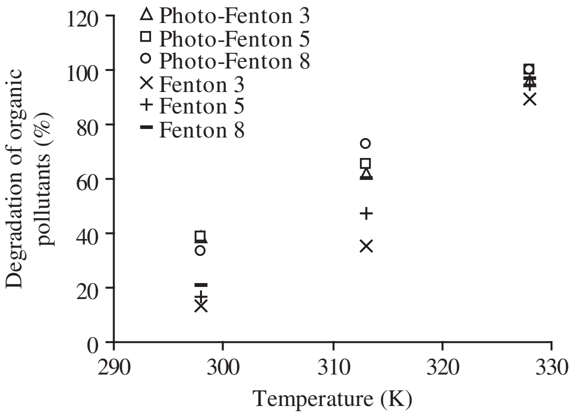

Fig. 7 The percentage degradation of organic pollutants by photo-Fenton and Fenton reactions in a stirred tank laboratory photoreactor. 3, 5 and 8 indicates the molar ratio of the reactant H_2O_2 to formic acid in the aqueous solutions. *Data Source* Farias et al. (2007)

where $k'_1 = k[H_2O_2]$. The reaction is quite fast at high temperature and pH, and it becomes quite difficult to be examined at 25 °C and pH 8. The reaction at 5 °C and pH 3.5 followed first-order kinetics with respect to Fe(II) for seawater samples, giving $k' = 0.0385 \pm 0.0009\ \text{min}^{-1}$ and $\log k = 1.50 \pm 0.02$ (k in $M^{-1}\ s^{-1}$) (Millero and Sotolongo 1989). At higher pH and temperature, the second-order reaction rate constants have been determined at the stoichiometric ratio [Fe(II)]/$[H_2O_2] = 2$, following Eq. (4.29) (Benson 1960)

$$1/[\mathrm{Fe(II)}] = 1/[\mathrm{Fe(II)}]_o + (k/2)t \tag{4.29}$$

where $[\mathrm{Fe(II)}]_o$ is the initial concentration of Fe(II).

The rate constant k ($M^{-1}\ s^{-1}$) for Eq. (4.29) is independent of pH below pH 4, and increases significantly at high pH values. It is a linear function of $[H^+]$ or $[HO^-]$ from pH 6 to 8 in seawater. The effect of pH is not affected by a variation of the temperature

The effects of temperature (T) and ionic strength (I) on k at pH 6 can be expressed as (Eq. 4.30) (Millero and Sotolongo 1989):

$$\log k = 13.73 - 2{,}948/T - 1.70I^{1/2} + 1.20I \tag{4.30}$$

The reaction rates can be depicted as (Eq. 4.31) (Millero and Sotolongo 1989):

$$d[\mathrm{Fe(II)}]/dt = -k_2[\mathrm{Fe(II)}][H_2O_2][HO^-] \tag{4.31}$$

where the values of k_2 are independent of temperature. This is attributed to the fact that the activation energy is of the same order of magnitude as the heat of ionization of water ($\Delta H_w{}^*$). The effect of the ionic strength on log k_2 can be depicted as (Eq. 4.32) (Millero and Sotolongo 1989):

$$\log k_2 = 11.72 - 2.14I^{1/2} + 1.38I \tag{4.32}$$

The overall reaction rate k over the entire range of pH, temperature and ionic strength can be expressed by (Eq. 4.33) (Millero and Sotolongo 1989):

$$k = k_o\alpha_{\mathrm{Fe}} + k_1\alpha_{\mathrm{FeOH}} \tag{4.33}$$

where α_{Fe} and α_{FeOH}, k_o and k_1 are the fractions of the two Fe(II) species and the rate constants for the oxidation of Fe^{2+} and $FeOH^+$, respectively. The values of k_o and k_1 can be expressed by (Eqs. 4.34, 4.35) (Millero and Sotolongo 1989):

$$\log k_0 = 8.37 - 1{,}866/T \tag{4.34}$$

$$\log k_1 = 17.26 - 2.948/T - 1.70I^{1/2} + 1.20I \tag{4.35}$$

The addition of HCO_3^- at constant pH linearly increases the reaction rate, independently of the temperature and salinity. This result can be attributed to $FeCO_3{}^0$ reacting faster than $FeOH^+$ with H_2O_2. At a given pH and ionic strength, the reaction rates in seawater are almost the same as in NaCl. These results can explain the differences in the reaction rates observed between estuarine waters of various alkalinity and seawater diluted with water (Millero and Sotolongo 1989).

A recent study demonstrates that the rates of the Fenton reaction do not vary in the presence of chloride, nitrate and perchlorate. However, in the presence of sulfate the rate of Fe(II) oxidation is higher and depends on pH and the concentration of sulfate. This result has been obtained under dark conditions at $\mathrm{pH} < 3$, 25 ± 0.5 °C and controlled ionic strength (≤ 1 M) (Le Truong et al. 2004). It has also been shown that H_2O_2 is more stable in Fenton-like than in Fenton's systems, and that the lifetime of H_2O_2 is highly affected by the solution pH. Indeed, pH-buffered acidic conditions are preferred to ensure sufficient H_2O_2 lifetime, which is an important factor in the feasibility of Fenton's and Fenton-like reactions with haematite and magnetite for soil and groundwater remediation (Jung et al. 2009).

4.7 Photo-Fenton Reaction

The formation of $HO^{\bullet}$ in the photo-Fenton reaction ($\mathrm{Fe(III)} + H_2O_2 + h\nu$) significantly depends on light intensity, H_2O_2 and Fe(III) concentration, and pH (Zepp et al. 1992; Voelker et al. 1997; Southworth and Voelker 2003; Vermilyea and Voelker 2009). Studies on the ferrioxalate system (air- and argon-saturated) suggest that the Fe(II) photoproduction rates are not affected by the reducing intermediates ($CO_2^{\bullet-}$, $O_2^{\bullet-}$, scavenger-derived radicals) produced in the aqueous solution (Zepp et al. 1992). The results demonstrate that the photolytically generated Fe(II) can efficiently react with H_2O_2 to produce $HO^{\bullet}$ in water at pH 3–8 (Zepp et al. 1992). It has been shown that the Fe(II) concentration in upstream waters gradually increased from zero (0530 h JST, Japan standard time) to 3.8 μM (1300 h JST), and decreased to zero again after sunset (1900 h JST) (Fig. 8a) (Mostofa KMG and Sakugawa H unpublished data). In the meantime, pH varied from 7.0 to 7.6 (Mostofa and Sakugawa 2009). In downstream waters, the Fe(II) concentration increases from 2.3 (0530 JST) to 4.0 μM (1200 JST) and then decreased to 2.2 μM (1900 JST) after sunset (Fig. 8b) (Mostofa KMG and Sakugawa H unpublished data). The pH varied from 7.0 to 7.3 (Mostofa and Sakugawa 2009). The production of Fe(II) was the highest at noon, and it was almost the same in clean upstream river (3.8 μM, 7.3 % of the total Fe) and polluted river waters (4.0 μM, 1.9 % of the total Fe). In a similar way, the H_2O_2 production was also maximum at noon and reached 40 and 63 nM, respectively (Fig. 8, "Photoinduced and Microbial Generation of Hydrogen Peroxide and Organic Peroxides in Natural Waters") (Mostofa and Sakugawa 2009). Similarly, Fe^{2+} has been observed to reach up to 0.9 nM in a Swiss Lake at pH 8.0–8.5; 15 nM in a low-land lake in the United Kingdom at pH 7.0–7.5; and approximately 0–145 μM in a salt marsh at Skidaway Island in the USA (Viollier et al. 2000; Aldrich et al. 2001; Emmenegger et al. 2001). The peak concentration of Fe(II) ranged from 4 to 8 % of the total iron concentration at pH 8 in waters of Narragansett Bay. It was also observed an increase of Fe(II) concentration by lowering the pH over the entire

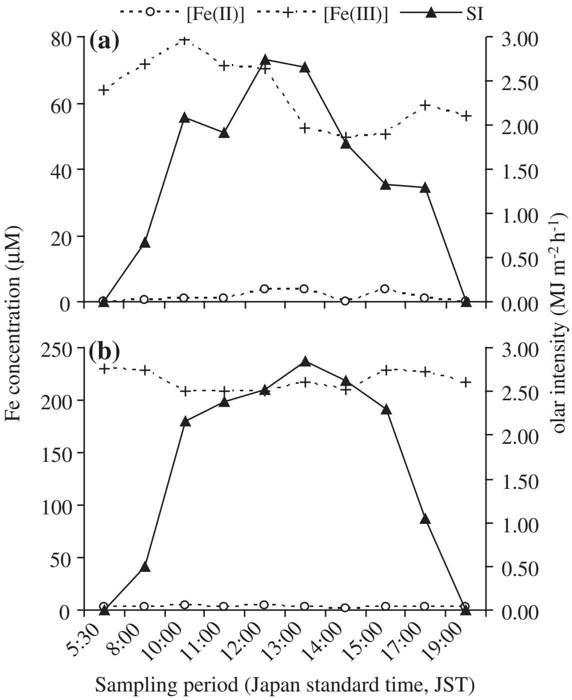

Fig. 8 Diurnal variations of Fe(II) and Fe(III) in the upstream waters (Site KR2, Shouriki) on 21 August 2003 and in the downstream waters (Site KR6, Hinotsume) on 26 September 2003, in the Kurose River, Japan. *Data Source* Mostofa and Sakugawa (unpublished data)

course of the experiment (Miller et al. 1995). All the reported results suggest that the photo-Fenton reaction under sunlight proceeds at the highest rate at noon in natural waters, in correspondence with the peak values of Fe^{2+} and H_2O_2. The diurnal changes in the concentrations of Fe(II) and H_2O_2 are strongly correlated to the losses in the DOM fluorescence: the latter was 28 % lower at noon than before sunrise in the river waters (Mostofa et al. 2005). However, the contribution of the photo-Fenton reaction to the production of $HO^\bullet$ was minor (2–29 %) as compared to NO_3^- (3–70 %) and NO_2^- (1–89 %) upon irradiation of river water samples from Japan (pH 6.7–9.0) (Nakatani et al. 2007). Interestingly, it has also been shown that the oxidation of Fe^{2+} by H_2O_2 is the key reaction step in the presence of high concentrations of Fe^{2+}; in contrast, the back reduction of Fe(III) by superoxide is important at low initial Fe^{2+} concentrations and high pH (Pham and Waite 2008). It has also been suggested that precipitation of Fe(III) has a marked effect on the overall Fe(II) oxidation, particularly at high pH. A recent study has shown that the inhibition of the photo-Fenton degradation of organic material (both synthetic phenol wastewater and an aqueous extract of Brazilian gasoline) in the presence of chloride ions can be circumvented, by maintaining the pH of the medium at or slightly above 3 throughout the process. In this way, it is possible to limit inhibition of the oxidation reactions even in the presence of 0.5 M chloride (Machulek et al. 2007).

4.7.1 Kinetics of the Photo-Fenton Reaction

The kinetics of the photo-Fenton reaction can be determined as a function of pH, based on the yield of $HO^\bullet$ formed per Fe(II) oxidized by H_2O_2, and considering the photoreactions of aqueous organic substrates (Zepp et al. 1992; Hoigné et al. 1988). Under illumination with constant irradiance of a diluted probe compound (P) that reacts with $HO^\bullet$ (Eq. 4.36), the hydroxyl radical would rapidly reach a steady-state concentration. In the presence of P and of other $HO^\bullet$ scavengers (S), the decay of $HO^\bullet$ can be expressed as follows (Eqs. 4.36, 4.37) (Zepp et al. 1992):

$$HO^\bullet + P \xrightarrow{K_P,\,[P]} \text{rection products} \tag{4.36}$$

$$HO^\bullet + S \xrightarrow{\sum K_s,\,[S]} \text{scavenging products} \tag{4.37}$$

where k_p is the second-order rate constant ($M^{-1}\ s^{-1}$) for the reaction of $HO^\bullet$ with the probe P, and $\sum k_s[S]$ is the pseudo-first order rate constant (s^{-1}) for $HO^\bullet$ scavenging by all the components present in the reaction medium, except the probe compound.

The scavenging rate of $HO^\bullet$ can be expressed as (Eq. 4.38) (Zepp et al. 1992):

$$r_S = \{k_P\,[P] + \sum k_s\left[S\,]\}[\,HO^\bullet\right] \tag{4.38}$$

If the concentration of P or the reaction rate for the P is sufficiently low (i.e., $\sum k_s[S] \gg k_P[P]$), it is $r_S = (\sum k_s[S])[HO^\bullet]$. Under the steady-state condition the rate of generation of $HO^\bullet$ is $r_{OH} = r_S$, from which the hydroxyl radical concentration becomes (Eq. 4..39) (Zepp et al. 1992):

$$\left[HO^\bullet\right]_{ss} = r_{HO}/\left(\sum k_s\,[S]\right) \tag{4.39}$$

The oxidation rate (Ms^{-1}) of the probe compound in an irradiated system (conversion per unit time) is described as (Eq. 4.40) (Zepp et al. 1992):

$$-d\,[P]\,/dt\ = k_P\left[HO^\bullet\right]_{ss}[P]\ = k\,[P] \tag{4.40}$$

If the concentrations of the photoactive Fe(III) species, H_2O_2, and the scavengers show a negligible variation as compared to [P], both r_{OH} and $\sum k_s[S]$ (and $[HO^\bullet]_{ss}$ as a consequence) would be about constant. That would give a pseudo-first order reaction with rate constant k. If the second-order rate constant, k_P and the scavenging rate constant, $\sum k_s[S]$ are known, then r_{OH} can be determined from k by the following equation (Eq. 4.41) (Zepp et al. 1992):

$$r_{HO} = k\left(\sum k_s\,[S]\right)/(k_P) \tag{4.41}$$

This steady-state approach has been successfully applied to examine the thermal production of $HO^\bullet$ in ozone-treated natural waters, as well as the photoinduced generation of $HO^\bullet$ upon irradiation of natural waters and of nitrate ions (Zepp et al. 1987, 1992; Haag and Hoigné 1985).

In natural waters for a thin layer at the surface of a water body, the photoinduced production rate of the reactive species (Schwarzenbach et al. 1993) can be expressed as (Eq. 4.42):

$$r_p = 2.3 \sum_{\lambda} I(\lambda) \times \varepsilon(\lambda) \times \Phi(\lambda) \times C \tag{4.42}$$

where r_P is the production rate (M s^{-1}), I is the incident light intensity (mEinstein cm^{-2} s^{-1}), φ is either the quantum yield (mol $Einstein^{-1}$) or the apparent quantum yield, ϵ and C are the absorption coefficient and the concentration of the relevant light-absorbing reactive species, respectively, and λ is the wavelength. Thus, it is possible to determine the near-surface production rate of $HO^\bullet$ from NO_3^- photolysis from Eq. (4.39), from which one gets (Eq. 4.43) (Southworth and Voelker 2003):

$$r_{\mathrm{NO3}} = \left(2 \times 10^{-7}\right) [\mathrm{NO}_3^-] \tag{4.43}$$

To obtain (Eq. 4.43), the light intensity values were integrated over wavelength for a solar declination of 20° (24-h averaged) (Schwarzenbach et al. 1993), adopting a quantum yield of 0.015 for the $HO^\bullet$ photoproduction upon nitrate irradiation at 25 °C (Zepp et al. 1987).

The degradation rate of formic acid in the photo-Fenton reaction increases with temperature (Fig. 7) (Farias et al. 2007). From the cited results it can be estimated that the conversion of HCOOH after 20 min of reaction time is increased approximately by 70–120 % at 313 K and 160–202 % at 328 K compared to the initial temperature of 298 K, with H_2O_2:HCOOH molar ratios in the range from 3 to 8 (Fig. 7). It is also observed that irradiation in the photo-Fenton system enhances degradation, compared to the corresponding dark Fenton system at equal temperature. However, the effect of irradiation is decreased dramatically as temperature increases, so that at 328 K there is little advantage in irradiating the system.

4.8 *Photo-Ferrioxalate/H_2O_2 Reaction: Dependence on pH and Reactants*

Without addition of H_2O_2 to the photo-ferrioxalate system, the reaction rate gradually increases with increasing pH as can be measured from the degradation of specific organic compounds (Jeong and Yoon 2005; Balmer and Sulzberger 1999). The pH effect is thought to involve two phenomena (Jeong and Yoon 2005; Balmer and Sulzberger 1999). First, an increase in pH may enhance the conversion of dominant ferric complexes such as $[Fe^{III}(C_2O_4)]^+$ and $[Fe^{III}(C_2O_4)_3]^{3-}$ (Eq. 3.19). It subsequently enhances the overall reaction rates through the chain reactions of $CO_2^{\bullet-}$ that form H_2O_2 and, through formation of Fe^{2+} (Eqs. 3.21, 3.23, 3.24), produce $HO^\bullet$ as a consequence (Eqs. 3.22, 3.43, 3.45, 4.23, 4.25). Second, the formation of the $Fe^{II}(C_2O_4)$ complex increases with pH and subsequently enhances the Fenton reaction, because $Fe^{II}(C_2O_4)$ can react with H_2O_2 at a faster rate (Eq. 3.25) than Fe^{2+} (Eq. 4.18). Thus, without addition of H_2O_2 the rate-determining step for the production of $HO^\bullet$ is the formation of H_2O_2. The latter is formed upon reaction of Fe(II) with $O_2^{\bullet-}$ or $HO_2^\bullet$, or from $O_2^- + H^+$ and chain propagation within $HO_2^\bullet$. $O_2^{\bullet-}$ is formed from $CO_2^{\bullet-}$ or from the reaction of O_2 with photoinduced electron (e^-), emitted upon photo-ionization of organic compounds. Therefore, an increase in pH will favor the occurrence of Fe(II), $CO_2^{\bullet-}$ and $O_2^{\bullet-}$, which leads to higher amounts of H_2O_2 and of $Fe^{II}(C_2O_4)$. Then, the reaction between H_2O_2 and $Fe^{II}(C_2O_4)$ favors the formation of $HO^\bullet$. It is obvious that higher $HO^\bullet$ photoproduction causes faster degradation of the dissolved organic substrates.

With addition of H_2O_2 to the photo-ferrioxalate system, the formation of $HO^\bullet$ depends on the concentration of H_2O_2 (Hislop and Bolton 1999; Jeong and Yoon 2005). With H_2O_2 above 10 mM the reaction rate may decrease, but the addition of H_2O_2 from 0.1 to 1 mM may enhance the degradation of organic substances. Therefore, a high concentration of H_2O_2 is a major factor for decreasing the overall formation rate of $HO^\bullet$. First of all, excess H_2O_2 can contribute significantly to the $HO^\bullet$ scavenging, consuming hydroxyl radicals and producing $HO_2^\bullet/O_2^{\bullet-}$. The latter species are then able to oxidize Fe(II), which might be kept low so that the formation rate of $HO^\bullet$ in the Fenton process is decreased. Lower $HO^\bullet$ formation and higher $HO^\bullet$ consumption by H_2O_2 can inhibit the degradation of dissolved organic compounds; the inhibition would be higher at higher pH, where the oxidation of Fe(II) by $HO_2^\bullet/O_2^{\bullet-}$ is favored.

On the other hand, relatively low levels of H_2O_2 (0.1 to 1 mM) can enhance degradation, because the addition of hydrogen peroxide would by-pass the slow step of H_2O_2 formation in the photo-ferrioxalate system without H_2O_2. Moreover, low H_2O_2 levels would not be able to scavenge $HO^\bullet$ significantly, nor to cause Fe(II) oxidation.

5 Significance of $HO^\bullet$ in Natural Waters

The $HO^\bullet$ radical is the most reactive transient among the reactive oxygen species (ROS) that can be present in natural waters. It is an effective, nonselective and strong oxidant in natural waters for the following reasons:

(i) Photoinduced transformation of DOM by $HO^\bullet$ into bioavailable compounds. An example is the degradation of persistent organic substances, which are otherwise recalcitrant to biological and chemical degradation in natural waters (Zepp et al. 1987; Miller and Chin 2002; Haag and Yao 1992; Vione et al. 2009; Grannas et al. 2006; Pullin et al. 2004; Draper and Crosby 1984; Ollis et al. 1991; Sun and Pignatello 1993; Zimbron and Reardon 2005).

(ii) Degradation of organic pollutants or DOM in natural waters (Brezonik and Fulkerson-Brekken 1998; Southworth and Voelker 2003; White et al. 2003; Westerhoff et al. 1999; Goldstone et al. 2002; Kang et al. 2000; Gao and Zepp 1998; Arslan et al. 1999; Katsumata et al. 2006; Muñoz et al. 2006; Farias et al. 2010). Suwannee River Fulvic Acid (SRFA) can produce H_2O_2, which can give $HO^\bullet$ by direct photolysis or through the Fenton reactions (Fig. 9) (Southworth and Voelker 2003). The Fenton process can also be exploited from a technological point of view. Recently, a new pilot-plant solar reactor for the photo-Fenton treatment of waters containing toxic organic substances has been developed. In this reactor, the combined photoinduced and thermal effects of sunlight can degrade 98.2 % of the initial pollutant, for a reaction time of 180 min and a relatively low iron concentration (Farias et al. 2010).

(iii) A great interest is presently devoted to the utilization of $HO^\bullet$ in the Advanced Oxidation Technology (AOT) for treatment of sewerage or industrial effluents, as a help to achieve sustainable development (Safazadeh-Amiri et al. 1996, 1997; Arslan et al. 2000; Venkatadri and Peters 1993).

(iv) The cycling of metals occurs through various redox chemical reactions in natural waters, to which $HO^\bullet$ gives a contribution (Faust 1994; Voelker et al. 1997; Jeong and Yoon 2005; Faust and Zepp 1993; Kwan and Voelker 2002; Emmenegger et al. 2001).

(v) Photoinduced generation of $HO^\bullet$ upon nitrite and nitrate photolysis in natural waters can cause hydroxylation, nitration and nitrosation reactions of many aromatic compounds or organic contaminants (Matykiewiczová et al. 2007; Torrents et al. 1997; Vione et al. 2003a, b, 2004). Some of the reaction intermediates are mutagenic or carcinogenic and are, therefore, of immense environmental concern in the water bodies.

(vi) The $HO^\bullet$ radical is for instance involved in the ultrasonically induced oxidation of arsenite, which plays a key role in the conversion of As(III) in aqueous media and may be applicable as a pretreatment step for the removal of arsenic from water (Xu et al. 2005).

6 Impact of Free Radicals on Biota (Proteins and Living Cells) and Plants

Free radicals are an unavoidable by-product in biological systems and can arise from foods containing unnecessary fat, smoking, alcohol, H_2O_2, ozone, toxins including the carcinogenic ones, ionization, environmental pollutants etc. The major sources of free radicals such as the superoxide ion (O_2^-) and the hydroperoxyl radical ($HO_2^\bullet$) are modest leakages from the electron transport chains of mitochondria, chloroplasts and the endoplasmic reticulum (Miller et al. 1990; Paradies et al. 2000; Blokhina et al. 2003). The $HO^\bullet$, alkoxyl radical ($RO^\bullet$), peroxyl radical ($ROO^\bullet$), and H_2O_2 produced from the autooxidation of biomolecules such as ascorbate, catecholamines or thiols, can damage the macromolecules such as DNA, proteins and lipids in biological systems (Miller et al. 1990; Buettner and Jurkiewicz 1996; Cadet et al. 1999; Blokhina et al. 2003; Berlett and Stadtman 1997; Morse et al. 1977; Radtke et al. 1992; Abele-Oeschger et al. 1994). These events have implications for numerous human health problems. Autoxidation reactions would mostly be catalyzed by transition metal ions (Fe^{2+}, Cu^+), and by semiquinones which can act as electron (e^-) donors (Buettner and Jurkiewicz 1996; Blokhina et al. 2003). Four-electron reduction of oxygen in the respiratory electron transport chain (ETC.) is generally associated with a partial one- to three-electron reduction, yielding reactive oxygen species such as $O_2^{\bullet-}$, $HO^\bullet$, H_2O_2, singlet oxygen ($^1O_2$) and O_3 (Blokhina et al. 2003). Both $O_2^{\bullet-}$ and $HO_2^\bullet$ undergo spontaneous dismutation to produce H_2O_2. In the presence of reduced transition metals such as Fe^{2+} or its complexes that are quite common in biological systems, the $HO^\bullet$ radical can be produced by the Fenton reaction. A mechanistic scheme for the generation of $HO^\bullet$ in biological systems can be depicted as follows (Eqs. 6.1–6.3) (Buettner et al. 1978; Buettner 1987; Buettner and Jurkiewicz 1996; Blokhina et al. 2003):

$$Fe^{3+}\text{-chelate} + O_2^{\bullet-}/AscH^\bullet \rightarrow Fe^{2+}\text{-chelate} + O_2/Asc^{\bullet-} \tag{6.1}$$

$$Fe^{2+}\text{-chelate} + H_2O_2 \rightarrow Fe^{3+}\text{-chelate} + OH^- + HO^\bullet \tag{6.2}$$

$$\text{Biomolecules} + HO^\bullet + O_2 \rightarrow Fe^{3+}\text{-chelate} + OH^- + HO^\bullet \tag{6.3}$$

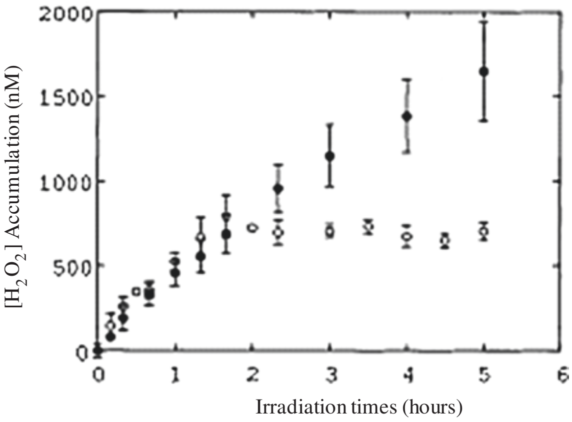

Fig. 9 H_2O_2 concentration during photoirradiation of Suwannee River Fulvic Acid (10 mg L^{-1}) solutions in the absence (●, average of five experiments) and the presence (○, average of three experiments) of Fe (10 μM) at pH 6.0. *Data source* Southworth and Voelker (2003)

where $O_2^{\bullet-}$ and ascorbate ($AscH^-$) can reduce the Fe^{3+}-chelate to form Fe^{2+}-chelate (Eq. 6.1), which subsequently reacts with H_2O_2 to form $HO^\bullet$ in the Fenton reaction (Eq. 6.2). $HO^\bullet$ then induces the oxidation of biomolecules (Eq. 6.3) in biological systems.

The presence of metals that can act as catalysts in biological systems is caused by the fact that many biomolecules bind transition metals, especially protein moieties containing oxygen, nitrogen or sulfur atoms. The transition metals are coordinated with biomolecules through the *d*-orbitals that can also permit the simultaneous binding of a biomolecule and dioxygen, thus providing a bridge between O_2 and the biomolecule (Miller et al. 1990; Buettner and Jurkiewicz 1996; Khan and Martell 1967; Valentine 1973). The major free radicals with the highest reduction potential are $HO^\bullet$, $RO^\bullet$, $LOO^\bullet$, $GS^\bullet$, urate, and even the tocopheroxyl radical ($TO^\bullet$). Ascorbate itself acts as an antioxidant by replacing a potentially very damaging radical ($X^\bullet$), through the following reaction (Buettner and Jurkiewicz 1996; Buettner 1993, 1988):

$$AscH^\bullet + X^\bullet \rightarrow Asc^{\bullet-} + XH \tag{6.4}$$

where $Asc^{\bullet-}$ is the ascorbate radical, which has low reduction potential and does not give additional reaction with O_2 to form further oxidizing species. The kinetics of these electron/hydrogen atom transfer reactions are very fast, as is observed for the equilibrium mixture of $AscH_2/AscH^-/Asc^{2-}$ at pH 7.4 which has been mentioned in earlier section (Buettner and Jurkiewicz 1996; Buettner 1988; Ross et al. 1994). Therefore, ascorbate is an excellent antioxidant from both a thermodynamic and kinetic point of view, but Asc^{2-} or $Asc^{\bullet-}$ can produce low levels of superoxide. The removal of $O_2^{\bullet-}$ by superoxide dismutase can prevent further free radical oxidation in biological systems (Buettner and Jurkiewicz 1996; Williams and Yandell 1982; Scarpa et al. 1983; Winterbourn 1993).

One of the most important impacts of harmful solar UV radiation in biological systems is the skin cancer, which is generally induced by the photoinduced production of free radicals. Formation of $^1O_2$ within cell membranes is caused by the photodynamic action of the photosensitizers photofrin and merocyanine 540 (Buettner and Jurkiewicz 1996). The $^1O_2$ reacts with the membrane lipids to form lipid hydroperoxides (LOOH). Skin is a significant iron excretion site (Green et al. 1968), and Fe(II) can react with LOOH to form highly oxidizing lipid alkoxyl radicals ($LO^\bullet$) by a Fenton-like reaction (Eq. 6.5):

$$Fe^{2+} + LOOH \rightarrow Fe^{3+} + LO^\bullet + OH^- \tag{6.5}$$

Applications of iron chelators to the skin can give photoprotection in the case of chronic exposure to UV radiation, by reducing the formation of free radicals (Bissett et al. 1991).

Second, another most important impact of $HO^\bullet$ is the declining of plants by the effect of $HO^\bullet$, which is formed in dew waters of plants by several sources such as NO_2^-, NO_3^- and H_2O_2 + Fe + oxalate system present in the plants

(Arakaki et al. 1998, 1999a, b; Arakaki and Faust 1998; Nakatani et al. 2001; Kobayashi et al. 2002). It is considered that the $HO^\bullet$ formed in the liquid phase on the needle surfaces of Japanese red pine, which are frequently present in the dew on sunny mornings in the warm-temperate region, are the cause of ecophysiological disorders in plants (Kobayashi et al. 2002).These effects subsequently affect to decrease in the maximum CO_2 assimilation rate, stomatal conductance, minimal fluorescence and needle lifespan (Kume et al. 2000).

7 Summary and Scope of the Future Challenges

The $HO^\bullet$ radical is the most reactive among the many oxygen transient species produced photolytically in natural waters. However, a few studies on $HO^\bullet$ production have been conducted on fresh- and seawater as a whole. The $HO^\bullet$ production in acidic lake waters is not well investigated, although it is known that acidification enhances the formation of $HO^\bullet$ (Vione et al. 2009). The $HO^\bullet$ production varies with the contents of DOM, which may be a key factor to understand the photoinduced processes in a variety of natural waters. Moreover, there is no study conducted about production of alkoxide radicals ($RO^\bullet$) and their role in the photodegradation kinetics of DOM along with $HO^\bullet$. An example of key possible research on free radicals needed for the future challenges are: (i) Effect of pH and temperature on the production of $HO^\bullet$ for a variation in quality and quantity of DOM in natural waters. (ii) Investigation on the sources of free radicals ($HO^\bullet$ and $RO^\bullet$), particularly from fluorescent dissolved organic matter (FDOM) for a variety of waters. (iii) Photoinduced generation of alkoxide radicals ($RO^\bullet$) and their relative reaction kinetics with respect to $HO^\bullet$ and other solution components. (iv) Impacts of free radicals on specific biota in the aquatic environment.

Problems

(1) List the various sources of $HO^\bullet$ and their role in natural waters.
(2) List three important free radical species except $HO^\bullet$ and their importance in natural waters.
(3) How is the steady state concentration of $HO^\bullet$ defined, and why does the steady state concentration vary for a variety of natural waters?
(4) Explain why the potential of $HO^\bullet$ formation is low in surface waters compared to those of deep lakes and the sea.
(5) Mention the important processes of $HO^\bullet$ formation in natural waters and explain the mechanism of in situ generation of $HO^\bullet$ from DOM via H_2O_2.
(6) Explain why the photo-Fenton reaction is more suitable than the Fenton reaction in the degradation of organic pollutants in aqueous solution.

(7) Explain how the photo-ferrioxalate/H_2O_2 reaction system degrades the organic pollutants in the aqueous solution.
(8) Explain how photocatalytic TiO_2 suspensions degrade the organic pollutants in aqueous solutions.
(9) What are the controlling factors for the production and decay of $HO^\bullet$? Explain how fulvic acid plays a dual role in production and decay of $HO^\bullet$.
(10) Explain the effect of wavelength spectrum, temperature, and pH on the formation of $HO^\bullet$ from nitrite and nitrate photolysis in aqueous solution.
(11) Explain the effect of wavelength spectrum and temperature on H_2O_2 photolysis in aqueous solution.
(12) Explain how the Fenton reaction is affected by pH, temperature and salinity in natural waters.
(13) Explain what the photo-Fenton reaction is and what is its kinetics.
(14) What is the photo-ferrioxalate/H_2O_2 reaction? How is this reaction system affected by variations in pH and reactants in aqueous solution?
(15) The quantum yield (Φ_{HO}) for the UV photoproduction of $HO^\bullet$ by nitrite photolysis at 308 nm is 0.07 at room temperature (298 K). Calculate Φ_{HO} at the temperatures of 288 and 328 K.
(16) The Φ_{HO} for the UV photoproduction of $HO^\bullet$ by nitrate photolysis at 308 nm is 0.017 at room temperature (298 K). Calculate the Φ_{HO} at the temperatures of 278 and 318 K.
(17) If the photolysis of aqueous H_2O_2 at 308 nm generates $HO^\bullet$ with $\Phi_{HO} = 1$ at room temperature (298 K), then calculate Φ_{HO} at 288 and 303 K.
(18) Explain shortly the significance of $HO^\bullet$ formation in natural waters.
(19) Explain how $HO^\bullet$ impacts on biota in natural waters.

Acknowledgments This work was financially supported jointly by the National Natural Science Foundation of China and the Chinese Academy of Sciences. This work was partly supported by Hiroshima University, Japan; PNRA—Progetto Antartide, University of Turin, Italy; Brook Byers Institute for Sustainable Systems at Georgia Institute of Technology, the United States; Aligarh Muslim University, India; and Northwest Missouri State University, USA. This chapter acknowledges the reprinted from reprinted (adapted) with permission from Kwan WP, Voelker BM, Decomposition of hydrogen peroxide and organic compounds in the presence of dissolved iron and ferrihydrite, Environmental Science & Technology, 36 (7), 1467–1476. Copyright (2002) Americal Chemical Society; reprinted (adapted) with permission from Farias J, Rossetti GH, Albizzati ED, Alfano OM, Solar degradation of formic acid: temperature effects on the photo-Fenton reaction. Industrial & Engineering Chemistry Research, 46(23):7580–7586). Copyright (2007) American Chemical Society; reprinted from Journal of Photochemistry and Photobiology A: Chemistry, 128(1–3), Mack J, Bolton JR, Photochemistry of nitrite and nitrate in aqueous solution: a review, 1–13. Copyright (1999), with permission from Elsevier; reprinted from Geochimica et Cosmochimica Acta, 53(8), Millero FJ, Sotolongo S, The oxidation of Fe(II) with H_2O_2 in seawater, 1867–1873. Copyright (1989), with permission from Elsevier; reprinted (adapted) with permission from Southworth BA, Voelker BM, Hydroxyl radical production via the photo-Fenton reaction in the presence of fulvic acid, Environmental Science & Technology, 37(6), 1130–1136. Copyright (2003) American Chemical Society; reprinted with permission from Zepp RG, Faust BC, Hoigné J, Hydroxyl radical formation in aqueous reactions (pH 3–8) of iron(II) with hydrogen peroxide: The Photo-Fenton reaction, Environmental Science & Technology, 26 (2), 313–319. Copyright

(1992) American Chemical Society; and reprinted from Water Research, 39(13), Jeong J, Yoon J, pH effect on OH radical production in photo/ferrioxalate system, 2893–2900. Copyright (2005), with permission from Elsevier; reprinted (adapted) with permission from Balmer ME, Sulzberger B, Atrazine degradation in irradiated iron/oxalate system: effects of pH and oxalate, Environmental Science & Technology, 33 (14), 2418–2424. Copyright (1999) American Chemical Society; Springer and the original Journal of Atmospheric Chemistry, 10, 1990, 411–425, Absolute OH quantum yields in the laser photolysis of nitrate, nitrite and dissolved H_2O_2 at 308 and 351 nm in the temperature range 278–353 K, Journal of Atmospheric Chemistry, Zellner R, Exner M, Herrmann H, with kind permission from Springer Science and Business Media; reprinted from Journal of Electrostatics, 39(3), Sun B, Sato M, Sid Clements J, Optical study of active species produced by a pulsed streamer corona discharge in water, 189–202, Copyright (1997), with permission from Elsevier; and Copyright (2004) by The Japan Society for Analytical Chemistry.

References

Abele-Oeschger D, Oeschger R, Theede H (1994) Biochemical adaptations of Nereis diversicolor (Polychaeta) to temporarily increased hydrogen peroxide levels in intertidal sandflats. Mar Ecol Prog Ser 106:101–110

al Housari F, Vione D, Chiron S, Barbati S (2010) Reactive photoinduced species in estuarine waters Characterization of hydroxyl radical, singlet oxygen and dissolved organic matter triplet state in natural oxidation processes. Photochem Photobiol Sci 9:78–86

Aldrich AP, van Berg den CMG, Thies H, Nickus U (2001) The redox speciation of iron in two lakes. Mar Freshw Res 52:885–890

Alegria AE, Ferrer A, Sepulveda E (1997) Photochemistry of water-soluble quinones production of a water-derived spin adduct. Photochem Photobiol 66:436–442

Allen JM, Lucas S, Allen SK (1996) Formation of hydroxyl radical in illuminated surface waters contaminated with acid mine drainage. Environ Sci Technol 15:107–113

Anastasio C, Jordan AL (2004) Photoformation of hydroxyl radical and hydrogen peroxide in aerosol particles from Alert, Nunavut: implications for aerosol and snowpack chemistry in the Arctic. Atmos Environ 38:1153–1166

Anastasio C, Newberg JT (2007) Sources and sinks of hydroxyl radical in sea-salt particles. J Geophys Res 112:D10306. doi:101029/2006JD008061

Anastasio C, Galbavy ES, Hutterli MA, Burkhart JF, Friel DK (2007) Photoformation of hydroxyl radical on snow grains at Summit Greenland. Atmos Environ 41:5110–5121

Arakaki T, Faust BC (1998) Sources, sinks, and mechanisms of hydroxyl radical (OH) photoproduction and consumption in authentic acidic continental cloud waters from Whiteface Mountain, New York: the role of the Fe(r) (r = II, III) photochemical cycle. J Geophys Res 103(D3):3487–3504

Arakaki T, Miyake T, Shibata M, Sakugawa H (1998) Measurement of photolytically formed hydroxyl radical in rain and dew waters. Nippon Kagaku Kaishi 9:619–625

Arakaki T, Miyake T, Hirakawa T, Sakugawa H (1999a) pH dependent photoformation of hydroxyl radical and absorbance of aqueous-phase N(III) (HNO2 and NO2-). Environ Sci Technol 33:2561–2565

Arakaki T, Miyake T, Shibata M, Sakugawa H (1999b) Photochemical formation and scavenging of hydroxyl radical in rain and dew waters. Nippon Kagaku Kaishi 5:335–340 (in Japanese)

Arslan I, Barcioglu A, Tuhkanen T (1999) Oxidative treatment of simulated dyehouse effluent by UV and near-UV light assisted Fenton's reagent. Chemosphere 39:2767–2783

Arslan I, Balcioglu IA, Bahnemann DW (2000) Advanced chemical oxidation of reactive dyes in simulated dyehouse effluents by ferrioxalate-Fenton/UV-A and TiO_2/UV-A processes. Dyes Pigm 47:207–218

Assel M, Laenen R, Laubereau A (1998) Ultrafast electron trapping in an aqueous NaCl-solution. Chem Phys Lett 289:267–274

Balmer ME, Sulzberger B (1999) Atrazine degradation in irradiated iron/oxalate system: effects of pH and oxalate. Environ Sci Technol 33:2418–2424

Barb WG, Boxendale JH, George P, Hargrove KR (1951) Reactions of ferrous and ferric ions with hydrogen peroxide, part II The ferric ion reaction. Trans Faraday Soc 47:591–616

Barbeni M, Minero C, Pelizzetti E (1987) Chemical degradation of chlorophenols with Fenton's reagent. Chemosphere 16:2225–2237

Bard AJ (1979) Photoelectro chemistry and heterogeneous photocatalysis at semiconductors. J Photochem 10:59–75

Baxendale JH, Wilson JA (1956) The photolysis of hydrogen peroxide at high light intensities. Trans Faraday Soc 53:344–356

Benson SW (1960) The foundation of chemical kinetics Ch 15. McGraw-Hill, New York

Berger P, Leitner N Karpel Vel, Doré M, Legube B (1999) Ozone and hydroxyl radicals induced oxidation of glycine. Water Res 33:433–441

Berlett BS, Stadtman ER (1997) Protein oxidation in aging, disease, and oxidative stress. J Biol Chem 272:20313–20316

Bertilsson S, Tranvik LJ (1998) Photolytically produced carboxylic acids as substrates for freshwater bacterioplankton. Limnol Oceanogr 43:885–895

Bielski BHJ, Cabelli DE, Arudi RL, Ross AB (1985) Reactivity of $HO2^{\bullet}/O2^{\bullet -}$ radicals in aqueous solution. J Phys Chem Ref Data 14:1041–1100

Bissett DL, Chatterjee R, Hannon DP (1991) Chronic ultraviolet radiation-induced increase in skin iron and the photoprotective effects of topically applied iron chelators. Photochem Photobiol 54:215–223

Blokhina O, Virolainen E, Fagerstedt KV (2003) Antioxidants, oxidative damage and oxygen deprivation stress: a review. Ann Bot 91:179–194

Blough NV (1988) Electron paramagnetic resonance measurements of photochemical radical production in humic substances: 1 Effects of O_2 and charge on radical scavenging by nitroxides. Environ Sci Technol 22:77–82

Blough NV, Zepp RG (1995) Reactive oxygen species in natural waters. In: Foote CS, Valentine JS (eds) Active oxygen in chemistry. Blackie Academic and Professional, New York, pp 280–333

Bossmann SH, Oliveros E, Gob S, Siegwart S, Dahlen EP, Payawan L, Straub M, Worner M, Braun AM (1998) New evidence against hydroxyl radicals as reactive intermediates in the thermal and photolytically enhanced Fenton reactions. J Phys Chem A 102:5542–5550

Bourdat A-G, Douki T, Frelon S, Gasparutto D, Cadet J (2000) Tandem base lesions are generated by hydroxyl radical within isolated DNA in aerated aqueous solution. J Am Chem Soc 122:4549–4556

Brezonik PL, Fulkerson-Brekken J (1998) Nitrate-induced photolysis in natural waters: controls on concentrations of hydroxyl radical photo-intermediates by natural scavenging agents. Environ Sci Technol 32:3004–3010

Brigante M, Charbouillot T, Vione D, Mailhot G (2010a) Photochemistry of 1-nitronaphthalene: a potential source of singlet oxygen and radical species in atmospheric waters. J Phys Chem A 114:2830–2836

Brigante M, Charbouillot T, Vione D, Mailhot G (2010b) Photochemistry of 1-nitronaphthalene: a potential source of singlet oxygen and radical species in atmospheric waters. J Phys Chem A 114:2830–2836

Buettner GR (1987) Activation of oxygen by metal complexes and its relevance to autoxidative processes in living systems. Bioelectochem Bioenerg 18:29–36

Buettner GR (1988) In the absence of catalytic metals ascorbate does not autoxidize at pH 7: ascorbate as a test for catalytic metals. J Biochem Biophys Methods 16:27–40

Buettner GR (1993) The pecking order of free radicals and antioxidants: Lipid peroxidation, α-tocopherol, and ascorbate. Arch Biochem Biophys 300:535–543

Buettner GR, Jurkiewicz BA (1996) Catalytic metals, ascorbate and free radicals: combinations to avoid. Radiat Res 145:532–541

Buettner GR, Oberley LW, Leuthauser SWHC (1978) The effect of iron on the distribution of superoxide and hydroxyl radicals as seen by spin trapping and on the superoxide dismutase assay. Photochem Photobiol 28:693–695

Buxton GV, Greenstock CL, Helman WP, Ross AB (1988) Critical review of rate constants for reaction of hydrated electrons, hydrogen atoms and hydroxyl radicals (OH/O^-) in aqueous solution. J Phys Chem Ref Data 17:513–886

Cadet J, Delatour T, Douki T, Gasparutto D, Pouget J-P, Ravanat J-L, Sauvaigo S (1999) Hydroxyl radicals and DNA base damage. Mutat Res Fundam Mol Mech Mutagen 424:9–21

Canonica S, Kohn T, Mac M, Real FJ, Wirz J, von Gunten U (2005) Photosensitizer method to determine rate constants for the reaction of carbonate radical with organic compounds. Environ Sci Technol 39:9182–9188

Chen R, Pignatello JJ (1997) Role of quinone intermediates as electron shuttles in Fenton and photoassisted Fenton oxidations of aromatic compounds. Environ Sci Technol 31:2399–2406

Chen C, Li X, Ma W, Zhao J, Hidaka H, Serpone N (2001) Effect of transition metal ions on the TiO_2-assisted photodegradation of dyes under visible irradiation: a probe for the interfacial electron transfer process and reaction mechanism. J Phys Chem B 106:318–324

Chu L, Anastasio C (2003) Quantum yields of hydroxyl radical and nitrogen dioxide from the photolysis of nitrate on ice. J Phys Chem A 107:9594–9602

Chu L, Anastasio C (2005) Formation of hydroxyl radical from the photolysis of frozen hydrogen peroxide. J Phys Chem A 109:6264–6271

Cohen G, Heikkila E (1974) The Generation of hydrogen peroxide, superoxide radical, and hydroxyl radical by 6-hydroxydopamine, dialuric acid, and related cytotoxic agents. J Biol Chem 249:2447–2452

Collen J, del Rio MJ, Garcia-Reina G, Pedersen M (1995) Photosynthetic production of hydrogen peroxide by Ulva rigida C Ag (Chlorophyta). Planta 196:225–230

Cooper WJ, Zika RG, Petasne RG, Fischer AM (1988) Sunlight-induced photochemistry of humic substances in natural waters: major reactive species In: Suffett IH, MacCarthy P (eds) Aquatic humic substances. American Chemical Society, Washington, pp 333–362

Cooper WJ, Nickelson MG, Waite TD, Kurucz CN (1991) High energy electron beam irradiation: an advanced oxidation process for the treatment of aqueous based organic hazardous wastes. J Environ Sci Health A27:219

Cooper WJ, Sawal KL, Hoogland YS, Slifker R, Nickelsen MG, Kurucz CN, Waite TD (1996) Disinfection by-product precursor removal from natural waters using gamma radiation to stimulate an innovative water treatment process. In: Minear RA, Amy GL (eds) Disinfection bi-products in water treatment. CRC Press, Inc, Boca Raton, pp 151–162

Croot PL, Laan P, Nishioka J, Strass V, Cisewski B, Boye M, Timmermans KR, Bellerby RG, Goldson L, Nightingale P, de Baar HJW (2005) Spatial and temporal distribution of Fe(II) and H_2O_2 during EisenEx, an open ocean mescoscale iron enrichment. Mar Chem 95:65–88

Das R, Dutta BK, Maurino V, Vione D, Minero C (2009) Suppression of inhibition of substrate photodegradation by scavengers of hydroxyl radicals: the solvent-cage effect of bromide on nitrate photolysis. Environ Chem Lett 7:337–342

de Laat J, Gallard H (1999) Catalytic decomposition of hydrogen peroxide by Fe(III) in homogeneous aqueous solution: mechanism and kinetic modeling. Environ Sci Technol 33:2726–2732

del Vecchio R, Blough NV (2002) Photobleaching of chromophoric dissolved organic matter in natural waters: kinetics and modeling. Mar Chem 78:231–253

Dister B, Zafiriou OC (1993) Photochemical free-radical production-rates in the eastern Caribbean. J Geophys Res Oceans 98(C2):2341–2352

Draper WM, Crosby DG (1981) Hydrogen peroxide and hydroxyl radical intermediates in indirect photolysis reactions in water. J Agric Food Chem 32:231–237

Draper WM, Crosby DG (1984) Solar photooxidation of pesticides in dilute H_2O_2. J Agric Food Chem 32:231–237

Duesterberg CK, Waite TD (2006) Process optimization of Fenton oxidation using kinetic modeling. Environ Sci Technol 40:4189–4195

Duesterberg CK, Cooper WJ, Waite TD (2005) Fenton-mediated oxidation in the presence and absence of oxygen. Environ Sci Technol 39:5052–5058

Duesterberg CK, Mylon SE, Waite TD (2008) pH effects on iron-catalyzed oxidation using Fenton's reagent. Envion Sci Technol 42:8522–8527

Dykens JA, Shick JM, Benoit C, Buettner GR, Winston GW (1992) Oxygen radical production in the sea anemone Anthopleura Elegantissima and its endosymbiotic algae. J Exp Biol 168:219–241

Emilio CA, Jardim WF, Littera MI, Mansilla HD (2002) EDTA destruction using the solar ferrioxalate AOT comparison with solar photo-Fenton. J Photochem Photobiol A Chem 151:121–127

Emmenegger L, Schwarzenbach R, Sigg L, Sulzberger B (2001) Light-induced redox cycling of iron in circumneutral lakes. Limnol Oceanogr 46:49–61

Ervens B, Gligorovski B, Herrmann H (2003) Temperature-dependent rate constants for hydroxyl radical reactions with organic compounds in aqueous solutions. Phys Chem Chem Phys 5:1811–1824

Fang X, Mark G, von Sonntag C (1996) OH radical formation by ultrasound in aqueous solutions part I: the chemistry underlying the terephthalate dosimeter. Ultrason Sonochem 3:57–63

Farias J, Rossetti GH, Albizzati ED, Alfano OM (2007) Solar degradation of formic acid: temperature effects on the photo-Fenton reaction. Ind Eng Chem Res 46:7580–7586

Farias J, Albizzati ED, Alfano OM (2010) New pilot-plant photo-Fenton solar reactor for water decontamination. Ind Eng Chem Res 49:1265–1273

Faust BC (1994) A review of the photochemical redox reactions of iron species in atmosphere, oceanic, and surface waters: influences of geochemical cycles and oxidant formation. Helz GR, Zepp RG, Crosby DG (eds) Aquatic and surface photochemistry. Lewis Publishers, Boca Raton, pp 3–38

Faust BC, Allen JM (1992) Aqueous-phase photochemical sources of peroxyl radicals and singlet molecular-oxygen in clouds and fog. J Geophys Res Atmos 97(D12):12913–12926

Faust BC, Hoigne J (1987) Sensitized photooxidation of phenols by fulvic acid and in natural waters. Environ Sci Technol 21:957–964

Faust BC, Zepp RG (1993) Photochemistry of aqueous iron(III)-polycarboxylate complexes: roles in the chemistry of atmospheric and surface waters. Environ Sci Technol 27:2517–2522

Fenton HJ (1894) Oxidation of tartaric acid in presence of iron. J Chem Soc 65:899–910

Fischer AM, Kliger DS, Winterle JS, Mill T (1985) Direct observations of phototransients in natural waters. Chemosphere 14:1299–1306

Fox MA (1993) The role of hydroxyl radicals in the photocatalyzed detoxification of organic pollutants—pulse-radiolysis and time-resolved diffuse-reflectance measurements. In: Ollis DF, Alekabi H (eds) Trace metals in the environment, 3, pp 163–167

Fu P, Mostofa KMG, Wu FC, Liu CQ, Li W, Liao H, Wang L, Wang J, Mei Y (2010) Excitation-emission matrix characterization of dissolved organic matter sources in two eutrophic lakes (Southwestern China Plateau). Geochem J 44:99–112

Gallard H, De Laat J Legube B (1998) Effect of pH on the oxidation rate of organic compounds by FeII/H_2O_2 mechanisms and simulation. New J Chem 22:263–268

Gan D, Jia M, Vaughan PP, Falvey DE, Blough NV (2008) Aqueous photochemistry of methylbenzoquinone. J Phys Chem A 112:2803–2812

Gao H, Zepp RG (1998) Factors influencing photoreactions of dissolved organic matter in a coastal river of the southern United States. Environ Sci Technol 32:2940–2946

Gjessing ET, Källqvist T (1991) Algicidal and chemical effect of uv-radiation of water containing humic substances. Water Res 25:491–494

Goldstein S, Rabani J (2008) Polychromatic UV photon irradiance measurements using chemical actinometers based on NO_3^- and H_2O_2 excitation: applications for industrial photoreactors. Environ Sci Technol 42:3248–3253

Goldstein S, Aschengrau D, Diamant Y, Rabani J (2007) Photolysis of aqueous H_2O_2: quantum yield and applications for polychromatic UV actinometry in photoreactors. Environ Sci Technol 41:7486–7490

Goldstone JV, Pullin MJ, Bertilsson S, Voelker BM (2002) Reactions of hydroxyl radical with humic substances: bleaching, mineralization, and production of bioavailable carbon substrates. Environ Sci Technol 36:364–372

Gopinathan C, Damle PS, Hart EJ (1972) Gamma-Ray irradiated sodium chloride as a source of hydrated electrons. J Phys Chem 76:3694–3698

Grannas AM, Martin CB, Chin Y, Platz M (2006a) Hydroxyl radical production from irradiated Arctic dissolved organic matter. Biogeochemistry 78:51–66

Grannas AM, Martin CB, Chin Y, Platz M (2006b) Hydroxyl radical production from irradiated Arctic dissolved organic matter. Biogeochemistry 78:51–66

Grebel JE, Pignatello JJ, Song W, Cooper WJ, Mitch WA (2009) Impact of halides on the photobleaching of dissolved organic matter. Mar Chem 115:134–144

Green R, Charlton R, Seftel H, Bothwell T, Mayet F, Adams B, Finch C, Layrisse M (1968) Body iron excretion in man: a collaborative study. Am J Med 45:336–353

Haag WR, Hoigné J (1985) Photo-sensitized oxidation in natural water via OH radicals. Chemosphere 14:1659–1671

Haag WR, Yao CCD (1992) Rate constants for reaction of hydroxyl radicals with several drinking water contaminants. Environ Sci Technol 26:1005–1013

Haber F, Weiss J (1934) The catalytic decomposition of hydrogen peroxide by iron salts. Proc R Soc Lond Ser A 147:332–351

Han F, Kambala VSR, Srinivasan M, Rajarathnam D, Naidu R (2009) Tailored titanium dioxide photocatalysts for the degradation of organic dyes in wastewater treatment: a review. Appl Catal A Gen 359:25–40

Hardwick TJ (1957) The rate constant of the reaction between ferrous ions and hydrogen peroxide in acid solution. Can J Chem 35:428–436

Henglein A (1987) Sonochemistry: historical developments and modern aspects. Ultrasonics 25:6–16

Hislop KA, Bolton JR (1999) The photochemical generation of hydroxyl radicals in the UV-vis/ferrioxalate/H_2O_2 system. Environ Sci Technol 33:3119–3126

Ho P (1986) Photooxidation of 2,4 dinitrotoluene in aqueous solution in the presence of H_2O_2. Environ Sci Technol 20:260–267

Hoigné J, Bader H (1978) Ozone and hydroxyl radical-initiated oxidations of organic and organometallic trace impurities in water. In: Brinkman FE, Bellama JM (eds) Organometals and organometalloids occurrence and fate in the environment. American Chemical Society, Washington, pp 292–313

Hoigné J, Bader H (1979) Ozonation of water: oxidation-competition values of different types of waters used in Switzerland. Ozone Sci Eng 1:357–372

Hoigné J, Faust BC, Haag WR, Zepp RG (1988) In influence of aquatic humic substances on fate and treatment of pollutants. In: MacCarthy P, Suffet IH (eds) ACS Symposium Series 219. American Chemical Society, Washington, pp 363–383

Hoigné J, Faust BC, Haag WR, Scully FE, Zepp RG (1989) Aquatic humic substances as sources and sinks of photolytically produced transient reactants. In: Suffett IH, MacCarthy P (eds) Aquatic humic substances: influence on fate and treatment of pollutants. American Chemical Society, Washington, pp 363–381

Hoigne′ J (1998) Chemistry of aqueous ozone and transformation of pollutants by ozonation and advanced oxidation processes. In: Hrubec J (ed) The handbook of environmental chemistry. Springer Verlag, Heidelberg, pp 83–141

Holder-Sandvik SL, Bilski P, Pakulski JD, Chignell CF, Coffin RB (2000) Photogeneration of singlet oxygen and free radicals in dissolved organic matter isolated from the Mississippi and Atchafalaya River plumes. Mar Chem 69:139–152

Hunt JP, Taube H (1952) The photochemical decomposition of hydrogen peroxide quantum yields, tracer and fractionation effects. J Am Chem Soc 74:5999–6002

Huston PL, Pignatello JJ (1996) Reduction of perchloroalkanes by ferrioxalate-generated carboxylate radical preceding mineralization by the photo-Fenton reaction. Environ Sci Technol 30:3457–3463

Jakob DJ (1986) Chemistry of OH in remote clouds and its role in the production of formic acid and peroxymonosulfate. J Geophys Res 91:9807–9826

Jeong J, Yoon J (2004) Dual roles of $CO2^{-}$ for degrading synthetic organic chemicals in the photo/ferrioxalate system. Water Res 38:3531–3540

Jeong J, Yoon J (2005) pH effect on OH radical production in photo/ferrioxalate system. Water Res 39:2893–2900

Jung YS, Lim WT, Park JY, Kim YH (2009) Effect of pH on Fenton and Fenton-like oxidation. Environ Technol 30:183–190

Kang SF, Liao CH, Po ST (2000) Decolorization of textile wastewater by photo-Fenton oxidation technology. Chemosphere 41:1287–1294

Kang NG, Lee D, Yoon J (2002) Kinetic modeling of Fenton oxidation of phenol and monochlorophenols. Chemosphere 47:915–924

Katsumata H, Kaneco S, Suzuki T, Ohta K, Yobico Y (2006) Photo-Fenton degradation of alachlor in the presence of citrate solution. J Photochem Photobiol A Chem 180:38–45

Khan MMT, Martell AE (1967) Metal ion and metal chelate catalyzed oxidation of ascorbic acid by molecular oxygen I cupric and ferric ion catalyzed oxidation. J Am Chem Soc 89:4176–4185

Kieber DJ, Blough NV (1990) Determination of carboncentered radicals in aqueous solution by liquid chromatography with fluorescence detection. Anal Chem 62:2275–2283

Kobayashi T, Nakatani N, Hirakawa T, Suzuki M, Miyake T, Chiwa M, Yuhara T, Hashimoto N, Inoue K, Yamamura K, Agus N, Sinogaya JR, Nakane K, Kume A, Arakaki T, Sakugawa H (2002) Variation in CO2 assimilation rate induced by simulated dew waters with different sources of hydroxyl radical ($^{\bullet}OH$) on the needle surfaces of Japanese red pine (*Pinus densiflora* Sieb Et Zucc.). Environ Pollut 118:383–391

Komissarov GG (2003) Photosynthesis: the physical-chemical approach. J Adv Chem Phys 2:28–61

Konstantinou IK, Albanis TA (2004) TiO2-assisted photocatalytic degradation of azo dyes in aqueous solution: kinetic and mechanistic investigations: a review. Appl Catal B Environ 49:1–14

Kremer ML (1999) Mechanism of the Fenton reaction evidence for a new intermediate. Phys Chem Chem Phys 1:3595–3605

Kume A, Tsuboi N, Satomura T, Suzuki M, Chiwa M, Nakane K, Sakurai N, Horikoshi T, Sakugawa H (2000) Physiological characteristics of Japanese red pine, Pinus densiflora Sieb et Zucc, in declined forests at Mt Gokurakuji in Hiroshima Prefecture, Japan. Trees 14:305–311

Kwan WP, Voelker BM (2002) Decomposition of hydrogen peroxide and organic compounds in the presence of dissolved iron and ferrihydrite. Environ Sci Technol 36:1467–1476

Langford JH, Carey CH (1975) Outer-sphere oxidations of alcohols and formic acid by charge transfer excited states of iron(III) species. Can J Chem 53:2436–2440

Le Truong G, De Laat J, Legube B (2004) Effects of chloride and sulfate on the rate of oxidation of ferrous ion by H_2O_2. Water Res 38:2384–2394

Lee C, Sedlak DL (2009) A novel homogeneous Fenton-like system with Fe(III)-phosphotungstate for oxidation of organic compounds at neutral pH values. J Mol Catal A Chem 311:1–6

Lee Y, Jeong J, Lee C, Yoon J (2003a) Influence of various reaction parameters on 2,4-D removal in photo/ferrioxalate/H_2O_2 process. Chemosphere 51:901–912

Lee Y, Lee C, Yoon J (2003b) High temperature dependence of 2,4-dichlorophenoxyacetic acid degradation by Fe^{3+}/H_2O_2 system. Chemosphere 51:963–971

Lee C, Keenan CR, Sedlak DL (2008) Polyoxometalate-enhanced oxidation of organic compounds by nanoparticulate zero-valent iron and ferrous ion in the presence of oxygen. Environ Sci Technol 42:4921–4926

Legrini O, Oliveros E, Braun AM (1993) Photochemical processes for water treatment. Chem Rev 93:671–698

Lehninger AL (1970) Biochemistry. Worth, New York, p 478

Li SX, Hong HS, Zheng FY, Deng NS (2008) Effects of metal pollution and macronutrient enrichment on the photoproduction of hydroxyl radicals in seawater by the alga Dunaliella salina. Mar Chem 108:207–214

Lindsey ME, Tarr MA (2000a) Quantitation of hydroxyl radical during Fenton oxidation following a single addition of iron and peroxide. Chemosphere 41:409–417

Lindsey ME, Tarr MA (2000b) Inhibited hydroxyl radical degradation of aromatic hydrocarbons in the presence of dissolved fulvic acid. Water Res 34:2385–2389

Lloyd RV, Hanna PM, Mason RP (1997) The origin of the hydroxyl radical oxygen in the Fenton reaction. Free Radic Biol Med 22:885–888

Mabury SA (1993) Hydroxyl radical in natural waters. Ph D dissertation, University of California, Davis, California

Machulek A, Moraes JEF, Vautier-Giongo C, Silverio CA, Friedrich LC, Nascimento CAO, Gonzalez MC, Quina FH (2007) Abatement of the inhibitory effect of chloride anions on the photo-Fenton process. Environ Sci Technol 41:8459–8463

Mack J, Bolton JR (1999) Photochemistry of nitrite and nitrate in aqueous solution: a review. J Photochem Photobiol A Chem 128:1–13

Maddigapu PR, Bedini A, Minero C, Maurino V, Vione D, Brigante M, Mailhot G, Sarakha M (2010) The pH-dependent photochemistry of anthraquinone-2-sulfonate. Photochem Photobiol Sci 9:323–330

Maddigapu PR, Minero C, Maurino V, Vione D, Brigante M, Charbouillot T, Sarakha M, Mailhot G (2011) Photoinduced and photosensitised reactions involving 1-nitronaphthalene and nitrite in aqueous solution. Photochem Photobiol Sci 10:601–609. doi:http:dxdoiorg/101039/C0PP00311E

Mageli OL, Kolczynski JR (1966) Organic peroxides. Ind Eng Chem 58:25–32

Makino K, Mossoba MM, Riesz P (1983) Chemical effects of ultrasound on aqueous solutions formation of hydroxyl radicals and hydrogen atoms. J Phys Chem 87:1369–1377

Mark G, Korth H-G, Schuchmann H-P, von Sonntag C (1996) The photochemistry of aqueous nitrate ion revisited. J Photochem Photobiol A Chem 101:89–103

Matykiewiczová N, Kurková R, Klánová J, Klán P (2007) Photolytically induced nitration and hydroxylation of organic aromatic compounds in the presence of nitrate or nitrite in ice. J Photochem Photobiol A Chem 187:24–32

Maurino V, Borghesi D, Vione D, Minero C (2008) Transformation of phenolic compounds upon UVA irradiation of anthraquinone-2-sulfonate. Photochem Photobiol Sci 7:321–327

McKnight DM, Kimball BA, Bencala KE (1988) Iron photoreduction and oxidation in an acidic mountain stream. Science 240:637–640

Meyerstein D, Treinin A (1961) Absorption spectra of NO_3^- in solution. Tram Faraday Soc 57:2104–2112

Micinski E, Ball LA, Zafiriou OC (1993) Photochemical oxygen activation: Superoxide radical detection and production rates in the eastern Caribbean. J Geophys Res Oceans 98(C2):2299–2306

Mill T, Hendry DG, Richardson H (1980) Free-radical oxidants in natural waters. Science 207:886–887

Miller PL, Chin YP (2002) Photoinduced degradation of carbaryl in wetland surface water. J Agric Food Chem 50:6758–6765

Miller DM, Buettner GR, Aust SD (1990) Transition metals as a catalysts of "autoxidation" reactions. Free Radic Biol Med 8:95–108

Miller WL, King DW, Lin J, Kester DR (1995) Photochemical redox cycling of iron in coastal seawater. Mar Chem 50:63–77

Miller WL, Moran MA, Sheldon WM, Zepp RG, Opsahl S (2002) Determination of apparent quantum yield spectra for the formation of biologically labile photoproducts. Limnol Oceanogr 47:343–352

Millero FJ, Sotolongo S (1989) The oxidation of Fe(II) with H_2O_2 in seawater. Geochim Cosmochim Acta 53:1867–1873

Millington KR, Maurdev G (2004) The generation of superoxide and hydrogen peroxide by exposure of fluorescent whitening agents to UVA radiation and its relevance to the rapid photoyellowing of whitened wool. J Photochem Photobiol A Chem 165:177–185

Minakata D, Li K, Westerhoff P, Crittenden J (2009) Development of a group contribution method to predict aqueous phase hydroxyl radical ($HO^•$) reaction rate constants. Environ Sci Technol 43:6220–6227

Minella M, Rogora M, Vione D, Maurino V, Minero C (2011) A model approach to assess the long-term trends of indirect photochemistry in lake water. The case of Lake Maggiore (NW Italy). Sci Total Environ 409:3463–3471

Moffett JW, Zika RG (1987a) Reaction kinetics of hydrogen peroxide with copper and iron in seawater. Environ Sci Technol 21:804–810

Moffett JW, Zika RG (1987b) Photochemistry of a copper complexes in sea water In: Zika RG, Cooper WJ (eds) Photochemistry of environmental aquatic systems, ACS symposium Ser 327. American Chemical Society, Washington, pp 116–130

Moore CA, Farmer CT, Zika RG (1993) Influence of the Orinoko River on hydrogen peroxide distribution and production in the Eastern Caribean. J Geophys Res 98(C2):2289–2298

Mopper K, Kieber DJ (2000) Marine photochemistry and its impact on carbon cycling. In: de Mora S, Demers S, Vernet M (eds) The effects of UV radiation in the marine environment. Cambridge University Press, Cambridge, pp 101–129

Mopper K, Zhou X (1990) Hydroxyl radical photoproduction in the sea and its potential impact on marine processes. Science 250:661–664

Moran MA, Zepp RG (1997) Role of photoreactions in the formation of biologically labile compounds from dissolved organic matter. Limnol Oceanogr 42:1307–1316

Moran MA Jr, Sheldon WM, Zepp RG (2000) Carbon loss and optical property changes during long-term photochemical and biological degradation of estuarine dissolved organic matter. Limnol Oceanogr 45:1254–1264

Morse DE, Duncan H, Hooker N, Morse A (1977) Hydrogen peroxide induces spawning in mollusks, with activation of prostaglandin endoperoxide synthetase. Science 196:298–300

Mostofa KMG, Sakugawa H (2009) Spatial and temporal variations and factors controlling the concentrations of hydrogen peroxide and organic peroxides in rivers. Environ Chem 6:524–534

Mostofa KMG, Honda Y, Sakugawa H (2005) Dynamics and optical nature of fluorescent dissolved organic matter in river waters in Hiroshima prefecture Japan. Geochem J 39:257–271

Mostofa KMG, Yoshioka T, Konohira E, Tanoue E (2007) Photodegradation of fluorescent dissolved organic matters in river waters. Geochem J 41:323–331

Mostofa KMG, Wu FC, Yoshioka T, Sakugawa H, Tanoue E (2009a) Dissolved organic matter in the aquatic environments. In: Wu FC, Xing B (eds) Natural organic matter and its significance in the environment. Science Press, Beijing, pp 3–66

Mostofa KMG, Liu CQ, Wu FC, Fu PQ, Ying WL, Yuan J (2009b) Overview of key biogeochemical functions in lake ecosystem: impacts of organic matter pollution and global warming keynote speech. In: Proceedings of the 13th world lake conference Wuhan, China, 1–5 Nov 2009, pp 59–60

Mostofa KMG, Wu FC, Liu CQ, Yoshioka T, Sakugawa H, Tanoue E (2011) Photochemical, microbial and metal complexation behavior of fluorescent dissolved organic matter in the aquatic environments (Invited review). Geochem J 45:235–254

Mulazzani QG, D’Angelantonio M, Venturi M, Hoffmann MZ, Rodgers MA (1986) Interaction of formate and oxalate ions with radiation-generated radicals in aqueous solution Methylviologen as a mechanistic probe. J Phys Chem 90:5352–5437

Muñoz I, Rieradevall J, Torrades F, Peral J, Dome`nech X (2006a) Environmental assessment of different advanced oxidation processes applied to a bleaching kraft mill effluent. Chemosphere 62:9–16

Muñoz I, Rieradevall J, Torrades F, Peral J, Dome`nech X (2006b) Environmental assessment of different advanced oxidation processes applied to a bleaching kraft mill effluent. Chemosphere 62:9–16

Murov SL, Carmichael I, Hug GL (1993) Handbook of photochemistry, 2nd edn. Marcel Dekker, New York, pp 299–305

Nakatani N, Miyake T, Chiwa M, Hashimoto M, Arakaki T, Sakugawa H (2001) Photochemical formation of OH radicals in dew formed on the pine needles at Mt Gokurakuji. Water Air Soil Pollut 130:397–402

Nakatani N, Hashimoto N, Sakugawa H (2004) An evaluation of hydroxyl radical formation in river water and the potential for photodegradation of bisphenol A. In: Hill RJ, Leventhal J, Aizenshtat Z, Baedecker MJ, Claypool G, Eganhouse R, Goldhaber M, Peters K (eds) The geochemical society special publication series 9, Geochemical investigations in earth and space science: a tribute to Isaac R Kaplan. Elsevier, Amsterdam, pp 233–242

Nakatani N, Ueda M, Shindo H, Takeda K, Sakugawa H (2007) Contribution of the photo-Fenton reaction to hydroxyl radical formation rates in river and rain water samples. Anal Sci 23:1137–1142

Neta P, Huie RE, Ross AB (1988) Rate constants for reactions of inorganic radicals in aqueous solution. J Phys Chem Ref Data 17:1027–1284

Nogueira RP, Guimaraes JR (2000) Photodegradation of dichloroacetic acid and 2,4-dichlorophenol by ferrioxalate/H_2O_2 system. Water Res 34:895–901

Oda T, Akaike T, Sato K, Ishimatsu A, Takeshita S, Muramatsu T, Maeda H (1992) Hydroxyl radical generation by red tide algae. Arch Biochem Biophys 294:38–43

Ollis DF, Pellizetti E, Serpone N (1991) Photocatalytic destruction of water contaminants. Environ Sci Technol 25:1522–1529

Osburn CL, O'Sullivan DW, Boyd TJ (2009) Increases in the longwave photobleaching of chromophoric dissolved organic matter in coastal waters. Limnol Oceanogr 54:145–159

Page SE, Arnold WA, McNeill K (2011) Assessing the contribution of free hydroxyl radical in organic matter-sensitized photohydroxylation reactions. Environ Sci Technol 45:2818–2825

Paradies G, Petrosillo G, Pistolese M, Ruggiero FM (2000) The effect of reactive oxygen species generated from the mitochondrial electron transport chain on the cytochrome C oxidase activity and on the cardilipin content in bovine heart submitochondrial particles. FEBS Lett 466:323–326

Petasne RG, Zika RG (1987) Fate of superoxide in coastal sea water. Nature 325:516–518

Pham AN, Waite TD (2008) Oxygenation of Fe(II) in natural waters revisited: Kinetic modeling approaches, rate constant estimation and the importance of various reaction pathways. Geochim Cosmochim Acta 72:3616–3630

Pignatello JJ (1992) Dark and photoassisted Fe^{3+}-catalyzed degradation of chlorophenoxy herbicides by hydrogen peroxide. Environ Sci Technol 26:944–951

Pignatello JJ, Oliveros E, MacKay A (2006) Advanced oxidation processes for organic contaminant destruction based on the Fenton reaction and related chemistry. Crit Rev Environ Sci Technol 36:1–84

Pleskov YV, Gurevich YY (1986) Semiconductor photoelectron chemistry. Consultants Bureau, New York, p 29

Po HN, Sutin N (1968) The stability constant of the monochloro complex of iron (II). Inorg Chem 7:621–624

Pochon A, Vaughan PP, Gan DQ, Vath P, Blough NV, Falvey DE (2002) Photochemical oxidation of water by 2-methyl-1,4-benzoquinone: evidence against the formation of free hydroxyl radical. J Phys Chem A 106:2889–2894

Pozdnyakov IP, Glebov EM, Plyusnin VF, Grivin VP, Ivanov YV, Vorobyev DY, Bazhin NM (2000) Hydroxyl radical formation upon photolysis of the $Fe(OH)^{2+}$ complex in aqueous solution. Mendeleev Commun 10:185–186

Prousek J (1996) Advanced oxidation processes for water treatment photochemical processes. Chem Listy 90:307–315

Pullin MJ, Bertilsson S, Goldstone JV, Voelker BM (2004) Effects of sunlight and hydroxyl radical on dissolved organic matter: bacterial growth efficiency and production of carboxylic acids and other substrates. Limnol Oceanogr 49:2011–2022

Qian J, Mopper K, Kieber DJ (2001) Photochemical production of the hydroxyl radical in Antarctic waters. Deep-Sea Res I 48:741–759

Radtke K, Byrnes RW, Kerrigan P, Antholine WE, Petering DH (1992) Requirement of endogenous iron for cytotoxicity caused by hydrogen peroxide in euglena gracilis. Mar Environ Res 34:339–343

Randall CE, Harvey VL, Manney GL, Orsolini Y, Codrescu M, Sioris C, Brohede S, Haley CS, Gordley LL, Zawdony JM, Russell JM (2005) Stratospheric effects of energetic particle precipitation in 2003–2004. Geophys Res Lett LO5082 doi:101029/2004GL022003

Rex M, Harris NRP, der Gathen P, Lehman R, Braathen GO, Reimer E, Beck A, Chipperfield MP, Alfier R, Allaart M, O'Conner F, Dier H, Dorokhov V, Fast H, Gil M, Kyro E, Litynska Z, Mikkelsen IB, Molyneux MG, Nakane H, Notholt J, Rummukainen M, Viatte P, Wenger J (1997) Prolonged stratospheric ozone loss in the 1995–96 Arctic winter. Nature 389:835–838

Ross AB, Mallard WG, Helman WP, Buxton, Huie RE, Neta P (1994) NDRL-NIST Solution Kinetics Database: -Ver 20. National Institute for Standards and Technology, Gaithersburg

Rossetti GH, Albizzati ED, Alfano OM (2002) Decomposition of formic acid in a water solution employing the photo-Fenton reaction. Ind Eng Chem Res 41:1436–1444

Ruppert G, Bauer R, Heisler GJ (1993) The photo-Fenton reaction- an effective photochemical wastewater treatment process. J Photochem Photobiol A Chem 73:75–78

Rush JD, Bielski GHJ (1985) Pulse radiolytic studies of the reactions of HO2/O2-with Fe(II)/Fe(III) ions. The reactivity of HO2/O2-with ferric ions and its implications on the occurrence of the Haber-Weiss reaction. J Phys Chem 89:5062–5066

Russi H, Kotzias D, Korte F (1982) Photoinduzierte hydroxylierungsreaktionen organischer chemikalien in naturlichen gewassern: nitrate als potentielle OH-radikalquellen. Chemosphere 11:1041–1048

Safazadeh-Amiri A, Bolton JR, Cater SR (1996) Ferrioxalate-mediated solar degradation of organic contaminants in water. Sol Energy 56:439–443

Safazadeh-Amiri A, Bolton JR, Cater SR (1997) Ferrioxalate-mediated photodegradation of organic pollutants in contaminated water. Water Res 31:2079–2085

Sakugawa H, Kaplan IR, Tsai W, Cohen Y (1990) Atmospheric hydrogen peroxide. Environ Sci Technol 24:1452–1462

Saquib M, Tariq MA, Haque MM, Muneer M (2008) Photocatalytic degradation of disperse blue 1 using UV/TiO_2/H_2O_2 process. J Environ Manag 88:300–306

Scarpa M, Stevanato R, Viglino P, Rigo A (1983) Superoxide ion as active intermediate in the autooxidation of ascorbate by molecular oxygen. J Biol Chem 258:6695–6697

Schiavello M (1987) Basic concepts in photocatalysis. In: Schiavello M (ed) Photocatalysis and environmental trends and applications. Kluwer Academic Publishers, The Netherlands, pp 351–360

Schuchmann MN, von Sonntag C (1979) Hydroxyl radical-induced oxidation of 2-methyl-2-propanol in oxygenated aqueous solution: a product and pulse radiolysis study. J Phys Chem 83:780–784

Schwarzenbach RP, Gschwend PM, Imboden DM (1993) Environmental organic chemistry. Wiley, New York, pp 436–484

Sedlak DL, Hoigné J (1993) The role of copper and oxalate in the redox cycling of iron in atmospheric waters. Atmos Environ 27A:2173–2185

Senesi N (1990) Molecular and quantitative aspects of the chemistry of fulvic acid and its interactions with metal ions and organic chemicals Part II The fluorescence spectroscopy approach. Anal Chim Acta 232:77–106

Serpone N, Pelizzetti E (1989) Photocatalysis: fundamentals and applications. Wiley, New York, p 650

Shuali U, Ottolenghi M, Rabani J, Yelin Z (1969) On photochemistry of aqueous nitrate solutions excited in 195-nm band. J Phys Chem 73:3445–3451

Skinner JF, Glasel A, Hsu L-C, Funt BL (1980) Rotating ring disk electrode study of the hydrogen peroxide oxidation of Fe(II) and Cu(I) in hydrochloric acid. J Electrochem Soc 127:315–324

Song RG, Westerhoff P, Minear RA, Amy GL (1996) Interaction between bromine and natural organic matter. In: Minear RA, Amy GL (eds) Water disinfection and natural organic matter. American Chemical Society, Washington, pp 298–321

Southworth BA, Voelker BM (2003) Hydroxyl radical production via the photo-Fenton reaction in the presence of fulvic acid. Environ Sci Technol 37:1130–1136

Staehelin J, Hoigné J (1985) Decomposition of ozone in water in the presence of organic solutes acting as promoters and inhibitors of radical chain reactions. Environ Sci Technol 19:1206–1213

Strehlow H, Wagner I (1982) Flash photolysis of nitrite ions in aqueous solutions. Z Phys Chem Neue Folge 132:151–160

Strickler SJ, Kasha M (1963) Solvent effects on the electronic absorption spectrum of nitrite ion. J Am Chem Soc 85:2899–2901

Sun L, Bolton JR (1996) Determination of the quantum yield for the photochemical generation of hydroxyl radicals in TiO_2 suspensions. J Phys Chem 100:4127–4134

Sun Y, Pignatello J (1993) Photochemical reactions involved in the total mineralization of 2,4-D by Fe^{3+}/H_2O_2/UV. Environ Sci Technol 27:304–310

Sun B, Sato M, Sid Clements J (1997) Optical study of active species produced by a pulsed streamer corona discharge in water. J Electrostat 39(3):189–202

Sur B, Rolle M, Minero C, Maurino V, Vione D, Brigante M, Mailhot G (2011) Formation of hydroxyl radicals by irradiated 1-nitronaphthalene (1NN): oxidation of hydroxyl ions and water by the 1NN triplet state. Photochem Photobiol Sci 10:1817–1824

Sychev AY, Isak VG (1995) Iron compounds and the mechanisms of the homogeneous catalysis of the activation of O_2 and H_2O_2 and of the oxidation of organic substrates. Russ Chem Rev 64:1105–1129

Takahashi N, Nakai T, Satoh Y, Katoh Y (1995) Ozonolysis of humic acid and its effect on decoloration and biodegradability. Ozone Sci Eng 17:511–525

Takeda K, Takedoi H, Yamaji S, Ohta K, Sakugawa H (2004) Determination of hydroxyl radical photoproduction rates in natural waters. Anal Sci 20:153–158

Taylor RC, Cross PC (1949) Light absorption of aqueous hydrogen peroxide solutions in the near ultraviolet region. J Am Chem Soc 71:2266–2268

Torrents A, Anderson BG, Bilboulian S, Johnson WE, Hapeman CJ (1997) Atrazine photolysis: mechanistic investigations of direct and nitrate mediated hydroxy radical processes and the influence of dissolved organic carbon from the Chesapeake Bay. Environ Sci Technol 31:1476–1482

Tossell JA (2005) Calculation of the interaction of bicarbonate ion with arsenites in aqueous solution and with the surfaces of Al hydroxide minerals. ACS Symp Ser, Chapter 9, 915:118–130

Tranvik LJ (1992) Allochthonous dissolved organic matter as an energy source for pelagic bacteria and the concept of the microbial loop. Hydrobiologia 229:107–114

Treinin A, Hayon E (1970) Absorption spectra and reaction kinetics of NO_2, N_2O_3, and N_2O_4 in aqueous solution. J Am Chem Soc 92:5821–5828

Tseng JM, Haung CP (1991) Removal of chlorophenols from water by photocatalytic oxidation. Water Sci Technol 23:377–387

Ullah SS, Khan MGM, Rahman ABMS (1998) Photocatalytic decomposition of phenols by titanium dioxide under sunlight and UV. J Bang Acad Sci 22:29–37

Valentine JS (1973) The dioxygen ligand in mononuclear group VIII transition metal complexes. Chem Rev 73:235–345

Vaughn PP, Blough NV (1998) Photochemical formation of hydroxyl radical by constituents of natural waters. Environ Sci Technol 32:2947–2953

Vel Leitner NK, Dore M (1996) Hydroxyl radical induced decomposition of aliphatic acids in oxygenated and deoxygenated aqueous solutions. J Photochem Photobiol A Chem 99:137–143

Venkatadri R, Peters R (1993) Chemical oxidation technologies. Hazard Waste Hazard Mater 10:107–149

Vermilyea AW, Voelker BM (2009) Photo-Fenton reaction at near neutral pH. Environ Sci Technol 43:6927–6933

Viollier E, Inglett PW, Hunter K, Roychoudhury AN, van Cappellen P (2000) The ferrozine method revisited: Fe(II)/Fe(III) determination in natural waters. Appl Geochem 15:785–790

Vione D, Maurino V, Minero C, Pelizzetti E (2001a) Phenol photonitration upon UV irradiation of nitrite in aqueous solution II: effects of pH and TiO_2. Chemosphere 45:903–910

Vione D, Maurino V, Minero C, Pelizzetti E (2001b) Phenol photonitration upon UV irradiation of nitrite in aqueous solution II: effects of pH and TiO_2. Chemosphere 45:903–910

Vione D, Maurino V, Minero C, Vincenti M, Pelizzetti E (2003a) Aromatic photonitration in homogeneous and heterogeneous aqueous systems. Environ Sci Pollut Res 10:321–324

Vione D, Maurino V, Minero C, Borghesi D, Lucchiari M, Pelizzetti E (2003b) New processes in the environmental chemistry of nitrite 2 the role of hydrogen peroxide. Environ Sci Technol 37:4635–4641

Vione D, Merlo F, Maurino V, Minero C (2004a) Effect of humic acids on the fenton degradation of phenol. Environ Chem Lett 2:129–133

Vione D, Maurino V, Pelizzetti E, Minero C (2004b) Phenol photonitration and photonitrosation upon nitrite photolysis in basic solution. Int J Environ Anal Chem 84:493–504

Vione D, Falletti G, Maurino V, Minero C, Pelizzetti E, Malandrino M, Ajassa R, Olariu R-I, Arsene C (2006) Sources and sinks of hydroxyl radicals upon irradiation of natural water samples. Environ Sci Technol 40:3775–3781

Vione D, Maurino V, Cucu Man S, Khanra S, Arsene C, Olariu RI, Minero C (2008) Formation of organobrominated compounds in the presence of bromide under simulated atmospheric aerosol conditions. ChemSusChem 1:197–204

Vione D, Khanra S, Man SC, Maddigapu PR, Das R, Arsene C, Olariu RI, Maurino V, Minero C (2009a) Inhibition vs enhancement of the nitrate-induced phototransformation of organic substrates by the OH scavengers bicarbonate and carbonate. Water Res 43:4718–4728

Vione D, Maurino V, Minero C, Carlotti ME, Chiron S, Barbati S (2009b) Modelling the occurrence and reactivity of the carbonate radical in surface freshwater. Comptes Rendus Chimie 12:865–871

Vione D, Lauri V, Minero C, Maurino V, Malandrino M, Carlotti ME, Olariu RI, Arsene C (2009c) Photostability and photolability of dissolved organic matter upon irradiation of natural water samples under simulated sunlight. Aquat Sci 71:34–45

Vione D, Casanova I, Minero C, Duncianu M, Olariu RI, Arsene C (2009d) Assessing the potentiality of Romanian surface waters to produce hydroxyl and nitrite radicals. Revista De Chimie 60:123–126

Vione D, Ponzo M, Bagnus D, Maurino V, Minero C, Carlotti ME (2010) Comparison of different probe molecules for the quantification of hydroxyl raidcals in aqueous solution. Environ Chem Lett 8:95–100

Voelker BM, Sulzberger B (1996) Effects of fulvic acid on Fe(II) oxidation by hydrogen peroxide. Environ Sci Technol 30:1106–1114

Voelker BM, Morel FMM, Sulzberger B (1997) Iron redox cycling in surface waters: effects of humic substances and light. Environ Sci Technol 31:1004–1011

Voelker BM, Sedlak DL, Zafiriou OC (2000) Chemistry of superoxide radical in seawater: Reactions with organic Cu complexes. Environ Sci Technol 34:1036–1042

Volman DH, Chen JC (1959) The photochemical decomposition of hydrogen peroxide in aqueous solutions of allyl alcohol at 2537 A. J Am Chem Soc 81:4141–4144

von Gunten U, Oliveras Y (1997) Kinetics of the reaction between hydrogen peroxide and hypobromous acid: implication on water treatment and natural systems. Water Res 31:900–906

von Sonntag C (2006) Free-radical-induced DNA damage and its repair a chemical perspective. Springer Verlag, Berlin, pp 359–482

von Sonntag C (2007) The basics of oxidants in water treatment Part A: OH radical reactions. Water Sci Technol 55:19–23

von Sonntag C, Mark G, Mertens R, Schuchmann MN, Schuchmann H-P (1993) UV-radiation and/or oxidants in water pollution control. J Water Supply Res Technol Aquat 42:201–211

Wagner I, Strehlow H, Busse G (1980) Flash-photolysis of nitrate ions in aqueous-solution. Z Phys Chem 123:1–33

Walling C (1975) Fenton's reagent revisited. Acc Chem Res 8:125–131

Walling C, Weil T (1974) The ferric ion catalyzed decomposition of hydrogen peroxide in perchloric acid solution. Int J Chem Kinet 6:507–516

Wang GS, Liao CH, Wu FJ (2001) Photodegradation of humic acids in the presence of hydrogen peroxide. Chemosphere 42:379–387

Wang Z, Chen X, Ji H, Ma W, Chen C, Zhao J (2010) Photochemical cycling of iron mediated by dicarboxylates: special effect of malonate. Environ Sci Technol 44:263–268

Warneck P, Wurzinger C (1988) Product quantum yields for the 305-nm photodecomposition of nitrate in aqueous solution. J Phys Chem 92:6278–6283

Wells CF, Salam MA (1967) Complex formation between Fe(II) and inorganic anions. Trans Faraday Soc 63:620–629

Wells CF, Salam MA (1968) The effect of pH on the kinetics of the reaction of iron (II) with hydrogen peroxide in perchlorate media. J Chem Soc (A):24–29

Westerhoff P, Aiken G, Army G, Debroux J (1999) Relationships between the structure of natural organic matter and its reactivity towards molecular ozone and hydroxyl radicals. Water Res 33:2265–2276

Westerhoff P, Mezyk SP, Cooper WJ, Minakata D (2007) Electron pulse radiolysis determination of hydroxyl radical rate constants with Suwannee river fulvic acid and other dissolved organic matter isolates. Environ Sci Technol 41:4610–4646

White EM, Vaughan PP, Zepp RG (2003) Role of photo-Fenton reaction in the production of hydroxyl radicals and photobleaching of coloured dissolved organic matter in a coastal river of the southern United States. Aquat Sci 65:402–414

Williams NH, Yandell JK (1982) Outer-sphere electron-transfer reaction of ascorbate anions. Aust J Chem 35:1133–1144

Winterbourn CC (1993) Superoxide as an intracellular radical sink. Free Radic Biol Med 14:85–90

Wu F, Deng N, Zuo Y (1999) Discoloration of dye solutions induced by solar photolysis of ferrioxalate in aqueous solutions. Chemosphere 39:2079–2085

Xu T, Cai Y, Mezyk SP, O'Shea KE (2005) The roles of hydroxyl radical, superoxide anion radical, and hydrogen peroxide in the oxidation of arsenite by ultrasonic irradiation advances in arsenic research. American Chemical Society, Washington, pp 333–343

You J-L, Fong FK (1986) Superoxide photogeneration by chlorophyll A in water/acetone Electron spin resonance studies of radical intermediates in chlorophyll A photoreaction in vitro. Biochem Biophys Res Commun 139:1124–1129

Zafiriou OC (1974) Sources and reactions of OH and daughter radicals in seawater. J Geophys Res 79:4491–4497

Zafiriou OC (1990) Chemistry of superoxide ion-radical (O2-) in seawater: I pK$^*_{\mathrm{asw}}$ (HOO) and uncatalyzed dismutation kinetics studies by pulse radiolysis. Mar Chem 30:31–43

Zafiriou OC, Bonneau R (1987) Wavelength-dependent quantum yield of OH radical formation from photolysis of nitrite ion in water. Photochem Photobiol 15:723–727

Zafiriou OC, Dister B (1991) Photochemical free-radical production-rates-Guld of marine and Woods-Hole Miami transect. J Geophys Res Oceans 96(C3):4939–4945

Zafiriou OC, True MB (1979a) Nitrite photolysis in seawater by sunlight. Mar Chem 8:9–32

Zafiriou OC, True MB (1979b) Nitrate photolysis in seawater by sunlight. Mar Chem 8:33–42

Zafiriou OC, Joussot-Dubien J, Zepp RG, Zika RG (1984) Photochemistry of natural waters. Environ Sci Technol 18:356A–371A

Zafiriou OC, True Mary B, Hayon E (1987) Consequences of OH radical reaction in sea water: formation and decay of Br2- ion radical, Photochemistry of environmental aquatic systems. American Chemical Society, Washington, pp 89–105

Zafiriou OC, True Mary B, Hayon E (1987) Consequences of OH radical reaction in sea water: formation and decay of Br^{2-} ion radical, Photochemistry of environmental aquatic systems. American Chemical Society, Washington, pp 89–105

Zafiriou OC, Voelker BM, Sedlak DL (1998) Chemistry of the superoxide radical (O2^{-}) in seawater: Reactions with inorganic copper complexes. J Phys Chem A 102:5693–5700

Zang L-Y, Stone K, Pryor WA (1995) Detection of free radicals in aqueous extracts of cigarette tar by electron spin resonance. Free Radic Biol Med 19(2):161–167

Zellner R, Exner M, Herrmann H (1990) Absolute OH quantum yields in the laser photolysis of nitrate, nitrite and dissolved H_2O_2 at 308 and 351 nm in the temperature range 278–353 K. J Atmos Chem 10:411–425

Zepp RG (2002) Solar ultraviolet radiation and aquatic carbon, nitrogen, sulfur and metals cycles In: Helbling EW, Zagarese H (eds) UV effects in aquatic organisms and ecosystems. Royal Society of Chemistry, Cambridge, pp 137–183

Zepp RG, Hoigné J, Bader H (1987a) Nitrate-induced photooxidation of trace organic chemicals in water. Environ Sci Technol 21:443–450

Zepp RG, Skurlatov YI, Pierce JT (1987) Algal-induced decay and formation of hydrogen peroxide in water: its possible role in oxidation of anilines by algae. In: Zika RG, Cooper WJ (eds) Photochemistry of environmental aquatic systems, ACS Symp Ser 327. American Chemical Society, Washington, pp 213–224

Zepp RG, Faust BC, Hoigné J (1992) Hydroxyl radical formation in aqueous reactions (pH 3–8) of iron(II) with hydrogen peroxide: the Photo-Fenton reaction. Environ Sci Technol 26:313–319

Zhao B, Li X, He R, Cheng S, Wenjuan X (1989) Scavenging effect of extracts of green tea and natural antioxidants on active oxygen radicals. Cell Biochem Biophys 14:175–185

Zhou X, Mopper K (1990) Determination of photolytically produced hydroxyl radicals in seawater and freshwater. Mar Chem 30:71–88

Zika RG, Milne PJ, Zafiriou OC (1993) Photochemical studies of the eastern Caribbean—an introductory overview. J Geophys Res Oceans 98(C2):2223–2232

Zimbron JA, Reardon KF (2005) Hydroxyl free radical reactivity toward aqueous chlorinated phenols. Water Res 39:865–869

Zuo Y, Hoigné J (1992) Formation of hydrogen peroxide and depletion of oxalic acid in atmospheric water by photolysis of iron(III)-oxalato complexes. Environ Sci Technol 26:1014–1022